Causes and consequences of altered microRNA levels

Slezak-Prochazka, Izabella Helena

rijksuniversiteit groningen

Causes and consequences of altered microRNA levels

Regulation of microRNA biogenesis and identification of microRNA-155 target genes

Izabella Ślęzak-Prochazka

The studies described in this thesis were financially supported by:

Graduate School of Medical Sciences
J.K. de Cock Foundation

Printing of this thesis was financially supported by:
University of Groningen
Graduate School of Medical Sciences
Faculty of Medical Sciences, UMCG

Cover: Bartosz Prochazka
Layout: Izabella Ślęzak-Prochazka
Printed by: Advertdruk, Chorzow, Poland

ISBN: 978-90-367-5942-7 (print)
ISBN: 978-90-367-5943-4 (digital)

rijksuniversiteit groningen

Causes and consequences of altered microRNA levels

Regulation of microRNA biogenesis and identification of microRNA-155 target genes

Proefschrift

ter verkrijging van het doctoraat in de
Medische Wetenschappen
aan de Rijksuniversiteit Groningen
op gezag van de
Rector Magnificus, dr. E. Sterken,
in het openbaar te verdedigen op
maandag 14 januari 2013
om 16.15 uur

door

Izabella Helena Ślęzak-Prochazka

geboren op 13 juni 1984
te Będzin, Polen

Promotor:	Prof. dr. J.H.M. van den Berg
Copromotores:	Dr. B.J. Kroesen
	Dr. J.L. Kluiver
Beoordelingscommissie:	Prof. dr. P.M. Kluin
	Prof. dr. G. de Haan
	Prof. dr. J.J. Schuringa

Paranimfen: Debora de Jong

Marta Capała

Katarzyna Śmigielska-Czepiel

To my parents

CONTENTS

CHAPTER 1

Introduction
Scope of the thesis

Izabella Ślęzak-Prochazka

CONTENTS

INTRODUCTION

1. MicroRNAs

MicroRNAs (miRNAs) are single-stranded RNA molecules of ~22nt (Bartel, 2004) that belong to the larger family of non-coding RNAs. MiRNAs inhibit expression of genes by repressing their translation or stability (Filipowicz et al., 2008). The first miRNA, lin-4, was discovered in *Caenorhabditis elegans* (*C. elegans*) in 1993 (Lee et al., 1993). However, only after the second miRNA, let-7, was discovered in 2000 (Reinhart et al., 2000), more attention was paid to miRNAs. Since then a substantial number of miRNAs has been identified with, at present, more than 25,000 miRNAs in the miRBase database, including over 2,000 human miRNAs (miRbase Release 19, Kozomara and Griffiths-Jones, 2011). MiRNAs have been found in a total number of 193 species, including viruses, plants and animals. Approximately 55% of the *C. elegans* miRNAs have homologues in humans indicating that there is high degree of conservation during animal evolution (Ibanez-Ventoso et al., 2008). This high degree of conservation indicates the importance of miRNAs in cellular functioning.

Biogenesis of miRNAs

Genomic locations of miRNAs include introns and exons of protein-coding or noncoding genes as well as intergenic regions (Fig.1) (Kim and Nam, 2006). The majority of the miRNAs are located in introns of protein-coding genes. MiRNAs are transcribed together with their host gene as longer primary miRNA transcripts (pri-miRNA) (Cai et al., 2004). The canonical miRNA biogenesis pathway consists of two enzymatic steps (Fig. 2). Transcription of pri-miRNAs generally involves polymerase II and occasionally polymerase III (Borchert et al., 2006; Lee et al., 2004). The pri-miRNA transcripts contain one or more hairpin structures. Different miRNAs that are transcribed from one primary transcript with multiple hairpin structures are denoted as miRNA clusters (Lee et al., 2002). MiRNA clusters are not a rare finding. In fact, miRNA clusters constitute ~40% of all human miRNAs (Altuvia et al., 2005; Hertel et al., 2006).

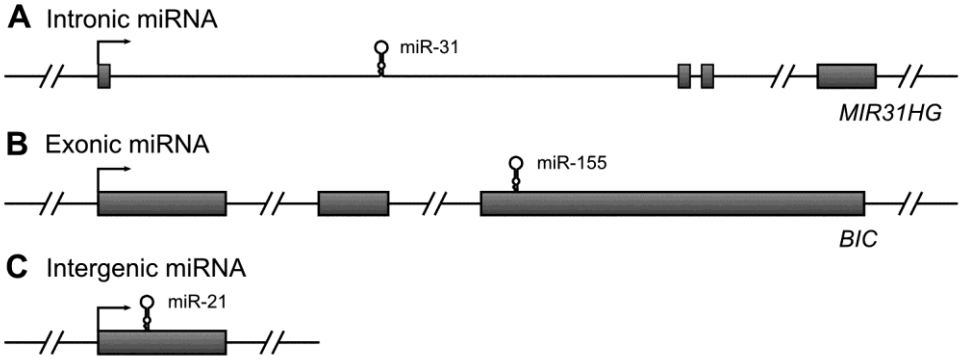

FIGURE 1. Genomic localization of miRNAs. (A) MiRNAs can be localized in introns of protein-coding or noncoding genes (intronic miRNAs). As an example the miR-31 primary transcript with the stem-loop in the intron of the noncoding *MIR31HG* gene is shown. (B) MiRNAs localized in exons of noncoding genes (exonic miRNAs). The location of the miR-155 stem-loop in exon 3 of the *BIC* noncoding gene. (C) MiRNAs that have their own promoter (intergenic miRNAs), as an example the miR-21 gene is shown.

Biogenesis of miRNAs is tightly regulated resulting in specific miRNA expression patterns in certain tissues or at specific developmental stages. Hairpin structures are processed by the Microprocessor complex that consists of DiGeorge syndrome critical region 8 (DGCR8) and the RNase III endonuclease Drosha (Denli et al., 2004; Gregory et al., 2004; Han et al., 2004; Landthaler et al., 2004; Lee et al., 2003). DGCR8 recognizes the hairpin structure by interacting with the ssRNA segments flanking the stem-loop structure and mediates cleavage of the hairpin structure by Drosha (Han et al., 2006; Zeng and Cullen, 2005). The resulting 60-70nt precursor miRNA (pre-miRNA) is exported to the cytoplasm by the Exportin 5 – RanGTP complex to be further processed by the RNase III endonuclease Dicer to a double stranded ~22nt miRNA/miRNA* duplex (Bohnsack et al., 2004; Grishok et al., 2001; Hutvagner et al., 2001; Lund et al., 2004; Yi et al., 2003). One strand, denoted as the miRNA, is incorporated into the RNA-induced silencing complex (RISC) while the other strand, denoted as the miRNA*, is often degraded (Eulalio et al., 2008; Filipowicz et al., 2008). Selection of the miRNA that will be retained in the RISC complex is thought to depend on the stability of the 5'ends of the miRNA/miRNA* duplex (Khvorova et al., 2003; Schwarz et al., 2003). Each of

the two strands of the duplex can be incorporated into the RISC complex. Therefore, miRNA-5p and -3p nomenclature is now more commonly used.

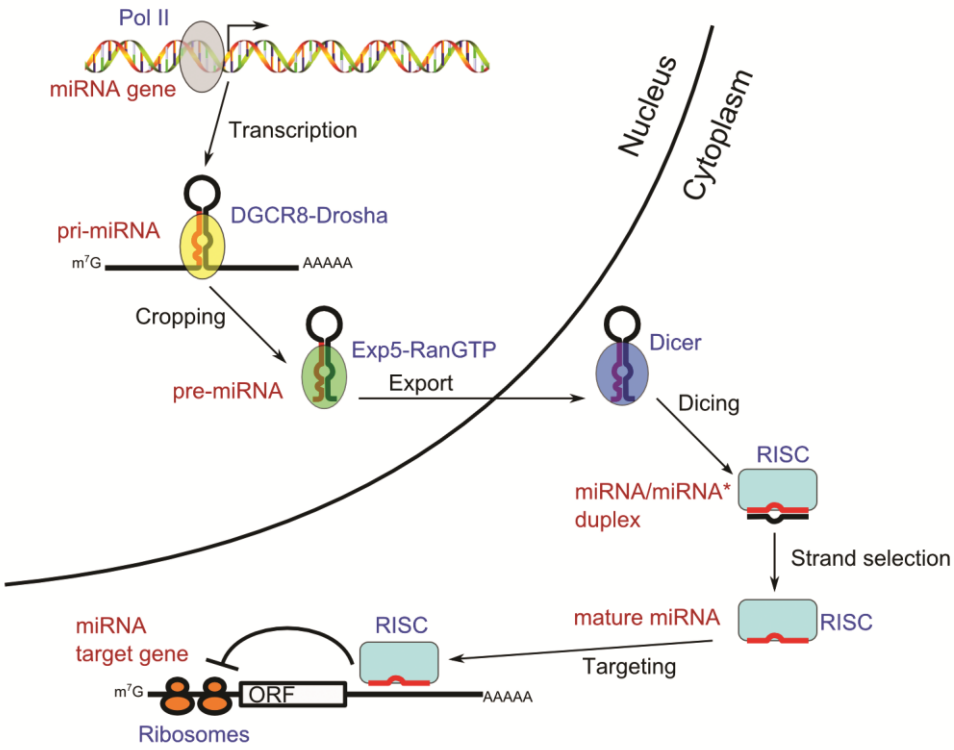

FIGURE 2. Canonical biogenesis of miRNAs. MicroRNAs are transcribed as long primary transcripts (pri-miRNA) that are processed by the Drosha-DGCR8 complex to precursor miRNA (pre-miRNA). These precursors are exported to the cytoplasm by Exportin-5 and further processed by Dicer to a miRNA/miRNA* duplex. The mature miRNA is incorporated into the RNA-induced silencing complex (RISC) and this complex binds to the 3'UTR of its target genes and inhibits the translation.

Function of miRNAs

RISC is a multiprotein complex that includes a miRNA and one of the four Argonaute proteins (Gregory et al., 2005; Hutvagner and Zamore, 2002; Mourelatos et al., 2002). The miRNA guides the RISC to its target transcripts based on partial complementarity between the mRNA and miRNA (Fig. 2). A high degree of complementarity of nucleotides 2-7 of the miRNA is the most important factor for effective targeting of the mRNA (Bartel, 2009). This region

is referred to as the "seed sequence". The degree of homology for the remaining part of the miRNA may be lower and thus adds to the promiscuous nature of single miRNAs that target different mRNAs (Doench and Sharp, 2004). MiRNAs that share "seed sequences" belong to the same miRNA seed family and may, at least in part, target the same set of genes. MiRNAs usually bind to the 3'UTR of the target gene and less frequent to the coding sequence or 5'UTR (Chi et al., 2009). MiRNA binding affects either mRNA translation or its stability (Pillai et al., 2007). Both target gene prediction programs and biochemical approaches have been widely applied to identify miRNA target genes and they indicated that each miRNA can target multiple mRNAs and each mRNA can be targeted by multiple miRNAs. It is estimated that more than one third of the genes can be regulated by miRNAs (Lewis et al., 2005). This suggests that miRNAs play a role in a large variety of cellular processes. Functional studies have indeed indicated that miRNAs are involved in virtually all biological processes including programmed cell death, proliferation, cell differentiation and metabolic control. In addition, miRNAs have been causally linked to many pathological conditions including diabetes, cardiovascular disease, autoimmune disorders and, most thoroughly investigated, cancer. A substantial number of human miRNAs are located in the cancer-associated genomic locations (Calin et al., 2004) and there are numerous studies that show altered miRNA levels in various cancer types (Lu et al., 2005; Sassen et al., 2008). Alteration of miRNA levels in cancer can be caused by genetic aberrations, deregulation of transcription and epigenetic factors, alterations in miRNA processing and/or miRNA stability.

2. B-cell lymphoma

The most common B-cell lymphoma subtypes include diffuse large B-cell lymphoma (DLBCL), Hodgkin lymphoma (HL), follicular lymphoma (FL), chronic lymphocytic leukemia (CLL), mantle cell lymphoma (MCL), marginal zone lymphoma (MZL) and Burkitt lymphoma (BL) (Kuppers, 2005). All these malignancies display distinct clinical, histological and immunophenotypic features, and vary greatly in short-term and long-term response to treatment.

A large proportion of the B-cell lymphomas are derived from B cells at the germinal center (GC) stage of maturation (Kuppers et al., 1999). GCs arise from foci of mature naïve B cells upon B-cell antigen receptor (BcR) stimulation in combination with co-stimulatory signals from T cells (MacLennan, 1994). GCs are characterized by proliferating B cells that have an active somatic hypermutation (SHM) machinery (Kuppers et al., 1993). During SHM, a high rate of mutations is introduced into the functionally rearranged immunoglobulin (Ig) genes, affecting their affinity. Fractions of these GC B cells undergo class-switch recombination, which is mediated by double-strand DNA breaks (Liu et al., 1996). These cells may undergo second rounds of affinity maturation and selection, after which they may differentiate into memory or plasma cells. Both processes are essential for successful antigen-driven maturation of B cells, but they also represent important risk factors for malignant transformation. Accordingly, an established hallmark of many types of B-cell lymphomas are reciprocal translocations involving one of the Ig gene loci (heavy and light chain genes) and a proto-oncogene. The result is uncontrolled constitutive expression of the translocated gene. Examples of such GC-derived translocations are BCL6-Ig in DLBCL, MYC-Ig in BL and DLBCL and BCL2-Ig in FL (Baron et al., 1993; Dalla-Favera et al., 1983; Ladanyi et al., 1991; Taub et al., 1982; Ye et al., 1993). The involvement of non-Ig gene loci is partially caused by the somatic hypermutation machinery which can also target many non-Ig genes.

3. MicroRNAs in B-cell lymphoma

Several miRNAs have been shown to have tumor suppressive or oncogenic activity in B-cell lymphoma. Tumor suppressive miRNAs may target oncogenes, and loss of such miRNAs leads to enhanced levels of oncogenic proteins. Tumor suppressive miR-15a and miR-16-1 are frequently deleted or downregulated in CLL (Calin et al., 2002; Calin et al., 2005). Mice with deletion of the genomic loci containing this miRNA locus developed CLL-like disease (Klein et al., 2010). The tumor suppressive role of miR-15a and miR-16-1 in CLL has been reported to involve inhibition of the anti-apoptotic oncogene Bcl-2 (Cimmino et al., 2005). Let-7a inhibits proliferation of BL cells through inhibition of the MYC oncogene

(Mayr et al., 2007; Sampson et al., 2007). Oncogenic miRNAs may target tumor suppressor genes, and enhanced expression of these oncogenic miRNAs may, as such, result in reduced levels of tumor suppressor proteins. For example, miR-21 is upregulated in most cancer types (Buscaglia and Li, 2011). Conditional overexpression of miR-21 in mice resulted in formation of tumors with pre-B cell malignant lymphoid-like phenotype that regressed completely when miR-21 was inactivated (Medina et al., 2010). This indicates that miR-21 is a genuine oncogene that plays a key role in tumor growth. Other oncogenic miRNAs strongly associated with both B-cell functioning and B-cell lymphoma are miR-155 and the miR-17~92 cluster (Hayashita et al., 2005; Kluiver et al., 2005; Kluiver et al., 2006).

MiR-155

MiR-155 is processed from the transcript of a noncoding gene called B-cell integration cluster (*BIC*) (Lagos-Quintana et al., 2002). Several studies have shown that *BIC* and miR-155 play a crucial role in the immune response (O'Connell et al., 2009; Rodriguez et al., 2007; Thai et al., 2007). *BIC* expression levels are highly induced in B cells upon stimulation via the B cell receptor (van den Berg et al., 2003). *BIC* and miR-155 are highly expressed in normal tonsillar GC B cells indicating a role in B-cell maturation (Kluiver et al., 2007). This was indeed demonstrated in *BIC*/miR-155-deficient mice (Rodriguez et al., 2007; Thai et al., 2007). These mice showed reduced numbers of germinal center B cells and diminished high-affinity IgG1 antibody production. Also, *in vitro* activated miR-155-deficient T cells showed increased tendency to differentiate into Th2-type cells (Rodriguez et al., 2007).

BIC/miR-155 was one of the first oncogenic miRNAs shown to be associated with B-cell lymphoma. Elevated miR-155 levels were observed in several B-cell lymphomas, such as HL, DLBCL and PMBL (Eis et al., 2005; Kluiver et al., 2005). Further evidence for an oncogenic role for miR-155 came from a study demonstrating that Eμ-miR-155 transgenic mice developed polyclonal pre-B-cell proliferations leading to B-cell malignancies at later stages (Costinean et al., 2006). Myeloproliferative disorders were induced by

overexpression of miR-155 in hematopoietic stem cells in a mouse model (O'Connell et al., 2008). Recently, Babar et al. showed that induction of miR-155 caused disseminated lymphoma in mice, characterized by clonal and transplantable neoplastic pre-B cells (Babar et al., 2012). Tumor cells were shown to be addicted to miR-155, as miR-155 withdrawal lead to rapid tumor regression due to increased apoptosis of the malignant cells. These studies suggest that inhibition of miR-155 can be used as a therapeutic strategy for miR-155-expressing lymphomas.

In contrast, to other GC B-cell-derived lymphomas, miR-155 is expressed at very low levels in Burkitt lymphoma suggesting that miR-155 may also have a tumor suppressive function (Kluiver et al., 2006). Consistent with this putative tumor suppressor function, miR-155 has been shown to target activation-induced cytidine deaminase (AID) (Dorsett et al., 2008). AID promotes immunoglobulin gene diversification in normal B cells, but thereby enhances the risk of chromosomal translocations involving the immunoglobulin loci (Dorsett et al., 2007; Liu et al., 2008; Ramiro et al., 2004). Translocations involving the MYC locus and one of the immunoglobulin gene loci are a hallmark of Burkitt lymphoma (Taub et al., 1982). Thus, these data indicate that downregulation of miR-155 may contribute to the initiation phase of Burkitt lymphoma by enhancing the formation of MYC translocations.

The miR-17~92 cluster

The miR-17~92 cluster consists of 6 miRNAs that are processed from a single primary transcript*, C13ORF25* (Figure 3). This miRNA cluster has two paralogs, i.e. the miR-106a~363 and miR-106b~25 clusters that share multiple seed family members and also some identical miRNAs (Tanzer and Stadler, 2004). *C13ORF25* is located in the 13q31 region, which is often amplified in B-cell lymphoma (Ota et al., 2004; Rinaldi et al., 2007). Mice deficient for miR-17~92 have a block in pro-B to pre-B-cell development, indicating an important role of this miRNA cluster in B-cell development (Ventura et al., 2008). Overexpression

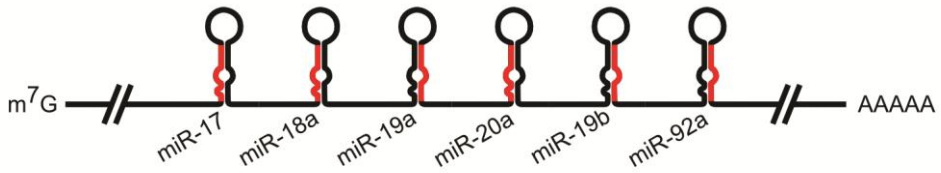

FIGURE 3. Schematic representation of the miR-17~92 cluster. Each dominant miRNA which is derived from the strand -3p or 5p is indicated in red.

of miR-17~92 in the Eμ-MYC mouse B-cell lymphoma model resulted in accelerated B-cell lymphoma development (He et al., 2005). More recently, miR-19a and miR-19b have been identified as the key oncogenic components necessary and sufficient for promoting MYC-induced lymphomagenesis by repressing apoptosis (Mu et al., 2009; Olive et al., 2009). Several individual members of this miRNA cluster play important roles in proliferation, tumor angiogenesis and suppression of apoptosis (Dews et al., 2006; Hayashita et al., 2005; Li et al., 2012; Matsumura et al., 2003).

SCOPE OF THE THESIS

Altered miRNA levels are observed in almost all types of cancer including B-cell lymphoma. The aim of this thesis is to investigate possible causes of altered miRNA levels and the specific consequences of altered miRNA-155 levels in B-cell lymphoma.

MiRNA levels are regulated at the level of transcription of the primary transcripts, miRNA processing and miRNA stability. In this thesis, we focus on the regulation of miRNA processing and the consequences of altered miR-155 levels. In **chapter 2**, we present an overview of established mechanisms to regulate miRNA processing. This chapter serves as an introduction to the experimental work described in chapters 3 and 4. In **chapter 3**, we present our results on processing of exonic miRNAs. It is still unclear whether exonic miRNAs are processed from unspliced or spliced pri-miRNA transcripts. To study this, we assessed the levels and cellular localization of unspliced and spliced pri-miRNA

transcripts of miR-155, miR-146a and miR-22. In addition, we overexpressed miR-155 using constructs containing pre-miR-155 and either exonic or intronic 5' upstream flanking sequence to determine if these upstream sequences affected the processing efficiency to miR-155. In **chapter 4**, we describe our study on processing of the miR-17~92 cluster. We assessed levels of the primary miR-17~92 transcript and the six mature miRNAs in normal B cells, 117 non-Hodgkin lymphoma (NHL) cases and in 21 NHL cell lines. We assessed the correlation between the levels of primary miR-17~92 transcripts with each of the six mature miRNAs in each NHL subtype. We also compared the levels of the individual miR-17~92 cluster members in NHL to the levels in their normal B-cell counterparts to identify which miRNAs are induced in NHL.

To determine the consequences of altered miRNA expression levels, it is crucial to effectively inhibit miRNAs. In **chapter 5**, we describe a straight-forward method to inhibit miRNAs using miRNA sponges. We showed how to generate retroviral miRNA sponges with variable numbers of miRNA binding sites. We confirmed their effectiveness and showed applications for loss-of-function studies. In **chapter 6**, we describe the consequence of altered miR-155 expression in B-cell lymphoma. To this end, we overexpressed miR-155 in Burkitt lymphoma cells with very low endogenous levels and determined the effect of miR-155 induction on cell growth. We next identified genes that are targeted by miR-155 using Ago2-RIP-Chip. We validated six selected genes by luciferase reporter assay and assessed whether their inhibition by shRNAs could phenocopy the effect of miR-155 induction on the growth of Burkitt lymphoma cells. We used a miR-155 sponge to determine whether the six selected targets are also regulated by endogenous miR-155 in Hodgkin lymphoma cells with high endogenous miR-155 level. Finally, in **chapter 7**, we summarize and discuss results presented in this thesis and discuss possible future perspectives.

REFERENCES

Altuvia, Y., Landgraf, P., Lithwick, G., Elefant, N., Pfeffer, S., Aravin, A., Brownstein, M.J., Tuschl, T. and Margalit, H. 2005. Clustering and conservation patterns of human microRNAs. *Nucleic Acids Res.* **33**: 2697-2706.

Babar, I.A., Cheng, C.J., Booth, C.J., Liang, X., Weidhaas, J.B., Saltzman, W.M. and Slack, F.J. 2012. Nanoparticle-based therapy in an in vivo microRNA-155 (miR-155)-dependent mouse model of lymphoma. *Proc. Natl. Acad. Sci. U. S. A.* **109**: E1695-704.

Baron, B.W., Nucifora, G., McCabe, N., Espinosa, R.,3rd, Le Beau, M.M. and McKeithan, T.W. 1993. Identification of the gene associated with the recurring chromosomal translocations t(3;14)(q27;q32) and t(3;22)(q27;q11) in B-cell lymphomas. *Proc. Natl. Acad. Sci. U. S. A.* **90**: 5262-5266.

Bartel, D.P. 2004. MicroRNAs: genomics, biogenesis, mechanism, and function. *Cell* **116**: 281-297.

Bartel, D.P. 2009. MicroRNAs: target recognition and regulatory functions. *Cell* **136**: 215-233.

Bohnsack, M.T., Czaplinski, K. and Gorlich, D. 2004. Exportin 5 is a RanGTP-dependent dsRNA-binding protein that mediates nuclear export of pre-miRNAs. *RNA* **10**: 185-191.

Borchert, G.M., Lanier, W. and Davidson, B.L. 2006. RNA polymerase III transcribes human microRNAs. *Nat. Struct. Mol. Biol.* **13**: 1097-1101.

Buscaglia, L.E. and Li, Y. 2011. Apoptosis and the target genes of microRNA-21. *Chin. J. Cancer.* **30**: 371-380.

Cai, X., Hagedorn, C.H. and Cullen, B.R. 2004. Human microRNAs are processed from capped, polyadenylated transcripts that can also function as mRNAs. *RNA* **10**: 1957-1966.

Calin, G.A., Dumitru, C.D., Shimizu, M., Bichi, R., Zupo, S., Noch, E., Aldler, H., Rattan, S., Keating, M., Rai, K. et al. 2002. Frequent deletions and down-regulation of micro- RNA genes miR15 and miR16 at 13q14 in chronic lymphocytic leukemia. *Proc. Natl. Acad. Sci. U. S. A.* **99**: 15524-15529.

Calin, G.A., Ferracin, M., Cimmino, A., Di Leva, G., Shimizu, M., Wojcik, S.E., Iorio, M.V., Visone, R., Sever, N.I., Fabbri, M. et al. 2005. A MicroRNA signature associated with prognosis and progression in chronic lymphocytic leukemia. *N. Engl. J. Med.* **353**: 1793-1801.

Calin, G.A., Sevignani, C., Dumitru, C.D., Hyslop, T., Noch, E., Yendamuri, S., Shimizu, M., Rattan, S., Bullrich, F., Negrini, M. et al. 2004. Human microRNA genes are frequently located at fragile sites and genomic regions involved in cancers. *Proc. Natl. Acad. Sci. U. S. A.* **101**: 2999-3004.

Chi, S.W., Zang, J.B., Mele, A. and Darnell, R.B. 2009. Argonaute HITS-CLIP decodes microRNA-mRNA interaction maps. *Nature* **460**: 479-486.

Cimmino, A., Calin, G.A., Fabbri, M., Iorio, M.V., Ferracin, M., Shimizu, M., Wojcik, S.E., Aqeilan, R.I., Zupo, S., Dono, M. et al. 2005. miR-15 and miR-16 induce apoptosis by targeting BCL2. *Proc. Natl. Acad. Sci. U. S. A.* **102**: 13944-13949.

Costinean, S., Zanesi, N., Pekarsky, Y., Tili, E., Volinia, S., Heerema, N. and Croce, C.M. 2006. Pre-B cell proliferation and lymphoblastic leukemia/high-grade lymphoma in E(mu)-miR155 transgenic mice. *Proc. Natl. Acad. Sci. U. S. A.* **103**: 7024-7029.

Dalla-Favera, R., Martinotti, S., Gallo, R.C., Erikson, J. and Croce, C.M. 1983. Translocation and rearrangements of the c-myc oncogene locus in human undifferentiated B-cell lymphomas. *Science* **219**: 963-967.

Denli, A.M., Tops, B.B., Plasterk, R.H., Ketting, R.F. and Hannon, G.J. 2004. Processing of primary microRNAs by the Microprocessor complex. *Nature* **432**: 231-235.

Dews, M., Homayouni, A., Yu, D., Murphy, D., Sevignani, C., Wentzel, E., Furth, E.E., Lee, W.M., Enders, G.H., Mendell, J.T. et al. 2006. Augmentation of tumor angiogenesis by a Myc-activated microRNA cluster. *Nat. Genet.* **38**: 1060-1065.

Doench, J.G. and Sharp, P.A. 2004. Specificity of microRNA target selection in translational repression. *Genes Dev.* **18**: 504-511.

Dorsett, Y., McBride, K.M., Jankovic, M., Gazumyan, A., Thai, T.H., Robbiani, D.F., Di Virgilio, M., Reina San-Martin, B., Heidkamp, G., Schwickert, T.A. et al. 2008. MicroRNA-155 suppresses activation-induced cytidine deaminase-mediated Myc-Igh translocation. *Immunity* **28**: 630-638.

Dorsett, Y., Robbiani, D.F., Jankovic, M., Reina-San-Martin, B., Eisenreich, T.R. and Nussenzweig, M.C. 2007. A role for AID in chromosome translocations between c-myc and the IgH variable region. *J. Exp. Med.* **204**: 2225-2232.

Eis, P.S., Tam, W., Sun, L., Chadburn, A., Li, Z., Gomez, M.F., Lund, E. and Dahlberg, J.E. 2005. Accumulation of miR-155 and BIC RNA in human B cell lymphomas. *Proc. Natl. Acad. Sci. U. S. A.* **102**: 3627-3632.

Eulalio, A., Huntzinger, E. and Izaurralde, E. 2008. Getting to the root of miRNA-mediated gene silencing. *Cell* **132**: 9-14.

Filipowicz, W., Bhattacharyya, S.N. and Sonenberg, N. 2008. Mechanisms of post-transcriptional regulation by microRNAs: are the answers in sight? *Nat. Rev. Genet.* **9**: 102-114.

Gregory, R.I., Chendrimada, T.P., Cooch, N. and Shiekhattar, R. 2005. Human RISC couples microRNA biogenesis and posttranscriptional gene silencing. *Cell* **123**: 631-640.

Gregory, R.I., Yan, K.P., Amuthan, G., Chendrimada, T., Doratotaj, B., Cooch, N. and Shiekhattar, R. 2004. The Microprocessor complex mediates the genesis of microRNAs. *Nature* **432**: 235-240.

Grishok, A., Pasquinelli, A.E., Conte, D., Li, N., Parrish, S., Ha, I., Baillie, D.L., Fire, A., Ruvkun, G. and Mello, C.C. 2001. Genes and mechanisms related to RNA interference regulate expression of the small temporal RNAs that control C. elegans developmental timing. *Cell* **106**: 23-34.

Han, J., Lee, Y., Yeom, K.H., Kim, Y.K., Jin, H. and Kim, V.N. 2004. The Drosha-DGCR8 complex in primary microRNA processing. *Genes Dev.* **18**: 3016-3027.

Han, J., Lee, Y., Yeom, K.H., Nam, J.W., Heo, I., Rhee, J.K., Sohn, S.Y., Cho, Y., Zhang, B.T. and Kim, V.N. 2006. Molecular basis for the recognition of primary microRNAs by the Drosha-DGCR8 complex. *Cell* **125**: 887-901.

Hayashita, Y., Osada, H., Tatematsu, Y., Yamada, H., Yanagisawa, K., Tomida, S., Yatabe, Y., Kawahara, K., Sekido, Y. and Takahashi, T. 2005. A polycistronic microRNA cluster, miR-17-92, is overexpressed in human lung cancers and enhances cell proliferation. *Cancer Res.* **65**: 9628-9632.

He, L., Thomson, J.M., Hemann, M.T., Hernando-Monge, E., Mu, D., Goodson, S., Powers, S., Cordon-Cardo, C., Lowe, S.W., Hannon, G.J. et al. 2005. A microRNA polycistron as a potential human oncogene. *Nature* **435**: 828-833.

Hertel, J., Lindemeyer, M., Missal, K., Fried, C., Tanzer, A., Flamm, C., Hofacker, I.L., Stadler, P.F. and Students of Bioinformatics Computer Labs 2004 and 2005. 2006. The expansion of the metazoan microRNA repertoire. *BMC Genomics* **7**: 25.

Hutvagner, G., McLachlan, J., Pasquinelli, A.E., Balint, E., Tuschl, T. and Zamore, P.D. 2001. A cellular function for the RNA-interference enzyme Dicer in the maturation of the let-7 small temporal RNA. *Science* **293**: 834-838.

Hutvagner, G. and Zamore, P.D. 2002. A microRNA in a multiple-turnover RNAi enzyme complex. *Science* **297**: 2056-2060.

Ibanez-Ventoso, C., Vora, M. and Driscoll, M. 2008. Sequence relationships among C. elegans, D. melanogaster and human microRNAs highlight the extensive conservation of microRNAs in biology. *PLoS One* **3**: e2818.

Khvorova, A., Reynolds, A. and Jayasena, S.D. 2003. Functional siRNAs and miRNAs exhibit strand bias. *Cell* **115**: 209-216.

Kim, V.N. and Nam, J.W. 2006. Genomics of microRNA. *Trends Genet.* **22**: 165-173.

Klein, U., Lia, M., Crespo, M., Siegel, R., Shen, Q., Mo, T., Ambesi-Impiombato, A., Califano, A., Migliazza, A., Bhagat, G. et al. 2010. The DLEU2/miR-15a/16-1 cluster

controls B cell proliferation and its deletion leads to chronic lymphocytic leukemia. *Cancer. Cell.* **17**: 28-40.

Kluiver, J., Haralambieva, E., de Jong, D., Blokzijl, T., Jacobs, S., Kroesen, B.J., Poppema, S. and van den Berg, A. 2006. Lack of BIC and microRNA miR-155 expression in primary cases of Burkitt lymphoma. *Genes Chromosomes Cancer* **45**: 147-153.

Kluiver, J., Poppema, S., de Jong, D., Blokzijl, T., Harms, G., Jacobs, S., Kroesen, B.J. and van den Berg, A. 2005. BIC and miR-155 are highly expressed in Hodgkin, primary mediastinal and diffuse large B cell lymphomas. *J. Pathol.* **207**: 243-249.

Kluiver, J., van den Berg, A., de Jong, D., Blokzijl, T., Harms, G., Bouwman, E., Jacobs, S., Poppema, S. and Kroesen, B.J. 2007. Regulation of pri-microRNA BIC transcription and processing in Burkitt lymphoma. *Oncogene* **26**: 3769-3776.

Kozomara, A. and Griffiths-Jones, S. 2011. miRBase: integrating microRNA annotation and deep-sequencing data. *Nucleic Acids Res.* **39**: D152-7.

Kuppers, R. 2005. Mechanisms of B-cell lymphoma pathogenesis. *Nat. Rev. Cancer.* **5**: 251-262.

Kuppers, R., Klein, U., Hansmann, M.L. and Rajewsky, K. 1999. Cellular origin of human B-cell lymphomas. *N. Engl. J. Med.* **341**: 1520-1529.

Kuppers, R., Zhao, M., Hansmann, M.L. and Rajewsky, K. 1993. Tracing B cell development in human germinal centres by molecular analysis of single cells picked from histological sections. *EMBO J.* **12**: 4955-4967.

Ladanyi, M., Offit, K., Jhanwar, S.C., Filippa, D.A. and Chaganti, R.S. 1991. MYC rearrangement and translocations involving band 8q24 in diffuse large cell lymphomas. *Blood* **77**: 1057-1063.

Lagos-Quintana, M., Rauhut, R., Yalcin, A., Meyer, J., Lendeckel, W. and Tuschl, T. 2002. Identification of tissue-specific microRNAs from mouse. *Curr. Biol.* **12**: 735-739.

Landthaler, M., Yalcin, A. and Tuschl, T. 2004. The human DiGeorge syndrome critical region gene 8 and Its D. melanogaster homolog are required for miRNA biogenesis. *Curr. Biol.* **14**: 2162-2167.

Lee, R.C., Feinbaum, R.L. and Ambros, V. 1993. The C. elegans heterochronic gene lin-4 encodes small RNAs with antisense complementarity to lin-14. *Cell* **75**: 843-854.

Lee, Y., Ahn, C., Han, J., Choi, H., Kim, J., Yim, J., Lee, J., Provost, P., Radmark, O., Kim, S. et al. 2003. The nuclear RNase III Drosha initiates microRNA processing. *Nature* **425**: 415-419.

Lee, Y., Jeon, K., Lee, J.T., Kim, S. and Kim, V.N. 2002. MicroRNA maturation: stepwise processing and subcellular localization. *EMBO J.* **21**: 4663-4670.

Lee, Y., Kim, M., Han, J., Yeom, K.H., Lee, S., Baek, S.H. and Kim, V.N. 2004. MicroRNA genes are transcribed by RNA polymerase II. *EMBO J.* **23**: 4051-4060.

Lewis, B.P., Burge, C.B. and Bartel, D.P. 2005. Conserved seed pairing, often flanked by adenosines, indicates that thousands of human genes are microRNA targets. *Cell* **120**: 15-20.

Li, Y., Vecchiarelli-Federico, L.M., Li, Y.J., Egan, S.E., Spaner, D., Hough, M.R. and Ben-David, Y. 2012. The miR-17-92 cluster expands multipotent hematopoietic progenitors whereas imbalanced expression of its individual oncogenic miRNAs promotes leukemia in mice. *Blood* **119**: 4486-4498.

Liu, M., Duke, J.L., Richter, D.J., Vinuesa, C.G., Goodnow, C.C., Kleinstein, S.H. and Schatz, D.G. 2008. Two levels of protection for the B cell genome during somatic hypermutation. *Nature* **451**: 841-845.

Liu, Y.J., Arpin, C., de Bouteiller, O., Guret, C., Banchereau, J., Martinez-Valdez, H. and Lebecque, S. 1996. Sequential triggering of apoptosis, somatic mutation and isotype switch during germinal center development. *Semin. Immunol.* **8**: 169-177.

Lu, J., Getz, G., Miska, E.A., Alvarez-Saavedra, E., Lamb, J., Peck, D., Sweet-Cordero, A., Ebert, B.L., Mak, R.H., Ferrando, A.A. et al. 2005. MicroRNA expression profiles classify human cancers. *Nature* **435**: 834-838.

Lund, E., Guttinger, S., Calado, A., Dahlberg, J.E. and Kutay, U. 2004. Nuclear export of microRNA precursors. *Science* **303**: 95-98.

MacLennan, I.C. 1994. Germinal centers. *Annu. Rev. Immunol.* **12**: 117-139.

Matsumura, I., Tanaka, H. and Kanakura, Y. 2003. E2F1 and c-Myc in cell growth and death. *Cell. Cycle* **2**: 333-338.

Mayr, C., Hemann, M.T. and Bartel, D.P. 2007. Disrupting the pairing between let-7 and Hmga2 enhances oncogenic transformation. *Science* **315**: 1576-1579.

Medina, P.P., Nolde, M. and Slack, F.J. 2010. OncomiR addiction in an in vivo model of microRNA-21-induced pre-B-cell lymphoma. *Nature* **467**: 86-90.

Mourelatos, Z., Dostie, J., Paushkin, S., Sharma, A., Charroux, B., Abel, L., Rappsilber, J., Mann, M. and Dreyfuss, G. 2002. miRNPs: a novel class of ribonucleoproteins containing numerous microRNAs. *Genes Dev.* **16**: 720-728.

Mu, P., Han, Y.C., Betel, D., Yao, E., Squatrito, M., Ogrodowski, P., de Stanchina, E., D'Andrea, A., Sander, C. and Ventura, A. 2009. Genetic dissection of the miR-17~92 cluster of microRNAs in Myc-induced B-cell lymphomas. *Genes Dev.* **23**: 2806-2811.

O'Connell, R.M., Chaudhuri, A.A., Rao, D.S. and Baltimore, D. 2009. Inositol phosphatase SHIP1 is a primary target of miR-155. *Proc. Natl. Acad. Sci. U. S. A.* **106**: 7113-7118.

O'Connell, R.M., Rao, D.S., Chaudhuri, A.A., Boldin, M.P., Taganov, K.D., Nicoll, J., Paquette, R.L. and Baltimore, D. 2008. Sustained expression of microRNA-155 in hematopoietic stem cells causes a myeloproliferative disorder. *J. Exp. Med.* **205**: 585-594.

Olive, V., Bennett, M.J., Walker, J.C., Ma, C., Jiang, I., Cordon-Cardo, C., Li, Q.J., Lowe, S.W., Hannon, G.J. and He, L. 2009. miR-19 is a key oncogenic component of mir-17-92. *Genes Dev.* **23**: 2839-2849.

Ota, A., Tagawa, H., Karnan, S., Tsuzuki, S., Karpas, A., Kira, S., Yoshida, Y. and Seto, M. 2004. Identification and characterization of a novel gene, C13orf25, as a target for 13q31-q32 amplification in malignant lymphoma. *Cancer Res.* **64**: 3087-3095.

Pillai, R.S., Bhattacharyya, S.N. and Filipowicz, W. 2007. Repression of protein synthesis by miRNAs: how many mechanisms? *Trends Cell Biol.* **17**: 118-126.

Ramiro, A.R., Jankovic, M., Eisenreich, T., Difilippantonio, S., Chen-Kiang, S., Muramatsu, M., Honjo, T., Nussenzweig, A. and Nussenzweig, M.C. 2004. AID is required for c-myc/IgH chromosome translocations in vivo. *Cell* **118**: 431-438.

Reinhart, B.J., Slack, F.J., Basson, M., Pasquinelli, A.E., Bettinger, J.C., Rougvie, A.E., Horvitz, H.R. and Ruvkun, G. 2000. The 21-nucleotide let-7 RNA regulates developmental timing in Caenorhabditis elegans. *Nature* **403**: 901-906.

Rinaldi, A., Poretti, G., Kwee, I., Zucca, E., Catapano, C.V., Tibiletti, M.G. and Bertoni, F. 2007. Concomitant MYC and microRNA cluster miR-17-92 (C13orf25) amplification in human mantle cell lymphoma. *Leuk. Lymphoma* **48**: 410-412.

Rodriguez, A., Vigorito, E., Clare, S., Warren, M.V., Couttet, P., Soond, D.R., van Dongen, S., Grocock, R.J., Das, P.P., Miska, E.A. et al. 2007. Requirement of bic/microRNA-155 for normal immune function. *Science* **316**: 608-611.

Sampson, V.B., Rong, N.H., Han, J., Yang, Q., Aris, V., Soteropoulos, P., Petrelli, N.J., Dunn, S.P. and Krueger, L.J. 2007. MicroRNA let-7a down-regulates MYC and reverts MYC-induced growth in Burkitt lymphoma cells. *Cancer Res.* **67**: 9762-9770.

Sander, S., Calado, D.P., Srinivasan, L., Kochert, K., Zhang, B., Rosolowski, M., Rodig, S.J., Holzmann, K., Stilgenbauer, S., Siebert, R. et al. 2012. Synergy between PI3K Signaling and MYC in Burkitt Lymphomagenesis. *Cancer. Cell.* **22**: 167-179.

Sassen, S., Miska, E.A. and Caldas, C. 2008. MicroRNA: implications for cancer. *Virchows Arch.* **452**: 1-10.

Schwarz, D.S., Hutvagner, G., Du, T., Xu, Z., Aronin, N. and Zamore, P.D. 2003. Asymmetry in the assembly of the RNAi enzyme complex. *Cell* **115**: 199-208.

Tanzer, A. and Stadler, P.F. 2004. Molecular evolution of a microRNA cluster. *J. Mol. Biol.* **339**: 327-335.

Taub, R., Kirsch, I., Morton, C., Lenoir, G., Swan, D., Tronick, S., Aaronson, S. and Leder, P. 1982. Translocation of the c-myc gene into the immunoglobulin heavy chain locus in human Burkitt lymphoma and murine plasmacytoma cells. *Proc. Natl. Acad. Sci. U. S. A.* **79**: 7837-7841.

Thai, T.H., Calado, D.P., Casola, S., Ansel, K.M., Xiao, C., Xue, Y., Murphy, A., Frendewey, D., Valenzuela, D., Kutok, J.L. et al. 2007. Regulation of the germinal center response by microRNA-155. *Science* **316**: 604-608.

van den Berg, A., Kroesen, B.J., Kooistra, K., de Jong, D., Briggs, J., Blokzijl, T., Jacobs, S., Kluiver, J., Diepstra, A., Maggio, E. et al. 2003. High expression of B-cell receptor inducible gene BIC in all subtypes of Hodgkin lymphoma. *Genes Chromosomes Cancer* **37**: 20-28.

Ventura, A., Young, A.G., Winslow, M.M., Lintault, L., Meissner, A., Erkeland, S.J., Newman, J., Bronson, R.T., Crowley, D., Stone, J.R. et al. 2008. Targeted deletion reveals essential and overlapping functions of the miR-17 through 92 family of miRNA clusters. *Cell* **132**: 875-886.

Ye, B.H., Rao, P.H., Chaganti, R.S. and Dalla-Favera, R. 1993. Cloning of bcl-6, the locus involved in chromosome translocations affecting band 3q27 in B-cell lymphoma. *Cancer Res.* **53**: 2732-2735.

Yi, R., Qin, Y., Macara, I.G. and Cullen, B.R. 2003. Exportin-5 mediates the nuclear export of pre-microRNAs and short hairpin RNAs. *Genes Dev.* **17**: 3011-3016.

Zeng, Y. and Cullen, B.R. 2005. Efficient processing of primary microRNA hairpins by Drosha requires flanking nonstructured RNA sequences. *J. Biol. Chem.* **280**: 27595-27603.

CHAPTER 2

MicroRNAs, macrocontrol: Regulation of miRNA processing

Izabella Slezak-Prochazka, Selvi Durmus,
Bart-Jan Kroesen and Anke van den Berg

RNA. 2010 Jun;16(6):1087-95

ABSTRACT

MicroRNAs (miRNAs) are a set of small, non-protein-coding RNAs that regulate gene expression at the post-transcriptional level. Maturation of miRNAs comprises several regulated steps resulting in ~22-nucleotide single-stranded mature miRNAs. Regulation of miRNA expression can occur both at the transcriptional level and at the post-transcriptional level during miRNA processing. Recent studies have elucidated specific aspects of the well-regulated nature of miRNA processing involving various regulatory proteins, editing of miRNA transcripts, and cellular location. In addition, single nucleotide polymorphisms in miRNA genes can also affect the processing efficiency of primary miRNA transcripts. In this review we present an overview of the currently known regulatory pathways of miRNA processing and provide a basis to understand how aberrant miRNA processing may arise and may be involved in pathophysiological conditions such as cancer.

INTRODUCTION

MicroRNAs (miRNAs) are small (22-nucleotide [nt]) noncoding RNA molecules that are single-stranded in the functional form (Bartel 2004). Unlike their small size, they play an important role in the regulation of gene expression at the post-transcriptional level. After their discovery in Caenorhabditis elegans (Lee et al. 1993; Wightman et al. 1993), there have been a large number of studies identifying miRNAs in animals, plants, and viruses. Their importance was confirmed in several cellular processes like development, cell fate determination, proliferation, and apoptosis. Moreover, altered miRNA expression profiles have been demonstrated in a large number of pathological conditions, such as cancer, suggesting that miRNAs are involved in disordered cellular function, such as malignant transformation.

MiRNAs are located within introns and exons of protein coding genes or in intergenic regions (Kim and Nam 2006). They are transcribed as long primary miRNA (pri-miRNA) transcripts containing one or more hairpin structures. Each hairpin structure consists of a double-stranded stem and a terminal loop. In the nucleus, the primary miRNA is cleaved by the Microprocessor complex, which consists of Drosha and DGCR8 (Lee et al. 2003; Denli et al. 2004; Gregory et al. 2004; Han et al. 2004; Landthaler et al. 2004). This cleavage step results in an ~65-nt precursor miRNA (pre-miRNA), which is exported from the nucleus to the cytoplasm in association with Exportin-5 and RanGTP (Yi et al. 2003; Bohnsack et al. 2004; Lund et al. 2004) and cleaved by Dicer to an ~22-nt miRNA duplex (Grishok et al. 2001; Hutvagner et al. 2001). One of the two strands is assembled into the RNA-induced silencing complex (RISC) together with one of the Argonaute (Ago) proteins. RISC can bind to the 3'-untranslated region (UTR) of the target mRNA based on a partial miRNA–mRNA complementarity. This binding causes a translational inhibition and/or degradation of the target mRNA (Eulalio et al. 2008; Filipowicz et al. 2008). However, not all miRNAs are processed by this so-called canonical biogenesis pathway. Alternatively, miRNAs can be generated from short intronic hairpins called mirtrons that are spliced and debranched to mimic pre-miRNA (Okamura et al. 2007; Ruby et al. 2007).

Mirtrons bypass cleavage by Drosha, but nuclear export and further processing are common with the canonical miRNA processing pathway (Okamura et al. 2007; Ruby et al. 2007).

Biogenesis of miRNAs is tightly regulated resulting in characteristic miRNA expression patterns for different organisms, tissues, cell types, and developmental stages. It is known that transcription of miRNA genes can be regulated by epigenetic factors (Scott et al. 2006; Lehmann et al. 2007; Lujambio et al. 2007) or transcription factors (Xi et al. 2006; He et al. 2007; mature miRNA expression levels clearly indicate that the level of mature miRNAs can also be regulated at the level of miRNA processing. This review focuses on the mechanisms and factors that regulate miRNA processing, for example, regulatory proteins, cellular localization, and genetic variation.

MECHANISMS FOR REGULATING MICRORNA PROCESSING

Processing of miRNAs can be regulated at multiple steps and leads to either elevated or decreased miRNA levels. Altered miRNA levels may be caused by regulatory proteins that influence miRNA processing, acquired variations in the miRNA transcript, and by changes in the nuclear export efficiency. In addition to these regulatory mechanisms, single nucleotide polymorphisms (SNPs) can also have a pronounced effect on the efficiency of the miRNA processing machinery.

Regulatory proteins

Recently, a number of proteins that regulate miRNA processing have been described as key elements in defining the unique expression patterns of miRNAs in different cell types, tissues, or in pathological conditions. These proteins can be subdivided into three groups, i.e., Drosha binding/associated proteins, Dicer binding proteins, and proteins that bind to the terminal loop of the pri- and/or pre-miRNAs.

Drosha binding/associated proteins

The Microprocessor complex consisting of Drosha and DGCR8 is sufficient to process pri-miRNA to pre-miRNA (Fig. 1A). However, Drosha was shown to be a component of a larger complex containing DEAD-box RNA helicases p68 (DDX5), p72 (DDX17), nuclear factor (NF) 90, and NF45 (Gregory et al. 2004). The p68/p72 and NF90/NF45 complexes have been shown to alter the miRNA processing efficiency for specific miRNAs (Fukuda et al. 2007; Davis et al. 2008; Sakamoto et al. 2009; Suzuki et al. 2009; Yamagata et al. 2009). Specifically, it has been shown that endogenous p68/p72 facilitate Drosha processing of a subset of pri-miRNAs based on reduced mature miRNA levels in both p72- and p68-helicase-deficient mouse embryos (Fukuda et al. 2007). Several studies showed that interaction of p68/p72 with other proteins also alters processing of specific primary miRNAs. Interaction of p68 with SMAD facilitates the processing of pri-miR-21 (Fig. 1B; Davis et al. 2008). The interaction of p68 with SMAD was induced by transforming growth factor β (TGF-β) and bone morphogenetic proteins (BMPs). Similarly, wild-type p53 has been shown to associate with p68 and enhance processing of several primary miRNAs by Drosha, including pri-miRNA of miR-16-1, miR-143, and miR-145, in response to DNA damage (Fig. 1C; Suzuki et al. 2009). Moreover, wild-type p53 positively regulates Drosha-mediated processing by promoting recruitment of Drosha complex to the target pri-miRNAs, whereas mutant p53 hinders assembly of the Drosha complex (Suzuki et al. 2009). Drosha-mediated processing can be inhibited by p68/p72-dependent mechanisms upon stimulation of estrogen receptor alpha (ERα) (Fig. 1D; Yamagata et al. 2009). This mechanism caused obstructed processing of a set of pri-miRNAs including miR-16, miR-125a, miR-143, miR-145, and miR-195 (Yamagata et al. 2009). Together these studies show that the p68/p72 complex is an important mediator of miRNA processing regulation and can direct Drosha toward either reduced or enhanced processing of specific miRNAs. The result of the interaction between Drosha, p68, and the target pri-miRNA depends on proteins interacting with p68 like SMAD, p53, or ERα. This indicates that the p68/p72-dependent mechanism is sensitive to cellular context.

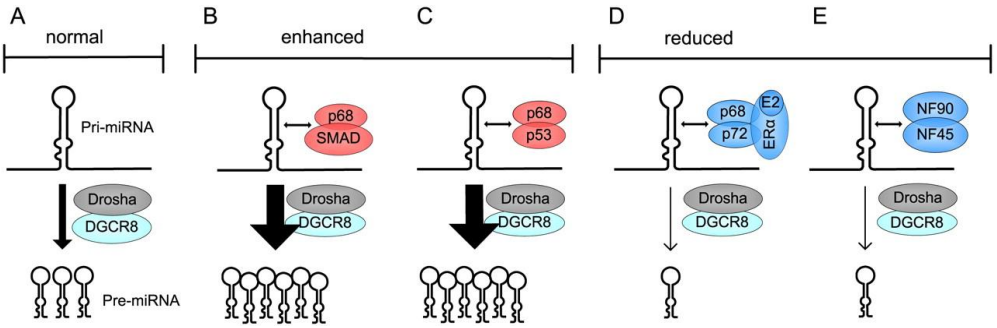

FIGURE 1. MicroRNA processing regulation by Drosha binding or Drosha-associated proteins. (A) Primary miRNA transcript (Pri-miRNA) is processed by Drosha/DGCR8 complex to precursor miRNA (Pre-miRNA). (B) SMAD associates with pri-miR-21, p68, and Drosha/DGCR8 complex to enhance pri-miR-21 processing. (C) Association of p53 with pri-miR-16-1 and pri-miR-143, p68, and Drosha/DGCR8 enhances pri-miR-16-1 and pri-miR-143 processing. (D) p68/p72 complex mediates inhibition of pri-miR-16, pri-miR-125a, pri-miR-143, pri-miR-145, and pri-miR-195 upon stimulation of estrogen receptor α (ERα) by estradiol (E2). (E) Nuclear factor (NF) 90/45 complex inhibits Drosha/DGCR8 processing by binding to stem/loop fragment of pri-miR-21, pri-miR-15~16-1, and pri-let-7a-1.

Two other members of the large Drosha-containing complex identified by Gregory et al. (2004), i.e., NF90 and NF45, were also shown to be involved in the regulation of miRNA processing (Fig. 1E). However, the interaction between Drosha and NF90/NF45 has not been confirmed for the endogenous Drosha–DGCR8 complex (Sakamoto et al. 2009). Nevertheless, overexpression of NF90/NF45 in 293T cells caused accumulation of pri-let-7a-1, pri-miR-21, and pri-miR-15a~16-1, without affecting the mature miRNA levels (Sakamoto et al. 2009). This suggests that the decreased processing efficiency induced by NF90/NF45 was compensated by other factors. Depletion of NF90 resulted in decreased pri-let-7a-1 levels and increased mature let-7a levels (Sakamoto et al. 2009). The higher binding affinity of NF90/NF45 to pri-let-7a-1, as compared to DGCR8 *in vitro*, suggested that the reduced miRNA processing efficiency was caused by reducing the accessibility for Drosha–DGCR8 (Sakamoto et al. 2009).

Current literature shows that regulatory proteins are a dominant factor in the regulation of Drosha-mediated pri-miRNA processing. Moreover, various signaling pathways enhance or reduce the efficiency of this step. It is likely that more Drosha-associated proteins regulate miRNA processing, and, as such, the

balance between positive and negative regulators may determine the efficiency of miRNA processing.

Dicer binding proteins

Dicer interacts with Tar RNA binding protein (TRBP) and protein activator of PKR (PACT) and one of the Ago (1–4) proteins, mainly Ago2 (Chendrimada et al. 2005; Haase et al. 2005; Lee et al. 2006). TRBP and PACT facilitate RISC assembly, and they are not essential for miRNA processing (Haase et al. 2005; Lee et al. 2006). However, phosphorylated TRBP stabilized the Dicer-containing complex (Paroo et al. 2009). Expression of phospho-mimic TRBP resulted in increased levels of growth-promoting miRNAs like miR-17, miR-20a, and miR-92 and decreased the level of the growth-inhibitory miRNA let-7a (Paroo et al. 2009). However, let-7a level is affected indirectly via a mechanism that may involve other proteins like Lin28 (Paroo et al. 2009). TRBP phosphorylation was mediated by the mitogen-activated protein kinase (MAPK) signaling pathway. Therefore, alteration of miRNA processing by ERK may result in a pro-growth phenotype.

Ago proteins are important for proper miRNA function. However, they can also influence miRNA expression. Ectopically expressed Ago proteins (Ago1–4) enhanced expression of some miRNAs including miR-215, miR-17-5p, miR-23b, and miR-92 (Diederichs and Haber 2007). Additionally, Ago2, which has intrinsic endonuclease activity in mammals (Song et al. 2004), induced cleavage of pre-miRNAs leading to an alternative processing intermediate with cleaved arms of the hairpin (Diederichs and Haber 2007). This intermediate did not change processing to mature miRNA, but may facilitate miRNA duplex dissociation and formation of RISC complex. Dicer-associated proteins, especially TRBP, clearly play a role in the regulation of miRNA processing. However, the mechanisms and specificity of this regulation remain unknown.

Terminal loop binding proteins

Processing of primary and precursor miRNAs (Fig. 2A) can be regulated by terminal loop binding proteins resulting in either reduced or enhanced

processing efficiency. Members of the let-7 family were shown to be post-transcriptionally regulated during differentiation of human embryonic stem cells (Suh et al. 2004), development of mice (Thomson et al. 2006), and neural differentiation of embryocarcinoma cells (Wulczyn et al. 2007). In all cases, Lin28, the developmentally regulated RNA binding protein, was shown to inhibit pri-let-7 processing (Fig. 2B; Newman et al. 2008; Piskounova et al. 2008; Rybak et al. 2008; Viswanathan et al. 2008). Lin28 interacted with the terminal loop region via a conserved sequence, inhibiting processing of pri- and pre-miRNA (Newman et al. 2008; Piskounova et al. 2008; Rybak et al. 2008; Viswanathan et al. 2008). Suppression of let-7 in neural stem cells led to upregulation of Lin28 and failure of pre-let-7 processing (Rybak et al. 2008). These results suggest a feedback loop between let-7 and Lin28. Lin28 causes terminal uridylation of pre-let-7 in the cytoplasm (Heo et al. 2008) leading to inhibition of Dicer processing and inducing guidance of pre-let-7 to a degradation pathway (Fig. 2B). A terminal uridylyl transferase 4 (TUTase 4, TUT4) has been shown to be responsible for the pre-let-7 uridylation (Hagan et al. 2009; Heo et al. 2009; Lehrbach et al. 2009). Binding of TUT4 to pre-let-7 is dependent on the presence of Lin28, confirming that Lin28 is necessary for recruiting TUT4.

The RNA binding protein heterogeneous nuclear ribonucleoprotein A1 (hnRNP A1) has been reported to facilitate processing of miR-18a, a member of the miR17~92 cluster (Fig. 2C; Guil and Caceres 2007). Knockdown of hnRNP A1 resulted in inhibition of pri- to pre-miR-18a processing, but did not affect other members of this cluster. This might in part explain variations in levels of the individual mature miRNA members of this cluster (Yu et al. 2006; Lu et al. 2007; Mendell 2008). hnRNP A1 binds to both the terminal loop and a region in the stem of pri-miR-18a (Michlewski et al. 2008), causing relaxation of the stem and facilitating Drosha/DGCR8 processing. The possible effect of hnRNP A1 binding on the Dicer processing step has not been investigated for miR-18a. hnRNP A1 also binds to the terminal loops of pri-let-7a-1 and pri-miR-101-1, indicating that this protein might also regulate processing of other pri-miRNAs.

This is consistent with the more general RNA binding properties of hnRNP A1 (Mayeda and Krainer 1992; Martinez-Contreras et al. 2006).

Another RNA binding protein proven to be involved in miRNA processing is the KH-type splicing regulatory protein (KSRP). KSRP is known as a key mediator of AU-rich element (ARE)-directed mRNA decay that facilitates recruitment of the degradation machinery to ARE-containing mRNAs (Gherzi et al. 2004; Garcıa-Mayoral et al. 2007). KSRP was shown to be a component of both Drosha and Dicer complexes and promoted biogenesis of a cohort of miRNAs including let-7a, miR-21, and miR-16 (Fig. 2D; Trabucchi et al. 2009). KSRP binds to the terminal loop of its target primary and/or precursor miRNAs and induces processing by Drosha and Dicer complexes through protein–protein interactions (Trabucchi et al. 2009). Moreover, KSRP mediates induction of miR-

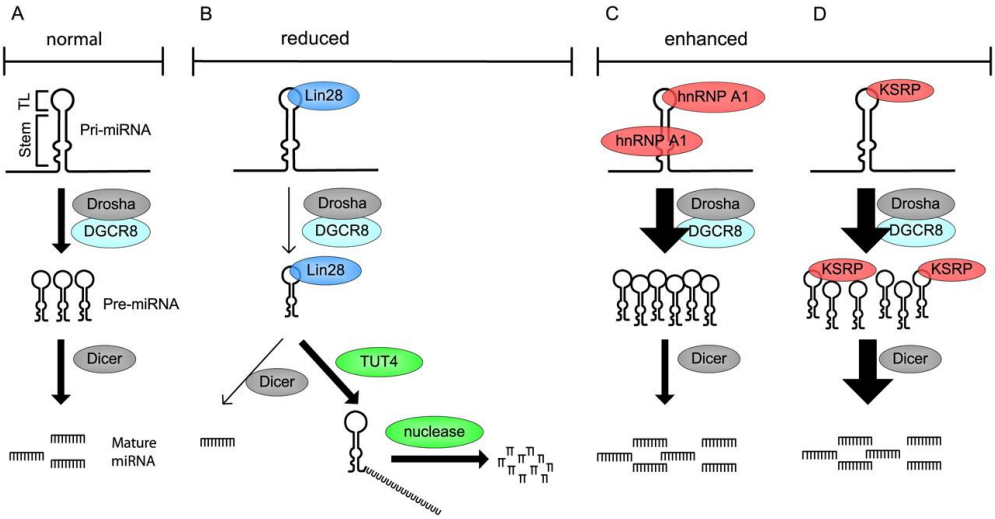

FIGURE 2. MicroRNA processing regulation by terminal loop binding proteins. (A) Primary miRNA transcript (pri-miRNA) is processed by Drosha/DGCR8 complex to precursor miRNA (pre-miRNA) and by Dicer to mature miRNA. Stem and terminal loop (TL) regions are assigned within pri-miRNA. (B) Lin28 protein binds to the terminal loop of pri- and pre-miRNAs from the let-7 family and impairs processing by reducing Drosha and Dicer cleavage and causing uridylation of pre-miR by terminal uridylyl transferase 4 (TUT4) leading to degradation of pre-miR by an unidentified nuclease. (C) Heterogeneous nuclear ribonucleoprotein (hnRNP) A1 binds to the terminal loop and stem of pri-miR-18a and facilitates its processing by Drosha. (D) KH-type splicing regulatory protein (KSRP) binds to the terminal loop of a set of pri- and pre-miRNAs including let-7a, miR-20, miR-26b, miR-106a, miR-21, miR-16, and enhances both Drosha/DGCR8 and Dicer processing.

155 processing in murine macrophages upon LPS stimulation that is also achieved by binding to the terminal loop (Ruggiero et al. 2009).

Conservation of terminal loop sequences across vertebrate species can be found in ~14% (74 out of 533) of the miRNAs indicating that the loops of these miRNAs are functionally important (Michlewski et al. 2008). To analyze the relevance of these conserved terminal loop sequences, Michlewski et al. (2008) showed that oligonucleotides complementary to the sequence of conserved terminal loops abolished the *in vitro* processing of pri-miR-18a, pri-miR-31, pri-miR-101-1, pri-miR-379, and pri-let-7a-1. Pri-miRNAs without conserved loops (pri-miR-16-1, pri-miR-27a) were not affected by antisense loop oligo's (Michlewski et al. 2008).

These studies clearly demonstrate that terminal loop binding proteins play an important role in the regulation of miRNA processing. Therefore, it is highly likely that other RNA binding proteins may also be involved in the regulation of processing of individual miRNAs.

Cellular location

Exportin-5 mediates the nuclear export of pre-miRNAs to the cytoplasm and protects pre-miRNAs from digestion (Bohnsack et al. 2004; Lund et al. 2004). The length of the double-stranded stem and presence of 3' overhangs but not the sequence or the loop structure are important for proper recognition of pre-miRNAs by Exportin-5 (Lund et al. 2004; Zeng and Cullen 2004).

A blockade in the transport of pre-miRNAs from nucleus to cytoplasm was suggested to explain the high levels of precursor and lack of mature miR-128a, miR-105, and miR-31 in some cancer cell lines. This was supported by the predominant nuclear localization of primary/precursors detected by in situ RT-PCR (Lee et al. 2008). A debatable example for premature nuclear export is *BIC* (pri-miR-155) (van den Berg et al. 2003; Eis et al. 2005; Kluiver et al. 2005). RNA *in situ* hybridization (ISH) using a probe complementary to the 3' part of exon 3 revealed a strong nuclear staining in various lymphoma subtypes and in normal B-cells. This exon contains the stem–loop region of miR-155, indicating an appropriate location. Eis at al. (2005) showed a cytoplasmic location of

spliced *BIC* transcripts and a nuclear location of the unspliced *BIC* transcript in two lymphoma cell lines by RT-PCR of RNA isolated from purified nuclear and cytoplasmic fractions. These data might indicate that the unspliced *BIC* transcript serves as a source for miR-155. However, this does not explain the specific nuclear localization for *BIC* using RNA-ISH. Since both cell lines tested by Eis at al. (2005) showed a high level of miR-155, it remains unclear if premature export of spliced *BIC* transcripts explains the low miR-155 levels observed in Burkitt lymphoma cell lines after induction of *BIC* (Kluiver et al. 2007). Based on current literature, the importance of nuclear export in miRNA processing regulation remains uncertain.

Sequence alterations in DNA/RNA

Alteration of miRNA processing can be caused not only by changes in the processing machinery, but also due to sequence alterations in the miRNA genes or RNA transcripts. In 15% of patients with chronic lymphocytic leukemia (CLL), but not in healthy controls, mutations were found in five of 42 analyzed miRNA genes (Calin et al. 2005). Moreover, a germline mutation located in the miR-15a~16-1 genomic DNA, 7 bp downstream from pre-miR-16-1, resulted in lower levels of the mature miRNAs (Calin et al. 2005). However, it remains to be established whether this effect is caused by aberrant transcription or processing.

Besides mutations, alterations at the miRNA transcript level caused by RNA editing can affect miRNA processing (Fig. 3). RNA editing is conducted by adenosine deaminases acting on RNA (ADARs) that convert adenosine (A) to inosine (I) in dsRNA structures (Bass 2002; Maas et al. 2003; Amariglio and Rechavi 2007). The primary transcript of miR-22 was the first miRNA shown to undergo A-to-I editing at positions that surround the Drosha cleavage site (Luciano et al. 2004). However, the physiological role of miR-22 editing has not been revealed yet. Another primary miRNA found to be edited by ADAR1 and ADAR2 isoforms *in vitro* is pri-miR-142 (Yang et al. 2006b). A-to-I editing of pri-miR-142 resulted in reduced Drosha processing in HEK293 cells. However, no accumulation of edited pri-miR-142 was observed in the nucleus. Edited pri-miR-142 was shown to be cleaved *in vitro* by Tudor-SN (Yang et al. 2006b), a

component of RISC, with ribonuclease activity specific to inosine-containing dsRNAs (Scadden 2005). However, the relevance of Tudor-SN for *in vivo* degradation of edited pri-miRNAs is still uncertain. ADAR editing of the pri-miRNA can also inhibit Dicer cleavage (Kawahara et al. 2007a). Editing of pri-miR-151 by ADAR1 did not affect pri-miRNA to pre-miRNA processing but caused inhibition of pre- to mature miR-151 processing as proven by accumulation of edited pre-miR-151. The inhibition at the Dicer cleavage step was investigated using synthetic pre-miR-151 *in vitro*. Although there was efficient binding of the Dicer–TRBP complex to pre-miR-151, the cleavage of pre- and release of mature form was blocked. Analysis of editing sites revealed that only a small proportion of the pri-miR-151 transcripts were edited at a specific site. Moreover, high frequency of pre-miR-151 editing has been shown *in vitro*. Therefore, A-to-I editing may occur also after processing of pri- to pre-miR-151 (Kawahara et al. 2007a). Moreover, ADAR editing may interfere with miRNA function by changing the ''seed'' region, which is crucial for target gene binding. The edited isoform of

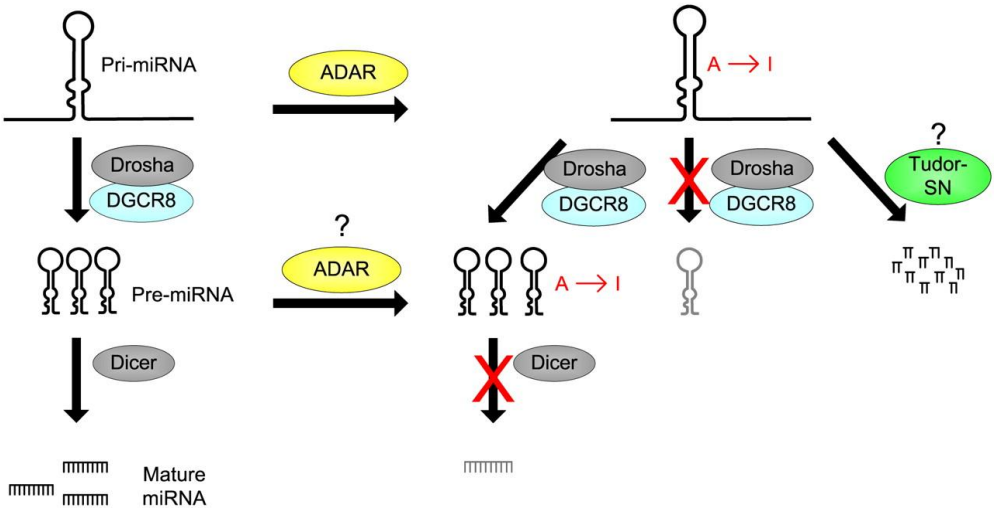

FIGURE 3. Regulation of miRNA processing by ADAR editing. Adenosine deaminases acting on RNA (ADARs) can convert adenosine to inosine in pri-miRNA; conversion of pre-miRNA is also possible, but has not been proven. ADAR editing can lead to blockade in Drosha cleavage of pri-miR-142 and degradation of edited pri-miR-142 by a ribonuclease Tudor-SN. ADAR editing can also block Dicer processing of pri-miR-151 causing accumulation of edited pre-miR-151.

miR-376 inhibited a different set of genes than the normal form supporting this concept (Kawahara et al. 2007b).

Since ADARs are predominantly nuclear enzymes, their targets are most likely pri-miRNAs and pre-miRNAs before nuclear export. However, some ADAR isoforms shuttle in and out of the nucleus (Desterro et al. 2003) and may edit pre-miRNA in the cytoplasm (Kawahara et al. 2007a). Although it is obvious that ADAR editing is a regulated event, there is not much known about the relevance of ADAR editing and the fate of edited miRNAs.

Single nucleotide polymorphisms

Polymorphisms in a miRNA gene may alter miRNA processing by changing the stem–loop structure. Although this is not an active processing regulation mechanism, it is evident that SNPs do alter the processing efficiency (Fig. 4). The first study that identified SNPs in miRNA precursors was performed by Iwai and Naraba (2005). However, no effect was observed for the processing efficiency of the two alleles of pre-miR-30c-2. The other nine SNPs that were identified in this study have not been tested (Iwai and Naraba 2005). Duan et al. (2007) systematically identified 323 SNPs that were associated with 227 human miRNA genes. Twelve of these SNPs were found in miRNA precursor sequences, and one SNP was located in the miR-125a seed sequence. Transfection of 293T cells with vectors expressing one of the two miR-125a precursor variants revealed that only one of the variants could be processed into mature miRNA. The blockade of the other allele occurred at the pri- to pre-miR-125a processing step (Duan et al. 2007). Difference in Drosha/DGCR8 processing was also proven for the two alleles of miR-146a (rs2910164), miR-502, miR-510, miR-890, and miR-892b (Jazdzewski et al. 2008; Sun et al. 2009). Possibly, the SNP affects the binding efficiency of the Drosha/DGCR8 complex. The T/G SNP in miR-934 altered processing efficiency, strand preference, and the mature miRNA sequence (Sun et al. 2009). In human lung cancer tissue, similar pre-miR-196a levels were observed for both alleles of the C/T SNP (rs11614913), whereas a marked difference was observed for the mature miR-196a levels, indicating an alteration in the pre- to mature miRNA processing step (Hu et al. 2008). This

suggests interference with the nuclear export or the Dicer processing step of pre-miR-196a by the SNP. Together, these studies demonstrate that SNPs in miRNA genes can significantly affect miRNA processing and in some cases also miRNA function.

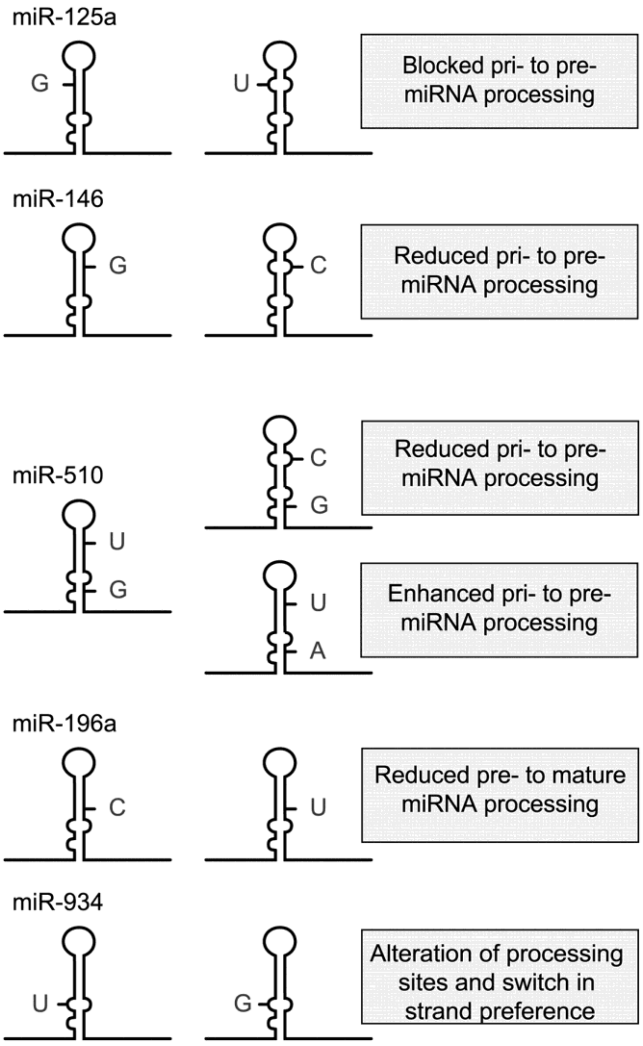

FIGURE 4. Influence of SNPs on miRNA processing. SNP variants of miR-125a, miR-146a, miR-510, miR-196a, and miR-934 are processed differently due to changes in a stem structure or processing sites. Major alleles are situated on the left side; minor alleles on the right.

CONCLUDING REMARKS

Recent studies have shown that miRNA biogenesis involves a number of tightly regulated processing steps that provide an important regulatory mechanism to define cellular levels of specific miRNAs. Therefore, biogenesis of miRNAs should not be regarded as a linear, unified mechanism. Based on current studies, Drosha, Dicer, and terminal loop binding proteins are the main factors involved in miRNA processing regulation. Cellular localization and ADAR editing influence processing of certain miRNAs, but their overall impact seems to be limited.

It is evident that proteins known to regulate transcription (p53, SMADs) or mRNA stability (KSRP) can also influence miRNA processing efficiency and therefore have the ability to control cellular levels of miRNAs. In some cases, complex networks have been reported to regulate processing of specific miRNAs; i.e., processing of miR-16, miR-143, and miR-145 is facilitated by p53 and inhibited by ERα in a p68/p72-dependent mechanism, and let-7 processing is negatively regulated by Lin28 and positively by KSRP. The terminal loop was shown to be an important target structure for regulation of miRNA expression by binding to activators and/or inhibitors of the miRNA processing machinery. This form of regulation may facilitate a much faster response to cellular changes as compared to the transcriptional control of miRNA genes. Moreover, the change in expression of one miRNA leads to differential expression of many miRNA target genes and may provide not only a quick but also a broad response to various stimuli.

Although knowledge about regulatory proteins is expanding rapidly, future studies should focus on identifying additional regulatory proteins. Human homologs of proteins regulating miRNA processing in plants, i.e., SERRATE and cap binding proteins CBP80/CBP20 (Lobbes et al. 2006; Yang et al. 2006a; Kim et al. 2008; Laubinger et al. 2008) need to be studied to define possible parallel regulatory functions in the processing of miRNA.

It is evident that several mechanisms regulate efficiency of miRNA processing. Nevertheless, for some miRNAs, inconsistencies between primary, precursor, and mature miRNA have been observed in certain normal or cancer

cells. The mechanisms for these inconsistencies (Table 1) are still unknown. For instance, no specific mechanism has been related to the tissue-specific expression levels of mature, but not precursor, miR-138 or miR-128 (Table 1; Obernosterer et al. 2006; Lee et al. 2008). An overall decrease of miRNA expression has been observed in many types of cancer as compared to their normal counterparts, and the underlying mechanisms remain unknown (Lu et al. 2005; Chen and Stallings 2007; Ozen et al. 2008). Inconsistencies between pri- and mature miRNAs are most obvious for the so-called polycistronic or miRNA clusters and indicate a miRNA-specific regulation. Based on current knowledge, it seems likely that the currently known mechanisms that regulate miRNA processing are, at least partially, involved in the deregulated miRNA expression levels in cancer. However, detailed comparisons between the regulations of miRNA processing in cancer cells as compared to their normal counterparts have not been performed. Elucidation of putative differences between normal and cancer cells and manipulation of these regulatory processes might provide a novel approach to restore a normal miRNA profile in cancer cells.

TABLE 1. miRNAs that may undergo processing regulation by a currently unknown mechanism

Altered miRNA[a]	Compared tissues or cells	Inconsistency between	Reference
miR-7↓	Glioblastoma/normal brain	Primary/precursor and mature	Kefas et al. 2008
miR-128↑	Brain, skeletal muscle/other tissues	Primary, precursor/mature	Lee et al. 2008
miR-138↑	Brain, neuroblastoma/other tissues	Precursor/mature	Obernosterer et al. 2006
miR-143↓ miR-145↓	Colorectal adenocarcinoma/normal mucosa	Precursor/mature	Michael et al. 2003
miR-155↓	Burkitt lymphoma with elevated pri-miR-155/other cells	Primary/mature	Kluiver et al. 2007
miR-206↓	Mouse myoblast cells with elevated pri-miR-206/other cells	Primary/mature	Sato et al. 2009

[a]Arrows indicate difference in miRNA levels between compared tissues or cells.

Undoubtedly, many factors regulating the cellular miRNA levels are still unknown. Further unraveling of the mechanisms responsible for regulation of the miRNA processing machinery will be an important step in elucidating the pathophysiological significance of miRNAs in malignancies and open up new venues for treatment.

REFERENCES

Amariglio N, Rechavi G. 2007. A-to-I RNA editing: a new regulatory mechanism of global gene expression. *Blood Cells Mol* **39**: 151-155.

Bartel DP. 2004. MicroRNAs: genomics, biogenesis, mechanism, and function. *Cell* **116**: 281-297.

Bass BL. 2002. RNA editing by adenosine deaminases that act on RNA. *Annu Rev Biochem* **71**: 817-846.

Bohnsack MT, Czaplinski K, Gorlich D. 2004. Exportin 5 is a RanGTP-dependent dsRNAbinding protein that mediates nuclear export of pre-miRNAs. *RNA* **10**: 185-191.

Calin GA, Ferracin M, Cimmino A, Di Leva G, Shimizu M, Wojcik SE, Iorio MV, Visone R,Sever NI, Fabbri M, et al. 2005. A MicroRNA signature associated with prognosis and progression in chronic lymphocytic leukemia. *N Engl J Med* **353**: 1793-1801.

Chen Y, Stallings RL. 2007. Differential patterns of microRNA expression in neuroblastomaare correlated with prognosis, differentiation, and apoptosis. *Cancer Res* **67**: 976–983.

Chendrimada TP, Gregory RI, Kumaraswamy E, Norman J, Cooch N, Nishikura K, Shiekhattar R. 2005. TRBP recruits the Dicer complex to Ago2 for microRNA processing and gene silencing. *Nature* **436:** 740–744.

Davis BN, Hilyard AC, Lagna G, Hata A. 2008. SMAD proteins control DROSHA-mediated microRNA maturation. *Nature* **454**: 56-61.

Denli AM, Tops BB, Plasterk RH, Ketting RF, Hannon GJ. 2004. Processing of primary microRNAs by Microprocessor complex. *Nature* **432**: 231-235.

Desterro JM, Keegan LP, Lafarga M, Berciano MT, O'Connell M, Carmo-Fonseca M. 2003.Dynamic association of RNA-editing enzymes with the nucleolus. *J Cell Sci* **116**: 1805-1818.

Diederichs S, Haber DA. 2007. Dual role for argonautes in microRNA processing and posttranscriptional regulation of microRNA expression. *Cell* **131**: 1097-1108.

Duan R, Pak C, Jin P. 2007. Single nucleotide polymorphism associated with mature miR-125a alters the processing of pri-miRNA. *Hum Mol Genet* **16**: 1124-1131.

Eis PS, Tam W, Sun L, Chadburn A, Li Z, Gomez MF, Lund E, Dahlberg JE. 2005. Accumulation of miR-155 and BIC RNA in human B cell lymphomas. *Proc Natl Acad Sci U S A* **102**: 3627-3632.

Eulalio A, Huntzinger E, Izaurralde E. 2008. Getting to the root of miRNA-mediated genesilencing. *Cell* **132**: 9-14.

Filipowicz W, Bhattacharyya SN, Sonenberg N. 2008. Mechanisms of post-transcriptional regulation by microRNAs: are the answers in sight? *Nat Rev Gene* **9**: 102-114.

Fukuda T, Yamagata K, Fujiyama S, Matsumoto T, Koshida I, Yoshimura K, Mihara M, Naitou M, Endoh H, Nakamura T, et al. 2007. DEAD-box RNA helicase subunits of the

Drosha complex are required for processing of rRNA and a subset of microRNAs. *Nat Cell Biol* **9**: 604-611.

García-Mayoral MF, Hollingworth D, Masino L, Díaz-Moreno I, Kelly G, Gherzi R, Chou CF, Chen CY, Ramos A. 2007. The structure of the C-terminal KH domains of KSRP reveals a noncanonical motif important for mRNA degradation. *Structure* **15**: 485-498.

Gherzi R, Lee KY, Briata P, Wegmüller D, Moroni C, Karin M, Chen CY. 2004. A KH domain RNA binding protein, KSRP, promotes ARE-directed mRNA turnover by recruiting the degradation machinery. *Mol Cell* **14**: 571-583.

Gregory RI, Yan KP, Amuthan G, Chendrimada T, Doratotaj B, Cooch N, Shiekhattar R. 2004. The Microprocessor complex mediates the genesis of MicroRNAs. *Nature* **432**: 235-240.

Grishok A, Pasquinelli AE, Conte D, Li N, Parrish S, Ha I, Baillie DL, Fire A, Ruvkun G, Mello CC. 2001. Genes and mechanisms related to RNA interference regulate expression of the small temporal RNAs that control C. elegans developmental timing. *Cell* **106**: 23-34.

Guil S, Cáceres JF. 2007. The multifunctional RNA-binding protein hnRNP-A1 is required for processing of miR-18a. *Nat Struct Mol Biol* **14**: 591-596.

Hagan JP, Piskounova E, Gregory RI. 2009. Lin28 recruits the TUTase Zcchc11 to inhibit let-7 maturation in mouse embryonic stem cells. *Nat Struct Mol Biol* **16**:1021-1025.

Han J, Lee Y, Yeom KH, Kim YK, Jin H, Kim VN. 2004. The Drosha-DGCR8 complex in primary microRNA processing. *Genes Dev* **18**: 3016-3027.

Haase AD, Jaskiewicz L, Zhang H, Lainé S, Sack R, Gatignol A, Filipowicz W. 2005. TRBP, a regulator of cellular PKR and HIV-1 virus expression, interacts with Dicer and functions in RNA silencing. *EMBO Rep* **6**: 961-967.

He L, He X, Lim LP, de Stanchina E, Xuan Z, Liang Y, Xue W, Zender L, Magnus J, Ridzon D, et al. 2007. A microRNA component of the p53 tumour suppressor network. *Nature* **447**: 1130–1134.

Heo I, Joo C, Cho J, Ha M, Han J, Kim VN. 2008. Lin28 mediates the terminal uridylation of let-7 precursor MicroRNA. *Mol Cell* **32**: 276-284.

Heo I, Joo C, Kim YK, Ha M, Yoon MJ, Cho J, Yeom KH, Han J, Kim VN. 2009. TUT4 in concert with Lin28 suppresses microRNA biogenesis through pre-microRNA uridylation. *Cell* **138**: 696-708.

Hu Z, Chen J, Tian T, Zhou X, Gu H, Xu L, Zeng Y, Miao R, Jin G, Ma H, Chen Y, Shen H. 2008. Genetic variants of miRNA sequences and non-small cell lung cancer survival. *J Clin Invest* **118**: 2600-2608.

Hutvagner G, McLachlan J, Pasquinelli AE, Balint E, Tuschl T, Zamore PD. 2001. A cellular function for the RNAinterference enzyme Dicer in the maturation of the let-7 small temporal RNA. *Science* **293**: 834–838.

Iwai N, Naraba H. 2005. Polymorphisms in human pre-miRNAs. *Biochem Biophys Res Commun* **331**: 1439-1444.

Jazdzewski K, Murray EL, Franssila K, Jarzab B, Schoenberg DR, de la Chapelle A. 2008. Common SNP in pre-miR-146a decreases mature miR expression and predisposes to papillary thyroid carcinoma. *Proc Natl Acad Sci U S A* **105**: 7269-7274.

Kawahara Y, Zinshteyn B, Chendrimada T P, Shiekhattar R, Nishikura K. 2007a. RNA editing of the microRNA-151 precursor blocks cleavage by the Dicer-TRBP complex. *EMBO Rep* **8**: 763-769.

Kawahara Y, Zinshteyn B, Sethupathy P, Iizasa H, Hatzigeorgiou AG, Nishikura K. 2007b. Redirection of silencing targets by Adenosine-to-Inosine editing of miRNAs. *Science* **315**: 1137-1140

Kefas B, Godlewski J, Comeau L, Li Y, Abounader R, Hawkinson M, Lee J, Fine H, Chiocca AE, Lawler S, Purow B. 2008. microRNA-7 Inhibits the Epidermal Growth Factor Receptor and the Akt Pathway and Is Down-regulated in Glioblastoma. *Cancer Res* **68**: 3566-3572.

Kim S, Yang JY, Xu J, Jang IC, Prigge MJ, Chua NH. 2008. Two CAP BINDING PROTEINS CBP20 and CBP80 are involved in processing primary microRNAs. *Plant Cell Physiol* **49**: 1634-1644.

Kim VN, Nam JW. 2006. Genomics of microRNA. *Trends Genet* **22:** 165-173.

Kluiver J, Poppema S, de Jong D, Blokzijl T, Harms G, Jacobs S, Kroesen BJ, van den Berg A. 2005. BIC and miR-155 are highly expressed in Hodgkin, primary mediastinal and diffuse large B cell lymphomas. *J Pathol* **207**: 243–249.

Kluiver J, van den Berg A, de Jong D, Blokzijl T, Harms G, Bouwman E, Jacobs S, Poppema S, Kroesen BJ. 2007. Regulation of pri-microRNA BIC transcription and processing in Burkitt lymphoma. *Oncogene* **26**: 3769-3776.

Landthaler M, Yalcin A, Tuschl T. 2004. The human DiGeorge syndrome critical region gene 8 and Its D. melanogaster homolog are required for miRNA biogenesis. *Curr Biol* **14**: 2162-2167.

Laubinger S, Sachsenberg T, Zeller G, Busch W, Lohmann JU, Rätsch G, Weigel D. 2008. Dual roles of the nuclear cap-binding complex and SERRATE in pre-mRNA splicing and microRNA processing in Arabidopsis thaliana. *Proc Natl Acad Sci U S A* **105**: 8795-8800.

Lehrbach NJ, Armisen J, Lightfoot HL, Murfitt KJ, Bugaut A, Balasubramanian S, Miska EA. 2009. LIN-28 and the poly(U) polymerase PUP-2 regulate let-7 microRNA processing in Caenorhabditis elegans. *Nat Struct Mol Biol* **16**:1016-1020.

Lee EJ, Baek M, Gusev Y, Brackett DJ, Nuovo GJ, Schmittgen TD. 2008. Systematic evaluation of microRNA processing patterns in tissues, cell lines, and tumors. *RNA* **14**:35-42.

Lee RC, Feinbaum RL, Ambros V. 1993. The C. elegans heterochronic gene lin-4 encodes small RNAs with antisense complementarity to lin-14. *C*ell **75**: 843–854.

Lee Y, Ahn C, Han J, Choi H, Kim J, Yim J, Lee J, Provost P, Radmark O, Kim S, et al. 2003. The nuclear RNase III Drosha initiates microRNA processing. *Nature* **425**: 415–419.

Lee Y, Hur I, Park SY, Kim YK, Suh MR, Kim VN. 2006. The role of PACT in the RNA silencing pathway. *EMBO J* **25:** 522–532

Lehmann U, Hasemeier B, Christgen M, Muller M, Romermann D, et al. 2007. Epigenetic inactivation of microRNA gene hsa-miR-9-1 in human breast cancer. *J Pathol* **214**: 17–24.

Lobbes D, Rallapalli G, Schmidt DD, Martin C, Clarke J. 2006. SERRATE: a new player on the plant microRNA scene. *EMBO Rep* **7**: 1052-1058.

Lu J, Getz G, Miska EA, Alvarez-Saavedra E, Lamb J, Peck D, Sweet-Cordero A, Ebert BL, Mak RH, Ferrando AA, et al. 2005. MicroRNA expression profiles classify human cancers. *Nature* **435**: 834-838.

Lu Y, Thomson JM, Wong HY, Hammond SM, Hogan BL. 2007. Transgenic over-expression of the microRNA miR-17-92 cluster promotes proliferation and inhibits differentiation of lung epithelial progenitor cells. *Dev Biol* **310**: 442-453.

Luciano DJ, Mirsky H, Vendetti NJ, Maas S. 2004. RNA editing of a miRNA precursor. *RNA* **10**: 1174-1177.

Lujambio A, Ropero S, Ballestar E, Fraga MF, Cerrato C, Setién F, Casado S, Suarez-Gauthier A, Sanchez-Cespedes M, Git A, et al. 2007. Genetic unmasking of an epigenetically silenced microRNA in human cancer cells. *Cancer Res* **67**: 1424–1429.

Lund E, Guttinger S, Calado A, Dahlberg JE, Kutay U. 2004. Nuclear export of microRNA precursors. *Science* **303**: 95 -98.

Maas S, Rich A, Nishikura K. 2003. A-to-I RNA editing: recent news and residual mysteries. *J Biol Chem* **278**: 1391-1394.

Martinez-Contreras R, Fisette JF, Nasim FU, Madden R, Cordeau M, Chabot B. 2006. Intronic binding sites for hnRNP A/B and hnRNP F/H proteins stimulate pre-mRNA splicing. *PLoS Biol* **4**: 172-185.

Mayeda A, Krainer AR. 1992. Regulation of alternative pre-mRNA splicing by hnRNPA1 and splicing factor SF2. *Cell* **68**: 365–375.

Mendell JT. 2008. miRiad roles for the miR-17-92 cluster in development and disease. *Cell* **133**: 217-222.

Michael MZ, O' Connor SM, van Holst Pellekaan NG, Young GP, James RJ. 2003. Reduced accumulation of specific microRNAs in colorectal neoplasia. *Mol Cancer Res* **1**: 882-891.

Michlewski G, Guil S, Semple CA, Cáceres JF. 2008. Posttranscriptional regulation of miRNAs harboring conserved terminal loops. *Mol Cell* **32**: 383-393.

Newman MA, Thomson JM, Hammond SM. 2008. Lin-28 interaction with the Let-7 precursor loop mediates regulated microRNA processing. *RNA* **14**: 1539-1549.

Obernosterer G, Leuschner PJ, Alenius M, Martinez J. 2006. Post-transcriptional regulation of microRNA expression. *RNA* **12**: 1161-1167.

Okamura K, Hagen JW, Duan H, Tyler DM**,** Lai EC. 2007. The mirtron pathway generates microRNA-class regulatory RNAs in Drosophila. *Cell* **130**: 89-100.

Ozen M, Creighton CJ, Ozdemir M, Ittmann M. 2008. Widespread deregulation of microRNA expression in human prostate cancer. *Oncogene* **27**: 1788-1793.

Paroo Z, Ye X, Chen S, Liu Q. 2009. Phosphorylation of the human microRNA-generating complex mediates MAPK/Erk signaling. *Cell* **139:** 112-122**.**

Piskounova E, Viswanathan SR, Janas M, Lapierre RJ, Daley GQ, Sliz P, Gregory RI. 2008. Determinants of microRNA processing inhibition by the developmentally regulated RNAbinding protein Lin28. *J Biol Chem* **283**: 21310-21314

Ruby JG, Jan CH, Bartel DP. 2007. Intronic microRNA precursors that bypass Drosha processing. *Nature* **448**: 83-86.

Ruggiero T, Trabucchi M, De Santa F, Zupo S, Harfe BD, McManus MT, Rosenfeld MG, Briata P, Gherzi R. 2009. LPS induces KH-type splicing regulatory protein-dependent processing of microRNA-155 precursors in macrophages. *FASEB J* **23**: 2898-2908.

Rybak A, Fuchs H, Smirnova L, Brandt C, Pohl EE, Nitsch R, Wulczyn FG. 2008. A feedback loop comprising lin-28 and let-7 controls pre-let-7 maturation during neural stem-cell commitment. *Nat Cell Biol* **10**: 987-993.

Sakamoto S, Aoki K, Higuchi T, Todaka H, Morisawa K, Tamaki N, Hatano E, Fukushima A, Taniguchi T, Agata Y. 2009. The NF90-NF45 complex functions as a negative regulator in the microRNA processing pathway. *Mol Cell Biol* **29**: 3754-3769.

Sato MM, Nashimoto M, Katagiri T, Yawaka Y, Tamura M. 2009. Bone morphogenetic protein-2 down-regulates miR-206 expression by blocking its maturation process. *Biochem Biophys Res Commun* **383**: 125-129.

Scadden AD. 2005. The RISC subunit Tudor-SN binds to hyper-edited double-stranded RNA and promotes its cleavage. *Nat Struct Mol Biol* **12**: 489-496.

Scott GK, Mattie MD, Berger CE, Benz SC, Benz CC. 2006. Rapid alteration of microRNA levels by histone deacetylase inhibition. *Cancer Res* **66**: 1277–1281.

Song JJ, Smith SK, Hannon GJ, Joshua-Tor L. 2004. Crystal structure of Argonaute and its implications for RISC slicer activity. *Science* **305**: 1434-1437.

Suh MR, Lee Y, Kim JY, Kim SK, Moon SH, Lee JY, Cha KY, Chung HM, Yoon HS, Moon SY et al. 2004. Human embryonic stem cells express a unique set of microRNAs. *Dev Biol* **270**: 488-498.

Sun G, Yan J, Noltner K, Feng J, Li H, Sarkis DA, Sommer SS, Rossi JJ. 2009. SNPs in human miRNA genes affect biogenesis and function. *RNA* **15**: 1640-1651.

Suzuki HI, Yamagata K, Sugimoto K, Iwamoto T, Kato S, Miyazono K. 2009. Modulation of microRNA processing by p53. *Nature* **460**: 529-533.

Thomson JM, Newman M, Parker JS, Morin-Kensicki EM, Wright T, Hammond SM. 2006. Extensive post-transcriptional regulation of microRNAs and its implications for cancer. *Genes Dev* **20**: 2202-2207.

Trabucchi M, Briata P, Garcia-Mayoral M, Haase AD, Filipowicz W, Ramos A, Gherzi R, Rosenfeld MG. 2009. The RNA-binding protein KSRP promotes the biogenesis of a subset of microRNAs. *Nature* **459**: 1010-1014.

van den Berg A, Kroesen BJ, Kooistra K, de Yong D, Briggs J, Blokzijl T, Jacobs S, Kluiver J, Diepstra A, Maggio E, Poppema S. 2003. High expression of B-cell receptor inducible gene BIC in all subtypes of Hodgkin's lymphoma. *Genes Chromosomes Cancer* **37**: 20-28.

Viswanathan SR, Daley GQ, Gregory RI. 2008. Selective blockade of microRNA processing by Lin28. *Science* **320**: 97-100.

Wightman B, Ha I, Ruvkun G. 1993. Posttranscriptional regulation of the heterochronic gene lin-14 by lin-4 mediates temporal pattern formation in C. elegans. *Cell* **75**: 855–862.

Woods K, Thomson JM, Hammond SM. 2007. Direct regulation of an oncogenic micro-RNA cluster by E2F transcription factors. *J Biol Chem* **282**: 2130–2134.

Wulczyn FG, Smirnova L, Rybak A, Brandt C, Kwidzinski E, Ninnemann O, Strehle M, Seiler A, Schumacher S, Nitsch R. 2007. Post-transcriptional regulation of the let-7 microRNA during neural cell specification. *FASEB J* **21**: 415-426.

Xi Y, Shalgi R, Fodstad O, Pilpel Y, Ju J. 2006. Differentially regulated microRNAs and actively translated messenger RNA transcripts by tumor suppressor p53 in colon cancer. *Clin Cancer Res* **12**: 2014–2024.

Yang L, Liu Z, Lu F, Dong A, Huang H. 2006. SERRATE is a novel nuclear regulator in primary microRNA processing in Arabidopsis. *Plant J* **47**:841-850.

Yang W, Chendrimada TP, Wang Q, Higuchi M, Seeburg PH, Shiekhattar R, Nishikura K. 2006. Modulation of microRNA processing and expression through RNA editing by ADAR deaminases. *Nat Struct Mol Biol* **13**: 13-21.

Yamagata K, Fujiyama S, Ito S, Ueda T, Murata T, Naitou M, Takeyama K, Minami Y, O'Malley BW, Kato S. 2009. Maturation of microRNA is hormonally regulated by a nuclear receptor. *Mol Cell* **36**: 340-347.

Yi R, Qin Y, Macara IG and Cullen BR. 2003. Exportin-5 mediates the nuclear export of premicroRNAs and short hairpin RNAs. *Genes Dev* **17**: 3011-3016.

Yu J, Wang F, Yang GH, Wang FL, Ma YN, Du ZW, Zhang JW. 2006. Human microRNA clusters: genomic organization and expression profile in leukemia cell lines. *Biochem Biophys Res Commun* **349**: 59-68.

Zeng Y, Cullen BR. 2004. Structural requirements for pre-microRNA binding and nuclear export by Exportin 5. *Nucleic Acids Res* **32**: 4776-4785.

CHAPTER 3

Cellular localization and processing of primary transcripts of exonic microRNAs

Izabella Slezak-Prochazka, Joost Kluiver, Debora de Jong,
Nancy Halsema, Sibrand Poppema,
Bart-Jan Kroesen and Anke van den Berg

Provisionally accepted in PLOS ONE

ABSTRACT

Processing of miRNAs occurs simultaneous with the transcription and splicing of their primary transcripts. For the small subset of exonic miRNAs it is unclear if the unspliced and/or spliced transcripts are used for miRNA biogenesis. We assessed endogenous levels and cellular location of primary transcripts of three exonic miRNAs. The ratio between unspliced and spliced transcripts varied markedly, i.e. >1 for *BIC*, <1 for pri-miR-146a and variable for pri-miR-22. Endogenous unspliced transcripts were located almost exclusively in the nucleus and thus were available for miRNA processing for all three miRNAs. Endogenous spliced pri-miRNA transcripts were present both in the nucleus and in the cytoplasm and thus were only partly available for miRNA processing. Overexpression of constructs containing the 5' upstream exonic or intronic sequence flanking pre-miR-155 resulted in strongly enhanced miR-155 levels, indicating that the flanking sequence does not affect processing efficiency. Exogenously overexpressed full-length spliced *BIC* transcripts were present both in the nucleus and in the cytoplasm and resulted in enhanced miR-155 levels. We conclude that both unspliced and spliced transcripts of exonic miRNAs can be used for pre-miRNA cleavage. Splicing and cytoplasmic transport of spliced transcripts may present a mechanism to regulate exonic microRNAs levels.

INTRODUCTION

MicroRNAs (miRNAs) are small (~22nt) noncoding RNA molecules that negatively regulate gene expression by binding to the 3'untranslated region (3'UTR) of their target mRNAs (Bartel, 2004). MiRNAs play an important role in cellular processes like apoptosis, proliferation and differentiation. Altered miRNA expression profiles have been associated with various diseases including most, if not all, types of cancer (Calin et al., 2004). This suggests that regulation of miRNA levels is important for normal cellular functioning. Regulation of the miRNA levels may include any of the regulatory mechanisms involved in normal gene expression, such as transcriptional or epigenetic control of transcription. Additionally, miRNA biogenesis is also regulated at the post-transcriptional level (reviewed in Slezak-Prochazka et al., 2010).

The first step in miRNA processing, i.e. cleavage of the primary transcript (pri-miRNA) by the Drosha/DGCR8 complex, is restricted to the nucleus (Denli et al., 2004; Gregory et al., 2004; Han et al., 2004; Landthaler et al., 2004). The miRNA stem-loop structures can be located in introns of protein-coding or noncoding RNA genes, in exons of noncoding genes or in intergenic regions (Kim and Nam, 2006). The vast majority of the human miRNAs are located in introns. Approximately 10% of the miRNAs, including miR-155, miR-146a, miR-22, miR-137, miR-34c and let-7b, reside within exons of noncoding genes (Kim and Kim, 2007; Rodriguez et al., 2007; Saini et al., 2008). Current knowledge about processing of pri-miRNAs has been obtained mainly for intronic or intergenic miRNAs (Ballarino et al., 2009; Janas et al., 2011; Kataoka et al., 2009; Kim and Kim, 2007; Morlando et al., 2008; Pawlicki and Steitz, 2008). Processing of intronic miRNAs occurs co-transcriptionally in cooperation with splicing of the primary transcript (Janas et al., 2011; Kataoka et al., 2009; Kim and Kim, 2007; Morlando et al., 2008; Pawlicki and Steitz, 2008). The Microprocessor complex and the spliceosome are associated in one complex, and co-produce precursor miRNAs (pre-miRNAs) and spliced transcripts from the unspliced pri-mRNA (Kataoka et al., 2009). Splicing is not required for pri-miRNA processing (Kim and Kim, 2007), but spliceosome assembly may

promote release of the pre-miRNA from introns of pri-miRNA (Kataoka et al., 2009). For exonic miRNAs, pre-miRNA release will disrupt the exon of the pri-miRNA and affect formation of spliced transcripts. Therefore, it is more likely that unspliced pri-miRNA transcripts of exonic miRNAs produce either pre-miRNAs or spliced transcripts. The processing of exonic miRNAs has not yet been studied in detail.

One well-known exonic miRNA, miR-155, is processed from the transcript of the B-cell integration cluster (*BIC*) gene, also known as the MIR155 host gene (*MIR155HG*) (Lagos-Quintana et al., 2002). The *BIC* gene consists of three exons separated by long (7.6 and 4kb) introns with the stem-loop pre-miR-155 sequence located in the third exon (Tam, 2001). MiR-155 is crucial for B-cell development and regulation of the immune response (Rodriguez et al., 2007; Thai et al., 2007; Vigorito et al., 2007). High miR-155 levels are observed in many types of cancer, including B-cell malignancies like Hodgkin, primary mediastinal and diffuse large B-cell lymphomas (Kluiver et al., 2005; van den Berg et al., 2003). In contrast, very low levels of miR-155 were observed in B cell-derived Burkitt lymphoma (Kluiver et al., 2006). Eis et al. showed that unspliced *BIC* is located in the nucleus, whereas spliced *BIC* is located mainly in the cytoplasm in two B-cell lymphoma cell lines that both show high miR-155 levels (Eis et al., 2005). RNA *in situ* hybridization in primary cases of Hodgkin lymphoma and non-Hodgkin lymphoma with high miR-155 levels revealed a strong nuclear staining of *BIC* and no staining in the cytoplasm (Kluiver et al., 2006; van den Berg et al., 2003).

In this study, we investigated processing of exonic miRNAs, with a main focus on miR-155. We determined the levels of endogenous unspliced and spliced *BIC*, pri-miR-22 and pri-miR-146a transcripts. We assessed cellular localization of endogenous unspliced and spliced *BIC*, pri-miR-22 and pri-miR-146a and showed that unspliced transcripts are located predominantly in the nucleus while spliced transcripts are partly transported to the cytoplasm. We also showed that the 5' exonic or intronic flanking sequence of pre-miR-155 does not alter processing efficiency of exogenous *BIC* transcripts and that upon

overexpression also spliced transcripts are efficiently processed to mature miR-155.

RESULTS

The unspliced/spliced transcript ratio is miRNA-specific in B-cell lymphoma

For exonic miRNAs, such as miR-155, miR-22 and miR-146a, both unspliced and spliced transcripts include the complete stem-loop pre-miRNA sequence and may serve as the primary miRNA template. To discriminate between unspliced and spliced transcripts we designed qRT-PCR primer sets specific for unspliced or spliced transcripts as indicated in Fig. 1A. We compared the levels of endogenous unspliced and spliced transcripts in twenty B-cell lymphoma cell lines with variable miRNA levels.

Endogenous miR-155 levels were highly variable in B-cell lymphoma cell lines. The difference between the cell line with the lowest (ST486) and the highest (OCI-Ly3) miR-155 level was ~500 fold (Fig. 1B). In general, cell lines with low miR-155 levels also showed low *BIC* transcript levels. The levels of endogenous unspliced *BIC* transcripts were 1,5 to 73 fold higher than the levels of spliced *BIC* transcripts in 17 out of 20 cell lines irrespective of the miR-155 levels (Fig. 1B). In two cell lines, the levels of unspliced and spliced *BIC* transcripts were equal. In L540 cells, the spliced *BIC* transcript levels were 1,5 fold higher than the levels of the unspliced *BIC* transcripts. In the two cells lines with the lowest miR-155 levels, i.e. ST486 and Ramos, only the unspliced *BIC* transcript was present. Both unspliced and spliced *BIC* transcript levels showed significant correlation with miR-155 levels resulting in R^2 of 0.53. The difference observed in levels of unspliced and spliced *BIC* transcripts did not result in a significant difference in the slope of the regression lines.

MiR-22 levels were low in all analyzed B-cell lymphoma cell lines (Fig. 1C). Pri-miR-22 has four alternative splice variants. Transcript variant 3 was almost exclusively detected in our panel of B-cell lymphoma cell lines (data not shown). We therefore restricted our subsequent analysis to this splice variant. Spliced

pri-miR-22 transcript levels were higher than unspliced pri-miR-22 transcript levels in 9, similar in 9 and lower in 2 of the analyzed cell lines (Fig. 1C). The spliced/unspliced pri-miR-22 transcript ratio varied from 0.2 in UHO1 to 8 in L540 cells. In SU-DHL-4 cells, only spliced pri-miR-22 transcript was present. No significant correlation was observed for either spliced or unspliced pri-miR-22 transcript levels with mature miR-22 levels. This might be caused by marked differences in the efficiency of the pri-miR-22 transcript to miR-22 processing, differences in the miR-22 stability, factors regulating the level of mature miR-22 or limiting amounts of factors involved in the biogenesis of miRNAs.

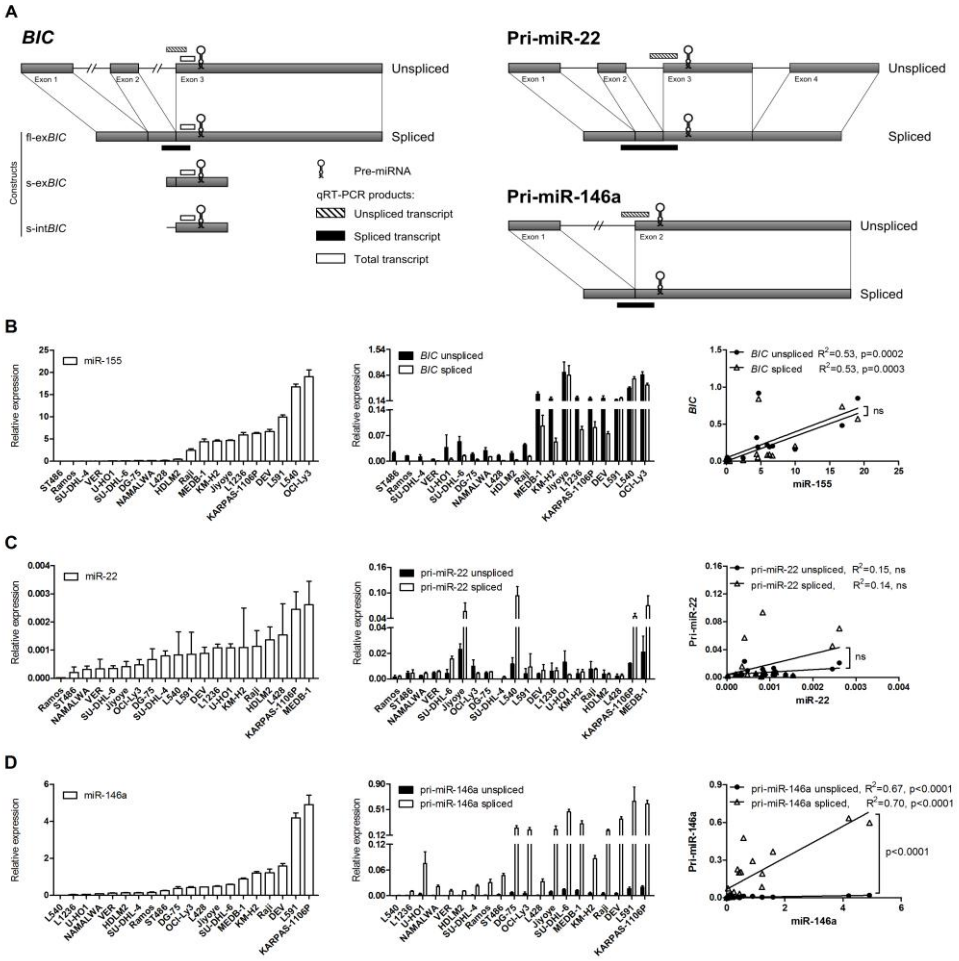

FIGURE 1. The unspliced/spliced ratio of pri-miRNA transcripts is miRNA-specific in B-cell lymphoma cell lines. (A) Schematic overview of the unspliced and spliced *BIC*, pri-miR-22 and pri-miR-146a transcripts and location of the PCR amplicons specific for unspliced, spliced transcripts and total (only for *BIC*) transcripts. Constructs used for miR-155 overexpression are also denoted. Short constructs, s-ex*BIC* and s-int*BIC*, constitute of pre-miR-155, ~150nt 3' flanking sequence from exon 3 and 5' flanking sequence derived from exon 2 (s-ex*BIC*) or intron 2 (s-int*BIC*) of *BIC* transcript, fl-ex*BIC* covers full-length spliced *BIC* transcript. Figures are not drawn to scale. (B) The endogenous levels of miR-155, unspliced and spliced *BIC* transcripts. In 17 out of 20 cell lines the level of unspliced *BIC* transcript was higher than the level of spliced *BIC* transcripts. Both spliced and unspliced *BIC* showed a similar significant correlation with miR-155 levels. (C) The endogenous levels of miR-22, unspliced and spliced pri-miR-22 transcripts. The unspliced/spliced transcript ratio is variable between cell lines and neither of the two transcripts shows a significant correlation with the miR-22 levels. (D) The endogenous levels of miR-146a, unspliced and spliced pri-miR-146a transcripts. In all tested cell lines, levels of spliced pri-miR-146a were much higher than unspliced pri-miR-146a transcripts. Both unspliced and spliced pri-miR-146a levels significantly correlate with the miR-146a levels. However, the slope of the regression line is significantly higher for spliced pri-miR-146a. Levels of *BIC*, pri-miR-22 and pri-miR-146a were normalized to HPRT and levels of miR-155, miR-22 and miR-146a were normalized to RNU48.

MiR-146a levels varied over a 1000-fold range between B-cell lymphoma cell lines with the lowest levels being observed in L540 and the highest levels in KARPAS-1106P (Fig. 1D). The levels of spliced pri-miR-146a transcripts were higher than unspliced pri-miR-146a transcripts for all cell lines. The spliced/unspliced pri-miR-146a transcript ratio varied from 14 to 72 fold. In L540 cells only the spliced pri-miR-146a transcript was present. Both unspliced and spliced pri-miR-146a transcript levels significantly correlated with miR-146a, showing R2 of 0.67 and 0.7, respectively. However, the slopes of the curves differ significantly ($p<0.0001$), due to lower unspliced pri-miR-146a transcript levels.

Thus, for all three exonic miRNAs, both unspliced and spliced primary transcripts are present albeit at a variable ratio. For *BIC*, the unspliced primary transcript is predominant, for pri-miR-146a the spliced primary transcripts is predominant, whereas for pri-miR-22 the unspliced/spliced transcript ratio varies between cell lines. Levels of the mature miRNAs correlated with the levels of both unspliced and spliced pri-miRNA transcripts for miR-155 and miR-146a, but not for miR-22.

Spliced pri-miRNA transcripts are partly transported to the cytoplasm

To further examine whether unspliced or spliced pri-miRNA transcripts are available for miRNA processing, we determined the subcellular localization of unspliced and spliced transcripts of *BIC*, pri-miR-22 and pri-miR-146a by qRT-PCR of nuclear and cytoplasmic fractions relative to the total fraction (Fig. 2). The pri-miRNA transcript levels in the cytoplasm were normalized to tRNA-Lys, which showed similar levels in total and cytoplasmic fraction. The pri-miRNA transcript levels in the nucleus were normalized to U3, which showed similar levels in total and nuclear fraction. To asses subcellular localization of unspliced and spliced *BIC* transcripts, we selected cell lines with low (L428), intermediate (Jiyoye) or high (L540) miR-155 levels (Fig. 1A). The same cell lines were used for subcellular localization of pri-miR-22 and pri-miR-146a to allow comparison between subcellular distributions of pri-miRNA transcripts.

Endogenous unspliced *BIC* transcripts were located exclusively in the nuclear fraction (more than 99%) in all three cell lines (Fig. 2). The fraction of spliced *BIC* transcripts located in the nucleus varied from 74% in L428 to 17% in Jiyoye cells and 47% in L540. The levels of the spliced and unspliced transcripts in cytoplasm and nucleus relative to their levels in the total fraction are shown in Supplementary Fig. 1. The highly abundant unspliced *BIC* transcripts most likely serve as the main endogenous primary miR-155 transcript. The spliced *BIC* transcripts that are located in the cytoplasm are not available for processing to miR-155 and the functional role of these cytoplasmic spliced *BIC* transcripts remains unclear.

Localization of unspliced pri-miR-22 transcripts was predominantly, but not exclusively, nuclear in all three cell lines (Fig. 2 and Supplementary Fig. 1). 88% in L428, 91% in Jiyoye and 97% in L540 of unspliced pri-miR-22 transcripts were present in the nucleus. The fraction of spliced pri-miR-22 transcripts that was present in the nucleus was 81% for L428, 53% for Jiyoye, and 50% for L540 cells.

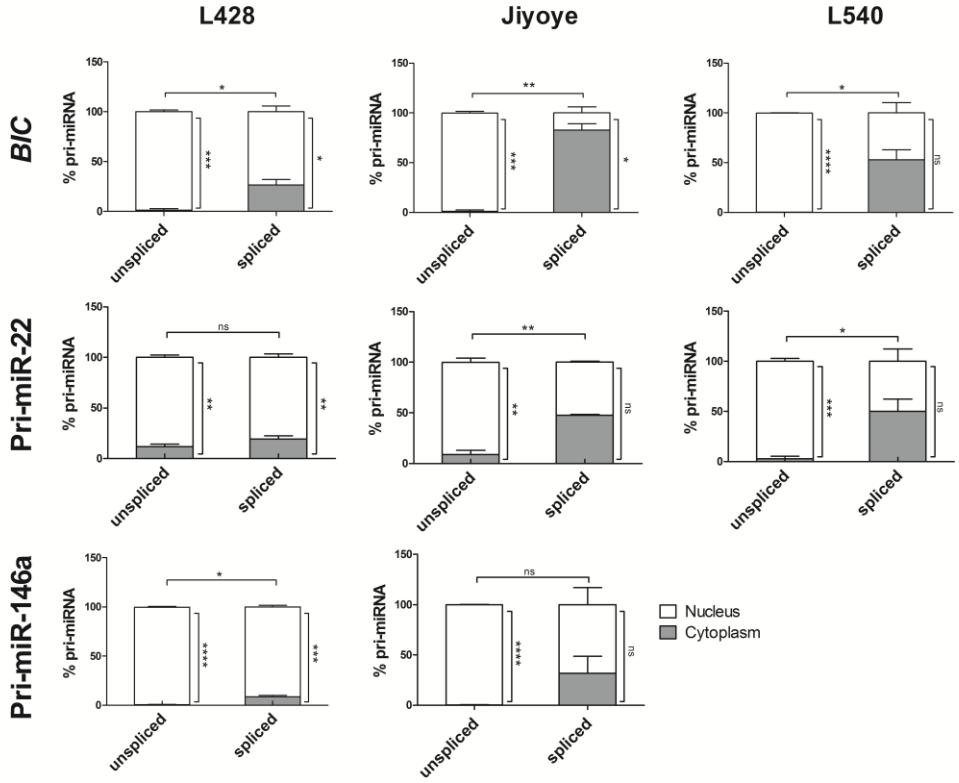

FIGURE 2. Cellular localization of unspliced and spliced pri-miRNA transcripts. The percentages of spliced and unspliced transcripts of *BIC*, pri-miR-22 and pri-miR-146a were shown in cytoplasmic and nuclear fractions of L428, Jiyoye and L540 cells. For all cell lines unspliced transcripts were located almost completely in the nucleus, whereas spliced transcripts were also detected in the cytoplasm. Pri-miR-146a was not detectable in L540. Transcript levels in the cytoplasm and in the nucleus were calculated relative to the total fractions. Average of three independent experiments was presented. P values were determined by a Student's t-test (* $p<0.05$, ** $p<0.01$, *** $p<0.001$, ****$p<0.0001$, ns - not significant).

Localization of unspliced pri-miR-146a transcripts was exclusively nuclear (above 99%) for both L428 and Jiyoye cells (Fig. 2 and Supplementary Fig. 1). In L540 cells, both mature and primary miR-146a transcripts were hardly detected, therefore it was not possible to determine the subcellular localization. 91% of spliced pri-miR-146a transcripts were present in the nucleus in L428 and 68% in Jiyoye cells.

Thus, part of the spliced *BIC*, pri-miR-22 and, to a lesser degree, pri-miR-146a transcripts are transported to the cytoplasm and as such unavailable for processing. Unspliced transcripts show an almost exclusive nuclear localization for *BIC*, pri-miR-22 and pri-miR-146a. Since the levels of spliced pri-miR-22 in L540 and Jiyoye cells and pri-miR-146a in Jiyoye and L428 were higher than the unspliced transcript levels in these cell lines (Fig. 1C and 1D), spliced pri-miR-22 and pri-miR-146a may still be the predominant miRNA substrate.

Exogenous spliced *BIC* can be processed to miR-155.

For further analysis we focused on miR-155, because previous studies have shown conflicting data concerning *BIC* to miR-155 processing (Kluiver et al., 2007; Zhang et al., 2008). The upstream pre-miR-155 flanking sequence is different in spliced and unspliced *BIC* transcripts. To determine if this upstream sequence affects the processing efficiency, we assessed the levels of miR-155 induction upon overexpression of *BIC* from two short fragments of *BIC* containing the stem-loop region, ~150nt 3' flanking sequence from exon 3 and ~150nt 5' flanking sequence derived either from intron 2 (s-int*BIC*) or from exon 2 (s-ex*BIC*) of the *BIC* transcript (Fig 1A). In addition, we also overexpressed the full-length spliced *BIC* (fl-ex*BIC*) transcript (Fig. 1A). We transduced these three *BIC* constructs into ST486, Ramos and U-HO1, i.e. cells that all have low endogenous miR-155 levels. A high expression of *BIC* was induced using either of the constructs (Fig. 3A), albeit at variable levels. Transduction with the short exon spanning *BIC* construct resulted in the highest increase and the full-length spliced *BIC* construct resulted in the lowest increase in total *BIC* transcript levels (Fig. 3A). Interestingly, the level of miR-155 induction was similar for all three constructs (Fig. 3B), despite the marked differences in total *BIC* levels. These data indicate that the upstream pre-miR-155 flanking sequence does not modify processing efficiency and suggest that at a certain level of primary miRNA transcript, other factors become limiting or regulate the level of mature miR-155.

Next, we determined the subcellular localization of *BIC* transcripts in Ramos cells transduced with fl-ex*BIC*. In empty vector control cells, endogenous

unspliced *BIC* transcripts showed a predominantly nuclear localization, whereas the endogenous spliced *BIC* transcripts were not detectable (Fig. 3C). Thus, total *BIC* levels can be completely attributed to the unspliced *BIC* transcript levels. Localization of the overexpressed fl-ex*BIC* was both cytoplasmic and nuclear (32% versus 68%). Localization of endogenous unspliced *BIC* transcripts remained predominantly nuclear, i.e. similar to the empty vector control. Localization of total *BIC* resembled the pattern of spliced *BIC,* since the exogenous spliced *BIC* levels were ~100 fold higher than the endogenous unspliced *BIC* levels. Overexpression of fl-ex*BIC* was followed by a strong induction of miR-155 (Fig. 3B), indicating that upon overexpression nuclear spliced *BIC* transcripts can also serve as the primary miR-155 transcript.

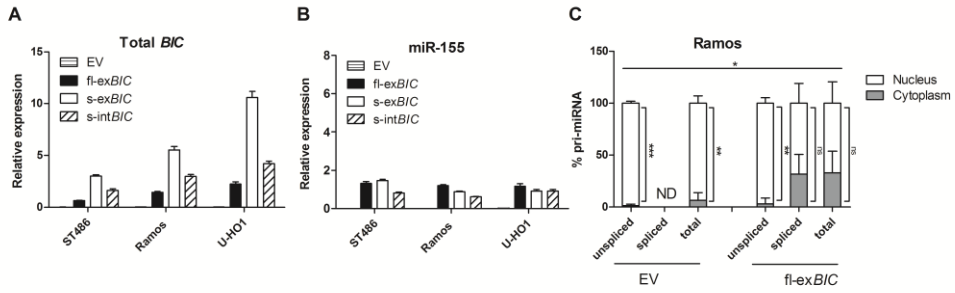

FIGURE 3. Processing and cellular localization of exogenous *BIC* transcripts. Levels of total *BIC* (A) and miR-155 (B) upon overexpression of the three constructs and empty vector (EV) in ST486, Ramos and U-HO1 cells. For the three *BIC* overexpression constructs, the increase in total *BIC* was variable and the highest levels were observed for short *BIC* transcript containing exon 2 derived 5' pre-miR-155 flanking sequence (s-ex*BIC*). However, miR-155 induction was similar for all *BIC* overexpression constructs. (C) The percentages of spliced, unspliced and total *BIC* transcripts in nuclear and cytoplasmic fractions of Ramos EV and Ramos full-length spliced *BIC* (fl-ex*BIC*). For both Ramos EV and fl-ex*BIC*, unspliced *BIC* was located predominantly in the nucleus. Spliced *BIC* was not detectable (ND) in Ramos EV. Upon overexpression of the fl-ex*BIC* construct, spliced *BIC* transcripts were partly exported to the cytoplasm. Localization of total *BIC* was similar to the dominant transcript forms, i.e. unspliced *BIC* for Ramos EV and spliced *BIC* for Ramos fl-ex*BIC*. Transcript levels in the cytoplasm and the nucleus were calculated relative to the total fraction. Average of three independent experiments was presented. P value was determined by 1-way ANOVA and by a Student's t-test for cytoplasmic versus nuclear localization. For both tests, * $p<0.05$, ** $p<0.01$, *** $p<0.001$, ns - not significant.

The unspliced/spliced ratio of *BIC* transcripts changes upon cellular activation

To investigate whether the ratio between unspliced and spliced *BIC* transcripts is altered upon induction *of BIC*, we activated three B-cell lymphoma cell lines using PMA/Ionomycin. Activation of DG-75, L428 and KM-H2 cells resulted in 3- to 13-fold increase in miR-155 levels (Fig. 4A). Induction of unspliced *BIC* transcript levels showed a 1.6 to 5.5 fold increase, whereas spliced *BIC* transcript levels showed a 5.4 to 31 fold increase compared to untreated cells (Fig. 4B). Although the unspliced *BIC* transcript remained the predominant transcript, the unspliced/spliced *BIC* transcript ratio significantly changed in favour of the spliced *BIC* transcript (Fig. 4C). Thus, both processing of unspliced *BIC* transcript to miR-155 and to spliced *BIC* transcripts are enhanced upon activation-induced expression of *BIC*.

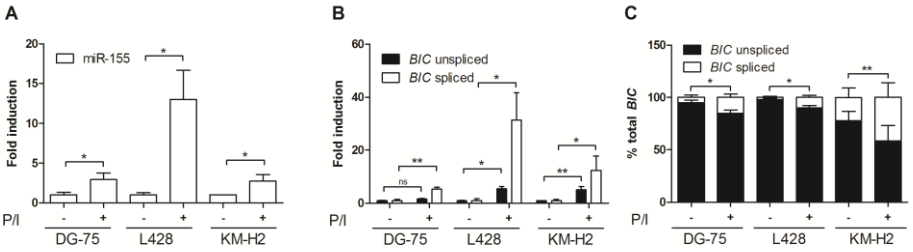

FIGURE 4. Induction of unspliced and spliced *BIC* transcripts upon cellular activation. Fold induction in miR-155 (A), unspliced *BIC* and spliced *BIC* transcript (B) levels upon PMA/Ionomycin (P/I) treatment. Levels of miR-155 and *BIC* transcripts in untreated cells were averaged and fold induction upon P/I treatment was calculated. In all three cell lines, induction of spliced *BIC* was higher that of unspliced *BIC* transcripts. (C) Unspliced *BIC* transcripts were predominant in both untreated and P/I-treated cells, however unspliced/spliced *BIC* ratio significantly decreased upon P/I treatment. Sum of spliced and unspliced *BIC* transcript levels was set as 100%. Average of three (DG-75 and L428) or four (KM-H2) experiments was presented. P values were determined by a Student's t-test (* $p<0.05$, ** $p<0.01$, ns - not significant).

DISCUSSION

Exonic miRNAs constitute a small group of the known human miRNAs. The vast majority of exonic miRNAs are located in noncoding RNA genes of which the only known function is being a miRNA host gene. In contrast to intronic miRNAs, processing of the pri-miRNA transcripts of exonic miRNAs to pre-miRNAs interferes with the normal splicing process of the transcript. Exonic miRNAs regulate important physiological pathways, i.e. miR-155 and miR-146a are crucial regulatory components of the immune response, hematopoiesis and carcinogenesis (reviewed in Rusca and Monticelli, 2011; Tili et al., 2009) and miR-22 plays a role in carcinogenesis (Alvarez-Diaz et al., 2012; Xu et al., 2011).

In this study, we showed that unspliced pri-miRNA transcripts of exonic miRNAs, i.e. miR-155, miR-22 and miR-146a, are located predominantly in the nucleus. The spliced transcripts are present both in the nucleus and the cytoplasm. Since the first processing step of pri-miRNAs takes place in the nucleus (Lee et al., 2002; Yeom et al., 2006), both nuclear unspliced and spliced transcripts can serve as pri-miRNA templates. Overexpression constructs containing either the exonic 5' flanking sequence or the intronic 5' flanking sequence of pre-miR-155 both resulted in a marked miR-155 induction. Consistent with these findings we also observed a marked induction of miR-155 upon exogenously overexpressed full-length spliced *BIC* transcripts. These data indicate that the Microprocessor complex can use spliced and unspliced *BIC* transcripts for processing to pre-miR-155. Since the unspliced *BIC* transcripts are much more abundant and are almost exclusively located in the nucleus, we conclude that unspliced nuclear *BIC* transcripts are the primary template for miR-155 processing in B-cell lymphoma. In contrast to pri-miR-155, the spliced transcripts are the most abundant form of pri-miR-146a and, for part of the cell lines of pri-miR-22. Unspliced pri-miR-146a showed very low levels in all cell lines. This might indicate that the unspliced pri-miR-146 is directly used for processing to pre-miR-146a or for splicing. The level of spliced pri-miR-146a might thus represent the level of pri-miRNA that was not used for miRNA

processing. Alternatively, despite the partial cytoplasmic location, the spliced transcripts can still be the most important source for the biogenesis of mature miR-146a. Overexpression of miRNAs from constructs that do not contain introns show very effective processing to mature miRNAs, similar to our results using the *BIC* constructs. This indicates that although splicing enhances processing (Kataoka et al., 2009; Morlando et al., 2008), it is not required to allow processing to mature miRNAs. Pawlicki *et al.* showed that overexpressed pri-miRNAs that are artificially prematurely released from the transcription site accumulate in the nucleoplasm and are not efficiently processed to pre-miRNA (Pawlicki and Steitz, 2008; Pawlicki and Steitz, 2009). These studies implicate that spliced pri-miRNA transcripts may be less efficient templates for the miRNA processing machinery when released from the transcription site. *In vitro* processing of radiolabeled pri-miRNAs using whole-cell extract or immunoprecipitated Microprocessor (Han et al., 2004) indicates that presence at the transcriptional start site is not required for release of the pre-miRNA. Although we do not know if spliced exonic pri-miRNA transcripts are released from the transcription start site before miRNA processing, our data show that spliced transcripts can be used for miRNA processing.

We observed that induction of *BIC* using three different constructs was variable. However, the induction of mature miR-155 was strikingly similar in the three cell lines. Thus, induction of higher *BIC* transcripts levels did not result in higher miR-155 levels. This suggests that the miR-155 levels are regulated in these cell lines that are characterized by very low endogenous miR-155 levels. Notably, the level of miR-155 obtained with these three constructs was still ~10 fold lower than the highest observed endogenous miR-155 levels (OCI-Ly3 cell line). An alternative explanation could be that factors required for miRNA biogenesis become limiting and preclude induction of higher levels.

For *BIC*, we demonstrated that part of the spliced transcripts are exported to the cytoplasm and are thus not available for processing. Similarly, spliced pri-miR-22 and to a lesser degree spliced pri-miR-146a are exported to the cytoplasm. Alteration of the efficiency of splicing and nuclear export of spliced pri-miRNA transcripts may rapidly change the amount of pri-miRNA available for

miRNA processing and therefore serve as a mechanism to regulate mature miRNA levels. Consistent with this hypothesis, we observed differences in the ratio of unspliced to spliced *BIC* transcript levels upon PMA/Ionomycin treatment. Cellular conditions and external stimuli may thus affect exonic miRNA levels by inducing changes to the amount of unspliced pri-miRNA used for miRNA processing at the expense of the amount of unspliced transcript available for splicing.

Both unspliced and spliced exonic miRNA transcripts can be used as template for miRNA processing. The level and ratio of spliced and unspliced transcripts, their cellular location and the processing efficiency together determine which form is the most likely endogenous pri-miRNA. For exonic miRNA processing studies it is important to assess total transcript levels and not only examine either spliced or unspliced transcripts. Conflicting data as presented in the current literature concerning the processing efficiency of *BIC* may, at least partially, be explained by differences in the analyzed transcripts (Kluiver et al., 2007; Zhang et al., 2008).

Many proteins were reported to inhibit or promote miRNA processing by binding to stem-loop of pri-miRNA and/or pre-miRNA (reviewed in Slezak-Prochazka et al., 2010). These proteins have been identified to regulate both intronic and exonic miRNA processing. KH-type splicing regulatory protein (KSRP) was shown to enhance miR-155 processing in mouse activated macrophages by binding to the terminal loop of both *BIC* transcript and pre-miR-155 (Ruggiero et al., 2009). Moreover, monocyte chemoattractant protein [MCP]-1-induced protein 1 (MCPIP1) was shown to suppress miRNA processing of a panel of miRNAs, including miR-155 and miR-146a, by induction of pre-miRNA terminal loops cleavage (Suzuki et al., 2011). Some of these proteins, like KSRP or hnRNP A1, regulate both miRNA and mRNA processing (Gherzi et al., 2010; Michlewski et al., 2008; Trabucchi et al., 2009). These, and possibly other, regulatory proteins may thus regulate exonic miRNA levels by promoting either pre-miRNA cleavage or splicing of exonic pri-miRNA transcripts.

It is unclear whether cytoplasmic spliced transcripts have additional functions in the cytoplasm. To date, the only known function of the three noncoding genes studied in this paper is being the host gene for the miRNAs. Splicing of the transcripts and the subsequent transport to the cytoplasm might serve as a mechanism to prevent processing to pre-miRNA (Fig. 5). This is supported by the finding that upon inhibition of DGCR8 with shRNA in L1236 cells we saw a marked induction of the spliced *BIC* transcript, which resulted in a change of the unspliced/spliced *BIC* transcript ratio from 2.5 to 0.3 (data not shown). This indicates that when pre-miRNA processing is inhibited, splicing of the unspliced *BIC* transcript is enhanced. Another possible role of the cytoplasmic spliced transcripts is that they may function as competing endogenous RNA (ceRNA) transcripts for the mature miRNAs. MiR-155 and miR-155* sequences are highly complementary and the *BIC* transcript (MIR155HG) is a predicted miR-155 target by the miRanda-mirSVR and PITA algorithms (http://www.microrna.org, Betel et al., 2010; http://genie.weizmann.ac.il/pubs/mir07/mir07_prediction.html, Kertesz et al., 2007). Up to date, various transcripts were shown to function as ceRNA, e.g. protein-coding transcripts, pseudogenes, and long noncoding RNAs (Cesana et al., 2011; Poliseno et al., 2010; Tay et al., 2011). Spliced pri-miRNA transcripts of exonic miRNAs could prevent binding of the mature miRNA to their endogenous protein-coding target genes and thereby prevent efficient knockdown of the target proteins. This would be a novel mechanism, by which cytoplasmic pri-miRNA transcripts function in a negative feedback loop to regulate miRNA function.

In conclusion, we showed that unspliced *BIC*, pri-miR-146a and pri-miR-22 transcripts were predominantly localized in the nucleus, although they were not always more abundant than the spliced *BIC* transcripts. We also showed that spliced *BIC*, pri-miR-146a and pri-miR-22 transcripts are partly localized in the cytoplasm and thus not fully available for processing to the mature miRNAs. Pre-miRNAs and spliced transcripts appear to be two mutually exclusive products of unspliced pri-miRNA transcripts of exonic miRNA. Splicing and transport to the

cytoplasm may represent a novel mechanism to regulate cellular exonic miRNA levels and function.

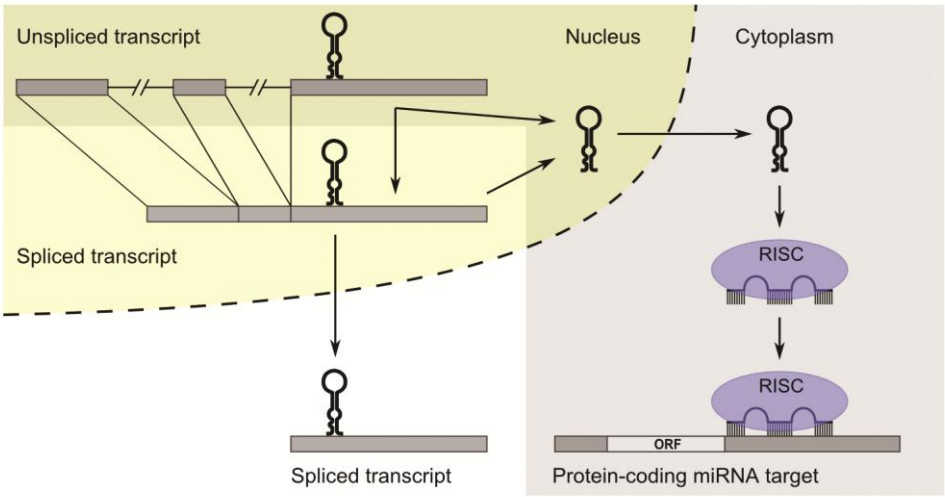

FIGURE 5. Model of processing and function of exonic miRNA primary transcripts. The classical miRNA processing and functioning pathway (indicated in dark colors) shows that the main pri-miRNA, the unspliced nuclear transcript, is processed to pre-miRNA. Pre-miRNA is transported to the cytoplasm and further processed to mature miRNA. Mature miRNA guides the RNA-induced silencing complex (RISC) to protein-coding miRNA targets and inhibits their expression. Unspliced transcripts can also be spliced instead of being processed to pre-miRNA. The pre-miRNA stem-loop structure might also be processed from the spliced transcripts. Spliced transcript can be transported to the cytoplasm. This may represent a mechanism to prevent processing to pre-miRNA.

MATERIALS AND METHODS

Cell lines and treatment. Burkitt lymphoma cell lines (Ramos, DG-75, NAMALWA, Raji, Jiyoye) were purchased from ATCC (ST486) and DSMZ (other cell lines). Diffuse large B-cell lymphoma cell lines (OCI-Ly3, SU-DHL-4, SU-DHL-6, VER) (Epstein et al., 1978; Tweeddale et al., 1987) were a kind gift of A. Epstein (UCLA, CA) (SU-DHL-4 and SU-DHL-6) or were established in our laboratory (VER). Hodgkin lymphoma cell lines (L540, L591, L1236, DEV, KM-H2, HDLM-2, L428, U-HO1) (Diehl et al., 1982; Diehl et al., 1985; Drexler et al., 1986; Kanzler et al., 1996; Mader et al., 2007; Schaadt et al., 1980) were purchased from DSMZ (L540, KM-H2), were a kind gift of V. Diehl (University of

Cologne, Germany) (L591, L1236, HDLM-2, L428) and P. Möller (University of Ulm, Germany) (U-HO1) or were established in our laboratory (DEV). Primary mediastinal B-cell lymphoma cell lines (KARPAS-1106P, MEDB-1) (Copie-Bergman et al., 2003) were a kind gift of M. Dyer (University of Leicester, UK). Cell lines were cultured at 37°C under an atmosphere containing 5% CO_2 in Iscove's Modified Dulbecco's Medium (OCI-Ly3) or RPMI-1640 (other cell lines) medium (Cambrex Biosciences, Walkersville, USA) supplemented with ultraglutamine (2 mM), penicillin (100 U/ml), streptomycin (0.1 mg/ml; Cambrex Biosciences), and 5% (L428), 20% (DEV, ST486, OCI-Ly3) or 10% (other cell lines) fetal calf serum (Cambrex Biosciences). DG-75, L428 and KM-H2 cells were treated for 24h with Phorbol 12-myristate 13-acetate (PMA)/Ionomycin (both Sigma-Aldrich, Saint Louis, MO) as previously described (Kluiver et al., 2007). The PMA/Ionomycin treatment was performed in triplicate (DG-75 and L428) or quadruplicate (KM-H2).

***BIC*/miR-155 constructs.** The pcDNA3.1(+) plasmid containing full-length spliced *BIC* (fl-ex*BIC*) was described previously (Kluiver et al., 2007). The MXW-PGK-IRES-GFP vector was a kind gift from C-Z. Chen (Stanford University, CA). The full-length spliced fl-ex*BIC* insert was subcloned from the pcDNA3.1(+) vector to the MXW-PGK-IRES-GFP vector using *PmeI* (pcDNA3.1(+) vector) and *HpaI* (MXW-PGK-IRES-GFP vector) restriction enzymes. The miR-155 stem-loop and ~150nt flanking sequences were amplified from genomic DNA (s-int*BIC*) or cDNA (s-ex*BIC*) using Taq polymerase. Primer sequences used for PCR were as follows, 5'-TGTCACCTCCAGCTTTATAACC-3' (forward, s-int*BIC*), 5'-AACCTACCAGAGACCTTACC-3' (forward, s-ex*BIC*), 5'-GGCTTTATCATTTTTCAATCT-3 (reverse, s-int*BIC* and s-ex*BIC*). An *XhoI* restriction site was added to the forward and an *EcoRI* site to the reverse primer to allow efficient cloning. PCR products were cloned to the retroviral MXW-PGK-IRES-GFP vector using standard laboratory procedures. The inserts were sequenced to confirm the correct sequences.

Retroviral transduction. To generate retroviral particles, Phoenix-Ampho packaging cells (Swift et al., 2001) were $CaPO_4$ transfected with 37,5µg of MXW-PGK-IRES-GFP constructs (empty vector or vector containing one of the *BIC* constructs) in T75 flasks. Viral particles were harvested after two days and concentrated with Retro-X concentrator (Clontech, Saint-Germain-en-Laye, France) according to the manufacturer's protocol. Target cells were transduced with the virus by spinning at 2,000rpm for 2hrs. Cells transduced with retroviral vectors were sorted for GFP using MoFlo sorter (Dako cytomation).

RNA isolation from total, nuclear and cytoplasmic fractions. Nuclear and cytoplasmic fractions were separated by adding 200µl of lysis buffer (140mM NaCl, 1.5mM MgCl2, 10mM Tris-HCl pH8.0, 1mM DTT, 0.5% Nonidet P-40) to pellets of ~4 million cells, followed by 5min incubation on ice and centrifugation for 3min at 4°C and 100xg. The supernatant was harvested as the cytoplasmic fraction. The pellet containing the nuclei was washed twice with lysis buffer. 1ml of Qiazol (Qiagen, Carlsbad, USA) was added to the ~200µl of cytoplasmic fraction, to the nuclear pellet and to the total cell pellet.

Quantitative RT-PCR. Total RNA was isolated using Trizol (Invitrogen, Carlsbad, USA) according to the manufacturer's protocol for the cell lines. RNA samples were treated with DNase (Ambion, Foster City, CA). For RNA isolation from cytoplamic/nuclear/total fractions, we used the miRNeasy kit (Qiagen) including a DNase treatment (Qiagen). The RNA concentration was measured with a NanoDropTM 1000 Spectrophotometer (Thermo Fisher Scientific Inc., Waltham, USA) and RNA integrity was evaluated by 1% agarose electrophoresis. cDNA was synthesized using 500ng input RNA, SuperScript II and random primers according to the manufacturers protocol (Invitrogen). The qPCR reaction contained SYBRgreen mix (Applied Biosystems, Foster City, USA), 300nM primers, and 1ng of cDNA in a total volume of 10µl. Levels of spliced, unspliced and total BIC as well as spliced and unspliced pri-miR-22, pri-miR-146a were normalized to HPRT. Transcript levels in nuclear fraction were normalized to U3 and in cytoplasmic fraction to tRNA-Lys. Normalized pri-miRNA transcript levels

in total fractions were set as 100% and percentage of pri-miRNA transcripts in the cytoplasm and in the nucleus were calculated relative to the total fraction. Percentages of each transcript in the cytoplasm and in the nucleus were added and recalculated to sum up to 100%. For qRT-PCR, we used the following primer sequences: for unspliced *BIC*, 5'- AGCTTTATAACCGCATGTGCATAC-3' (forward) and 5'- CAGATTTCCCCTTCCTGGTTT-3' (reverse); for total *BIC*, 5'-AAATTCTTTATGCCTCATCCTCTGA-3' (forward) and 5'-AGGCAAAAACCCCTATCACGAT-3' (reverse); for unspliced pri-miR-22, 5'-CTGCTCAGATCTTTCCCATTTTC-3' (forward) and 5'-CCAGGTGAGGGCGTGAGA-3' (reversed); for spliced pri-miR-22, 5'-GGGCTGATCACTGAACTCACATT-3' (forward) and 5'-TGAGGGCGTGAGAGGAACA-3' (reversed), for unspliced pri-miR-146a, 5'-ATTTACCAGGCTTTTCACTCTTGTATT-3' (forward) and 5'-GGCTTTTCAGAGATGGTGCAA-3' (reverse); for spliced pri-miR-146a, 5'-GACAGGAGACAGTAGCACAACGA-3' (forward) and 5'-CAGCCAGCGAGCTCCTAAAA-3' (reverse); primers for spliced *BIC*, HPRT, tRNA-Lys and U3 were described previously (Specht et al., 2001;Taft et al., 2010;van den Berg et al., 2003). Localization of unspliced or spliced transcript-specific qRT-PCR products are indicated in Fig. 2A. qRT-PCR for miR-155, miR-22, miR-146a and RNU48 was performed using miRNA qRT-PCR assays (Applied Biosystems, Foster City, USA) as described previously (Gibcus et al., 2009). Reverse transcription (RT) primers specific for a miRNA and RNU48 (control) were multiplexed in 15µl RT reactions containing 1µl of each RT primer. The miRNA levels were normalized to the RNU48 levels. Mean cycle threshold (Ct) values for all genes were quantified with the SDS software (version 2.1). Relative expression levels were calculated as 2-ΔCt.

REFERENCES

Alvarez-Diaz, S., Valle, N., Ferrer-Mayorga, G., Lombardia, L., Herrera, M., Dominguez, O., Segura, M.F., Bonilla, F., Hernando, E. and Munoz, A. 2012. MicroRNA-22 is induced by vitamin D and contributes to its antiproliferative, antimigratory and gene regulatory effects in colon cancer cells. *Hum. Mol. Genet.* **21**: 2157-2165.

Ballarino, M., Pagano, F., Girardi, E., Morlando, M., Cacchiarelli, D., Marchioni, M., Proudfoot, N.J. and Bozzoni, I. 2009. Coupled RNA processing and transcription of intergenic primary microRNAs. *Mol. Cell. Biol.* **29**: 5632-5638.

Bartel, D.P. 2004. MicroRNAs: genomics, biogenesis, mechanism, and function. *Cell* **116**: 281-297.

Betel, D., Koppal, A., Agius, P., Sander, C. and Leslie, C. 2010. Comprehensive modeling of microRNA targets predicts functional non-conserved and non-canonical sites. *Genome Biol.* **11**: R90.

Calin, G.A., Sevignani, C., Dumitru, C.D., Hyslop, T., Noch, E., Yendamuri, S., Shimizu, M., Rattan, S., Bullrich, F., Negrini, M. et al. 2004. Human microRNA genes are frequently located at fragile sites and genomic regions involved in cancers. *Proc. Natl. Acad. Sci. U. S. A.* **101**: 2999-3004.

Cesana, M., Cacchiarelli, D., Legnini, I., Santini, T., Sthandier, O., Chinappi, M., Tramontano, A. and Bozzoni, I. 2011. A long noncoding RNA controls muscle differentiation by functioning as a competing endogenous RNA. *Cell* **147**: 358-369.

Copie-Bergman, C., Boulland, M.L., Dehoulle, C., Moller, P., Farcet, J.P., Dyer, M.J., Haioun, C., Romeo, P.H., Gaulard, P. and Leroy, K. 2003. Interleukin 4-induced gene 1 is activated in primary mediastinal large B-cell lymphoma. *Blood* **101**: 2756-2761.

Denli, A.M., Tops, B.B., Plasterk, R.H., Ketting, R.F. and Hannon, G.J. 2004. Processing of primary microRNAs by the Microprocessor complex. *Nature* **432**: 231-235.

Diehl, V., Kirchner, H.H., Burrichter, H., Stein, H., Fonatsch, C., Gerdes, J., Schaadt, M., Heit, W., Uchanska-Ziegler, B., Ziegler, A. et al. 1982. Characteristics of Hodgkin's disease-derived cell lines. *Cancer Treat. Rep.* **66**: 615-632.

Diehl, V., Pfreundschuh, M., Fonatsch, C., Stein, H., Falk, M., Burrichter, H. and Schaadt, M. 1985. Phenotypic and genotypic analysis of Hodgkin's disease derived cell lines: histopathological and clinical implications. *Cancer Surv.* **4**: 399-419.

Drexler, H.G., Gaedicke, G., Lok, M.S., Diehl, V. and Minowada, J. 1986. Hodgkin's disease derived cell lines HDLM-2 and L-428: comparison of morphology, immunological and isoenzyme profiles. *Leuk. Res.* **10**: 487-500.

Eis, P.S., Tam, W., Sun, L., Chadburn, A., Li, Z., Gomez, M.F., Lund, E. and Dahlberg, J.E. 2005. Accumulation of miR-155 and BIC RNA in human B cell lymphomas. *Proc. Natl. Acad. Sci. U. S. A.* **102**: 3627-3632.

Epstein, A.L., Levy, R., Kim, H., Henle, W., Henle, G. and Kaplan, H.S. 1978. Biology of the human malignant lymphomas. IV. Functional characterization of ten diffuse histiocytic lymphoma cell lines. *Cancer* **42**: 2379-2391.

Gherzi, R., Chen, C.Y., Trabucchi, M., Ramos, A. and Briata, P. 2010. The role of KSRP in mRNA decay and microRNA precursor maturation. *Wiley Interdiscip. Rev. RNA* **1**: 230-239.

Gibcus, J.H., Tan, L.P., Harms, G., Schakel, R.N., de Jong, D., Blokzijl, T., Moller, P., Poppema, S., Kroesen, B.J. and van den Berg, A. 2009. Hodgkin lymphoma cell lines are characterized by a specific miRNA expression profile. *Neoplasia* **11**: 167-176.

Gregory, R.I., Yan, K.P., Amuthan, G., Chendrimada, T., Doratotaj, B., Cooch, N. and Shiekhattar, R. 2004. The Microprocessor complex mediates the genesis of microRNAs. *Nature* **432**: 235-240.

Han, J., Lee, Y., Yeom, K.H., Kim, Y.K., Jin, H. and Kim, V.N. 2004. The Drosha-DGCR8 complex in primary microRNA processing. *Genes Dev.* **18**: 3016-3027.

Janas, M.M., Khaled, M., Schubert, S., Bernstein, J.G., Golan, D., Veguilla, R.A., Fisher, D.E., Shomron, N., Levy, C. and Novina, C.D. 2011. Feed-forward microprocessing and splicing activities at a microRNA-containing intron. *PLoS Genet.* **7**: e1002330.

Kanzler, H., Hansmann, M.L., Kapp, U., Wolf, J., Diehl, V., Rajewsky, K. and Kuppers, R. 1996. Molecular single cell analysis demonstrates the derivation of a peripheral blood-derived cell line (L1236) from the Hodgkin/Reed-Sternberg cells of a Hodgkin's lymphoma patient. *Blood* **87**: 3429-3436.

Kataoka, N., Fujita, M. and Ohno, M. 2009. Functional association of the Microprocessor complex with the spliceosome. *Mol. Cell. Biol.* **29**: 3243-3254.

Kertesz, M., Iovino, N., Unnerstall, U., Gaul, U. and Segal, E. 2007. The role of site accessibility in microRNA target recognition. *Nat. Genet.* **39**: 1278-1284.

Kim, V.N. and Nam, J.W. 2006. Genomics of microRNA. *Trends Genet.* **22**: 165-173.

Kim, Y.K. and Kim, V.N. 2007. Processing of intronic microRNAs. *EMBO J.* **26**: 775-783.

Kluiver, J., Haralambieva, E., de Jong, D., Blokzijl, T., Jacobs, S., Kroesen, B.J., Poppema, S. and van den Berg, A. 2006. Lack of BIC and microRNA miR-155 expression in primary cases of Burkitt lymphoma. *Genes Chromosomes Cancer* **45**: 147-153.

Kluiver, J., Poppema, S., de Jong, D., Blokzijl, T., Harms, G., Jacobs, S., Kroesen, B.J. and van den Berg, A. 2005. BIC and miR-155 are highly expressed in Hodgkin, primary mediastinal and diffuse large B cell lymphomas. *J. Pathol.* **207**: 243-249.

Kluiver, J., van den Berg, A., de Jong, D., Blokzijl, T., Harms, G., Bouwman, E., Jacobs, S., Poppema, S. and Kroesen, B.J. 2007. Regulation of pri-microRNA BIC transcription and processing in Burkitt lymphoma. *Oncogene* **26**: 3769-3776.

Lagos-Quintana, M., Rauhut, R., Yalcin, A., Meyer, J., Lendeckel, W. and Tuschl, T. 2002. Identification of tissue-specific microRNAs from mouse. *Curr. Biol.* **12**: 735-739.

Landthaler, M., Yalcin, A. and Tuschl, T. 2004. The human DiGeorge syndrome critical region gene 8 and Its D. melanogaster homolog are required for miRNA biogenesis. *Curr. Biol.* **14**: 2162-2167.

Lee, Y., Jeon, K., Lee, J.T., Kim, S. and Kim, V.N. 2002. MicroRNA maturation: stepwise processing and subcellular localization. *EMBO J.* **21**: 4663-4670.

Mader, A., Bruderlein, S., Wegener, S., Melzner, I., Popov, S., Muller-Hermelink, H.K., Barth, T.F., Viardot, A. and Moller, P. 2007. U-HO1, a new cell line derived from a primary refractory classical Hodgkin lymphoma. *Cytogenet. Genome Res.* **119**: 204-210.

Michlewski, G., Guil, S., Semple, C.A. and Caceres, J.F. 2008. Posttranscriptional regulation of miRNAs harboring conserved terminal loops. *Mol. Cell* **32**: 383-393.

Morlando, M., Ballarino, M., Gromak, N., Pagano, F., Bozzoni, I. and Proudfoot, N.J. 2008. Primary microRNA transcripts are processed co-transcriptionally. *Nat. Struct. Mol. Biol.* **15**: 902-909.

Pawlicki, J.M. and Steitz, J.A. 2008. Primary microRNA transcript retention at sites of transcription leads to enhanced microRNA production. *J. Cell Biol.* **182**: 61-76.

Pawlicki, J.M. and Steitz, J.A. 2009. Subnuclear compartmentalization of transiently expressed polyadenylated pri-microRNAs: processing at transcription sites or accumulation in SC35 foci. *Cell. Cycle* **8**: 345-356.

Poliseno, L., Salmena, L., Zhang, J., Carver, B., Haveman, W.J. and Pandolfi, P.P. 2010. A coding-independent function of gene and pseudogene mRNAs regulates tumour biology. *Nature* **465**: 1033-1038.

Rodriguez, A., Vigorito, E., Clare, S., Warren, M.V., Couttet, P., Soond, D.R., van Dongen, S., Grocock, R.J., Das, P.P., Miska, E.A. et al. 2007. Requirement of bic/microRNA-155 for normal immune function. *Science* **316**: 608-611.

Ruggiero, T., Trabucchi, M., De Santa, F., Zupo, S., Harfe, B.D., McManus, M.T., Rosenfeld, M.G., Briata, P. and Gherzi, R. 2009. LPS induces KH-type splicing regulatory protein-dependent processing of microRNA-155 precursors in macrophages. *FASEB J.* **23**: 2898-2908.

Rusca, N. and Monticelli, S. 2011. MiR-146a in Immunity and Disease. *Mol. Biol. Int.* **2011**: 437301.

Saini, H.K., Enright, A.J. and Griffiths-Jones, S. 2008. Annotation of mammalian primary microRNAs. *BMC Genomics* **9**: 564.

Schaadt, M., Diehl, V., Stein, H., Fonatsch, C. and Kirchner, H.H. 1980. Two neoplastic cell lines with unique features derived from Hodgkin's disease. *Int. J. Cancer* **26**: 723-731.

Slezak-Prochazka, I., Durmus, S., Kroesen, B.J. and van den Berg, A. 2010. MicroRNAs, macrocontrol: regulation of miRNA processing. *RNA* **16**: 1087-1095.

Specht, K., Richter, T., Muller, U., Walch, A., Werner, M. and Hofler, H. 2001. Quantitative gene expression analysis in microdissected archival formalin-fixed and paraffin-embedded tumor tissue. *Am. J. Pathol.* **158**: 419-429.

Suzuki, H.I., Arase, M., Matsuyama, H., Choi, Y.L., Ueno, T., Mano, H., Sugimoto, K. and Miyazono, K. 2011. MCPIP1 ribonuclease antagonizes dicer and terminates microRNA biogenesis through precursor microRNA degradation. *Mol. Cell* **44**: 424-436.

Swift, S., Lorens, J., Achacoso, P. and Nolan, G.P. 2001. Rapid production of retroviruses for efficient gene delivery to mammalian cells using 293T cell-based systems. *Curr. Protoc. Immunol.* **Chapter 10**: Unit 10.17C.

Taft, R.J., Simons, C., Nahkuri, S., Oey, H., Korbie, D.J., Mercer, T.R., Holst, J., Ritchie, W., Wong, J.J., Rasko, J.E. et al. 2010. Nuclear-localized tiny RNAs are associated with transcription initiation and splice sites in metazoans. *Nat. Struct. Mol. Biol.* **17**: 1030-1034.

Tam, W. 2001. Identification and characterization of human BIC, a gene on chromosome 21 that encodes a noncoding RNA. *Gene* **274**: 157-167.

Tay, Y., Kats, L., Salmena, L., Weiss, D., Tan, S.M., Ala, U., Karreth, F., Poliseno, L., Provero, P., Di Cunto, F. et al. 2011. Coding-independent regulation of the tumor suppressor PTEN by competing endogenous mRNAs. *Cell* **147**: 344-357.

Thai, T.H., Calado, D.P., Casola, S., Ansel, K.M., Xiao, C., Xue, Y., Murphy, A., Frendewey, D., Valenzuela, D., Kutok, J.L. et al. 2007. Regulation of the germinal center response by microRNA-155. *Science* **316**: 604-608.

Tili, E., Croce, C.M. and Michaille, J.J. 2009. miR-155: on the crosstalk between inflammation and cancer. *Int. Rev. Immunol.* **28**: 264-284.

Trabucchi, M., Briata, P., Garcia-Mayoral, M., Haase, A.D., Filipowicz, W., Ramos, A., Gherzi, R. and Rosenfeld, M.G. 2009. The RNA-binding protein KSRP promotes the biogenesis of a subset of microRNAs. *Nature* **459**: 1010-1014.

Tweeddale, M.E., Lim, B., Jamal, N., Robinson, J., Zalcberg, J., Lockwood, G., Minden, M.D. and Messner, H.A. 1987. The presence of clonogenic cells in high-grade malignant lymphoma: a prognostic factor. *Blood* **69**: 1307-1314.

van den Berg, A., Kroesen, B.J., Kooistra, K., de Jong, D., Briggs, J., Blokzijl, T., Jacobs, S., Kluiver, J., Diepstra, A., Maggio, E. et al. 2003. High expression of B-cell receptor inducible gene BIC in all subtypes of Hodgkin lymphoma. *Genes Chromosomes Cancer* **37**: 20-28.

Vigorito, E., Perks, K.L., Abreu-Goodger, C., Bunting, S., Xiang, Z., Kohlhaas, S., Das, P.P., Miska, E.A., Rodriguez, A., Bradley, A. et al. 2007. microRNA-155 regulates the generation of immunoglobulin class-switched plasma cells. *Immunity* **27**: 847-859.

Xu, D., Takeshita, F., Hino, Y., Fukunaga, S., Kudo, Y., Tamaki, A., Matsunaga, J., Takahashi, R.U., Takata, T., Shimamoto, A. et al. 2011. miR-22 represses cancer progression by inducing cellular senescence. *J. Cell Biol.* **193**: 409-424.

Yeom, K.H., Lee, Y., Han, J., Suh, M.R. and Kim, V.N. 2006. Characterization of DGCR8/Pasha, the essential cofactor for Drosha in primary miRNA processing. *Nucleic Acids Res.* **34**: 4622-4629.

Zhang, T., Nie, K. and Tam, W. 2008. BIC is processed efficiently to microRNA-155 in Burkitt lymphoma cells. *Leukemia* **22**: 1795-1797.

SUPPLEMENTARY FIGURES

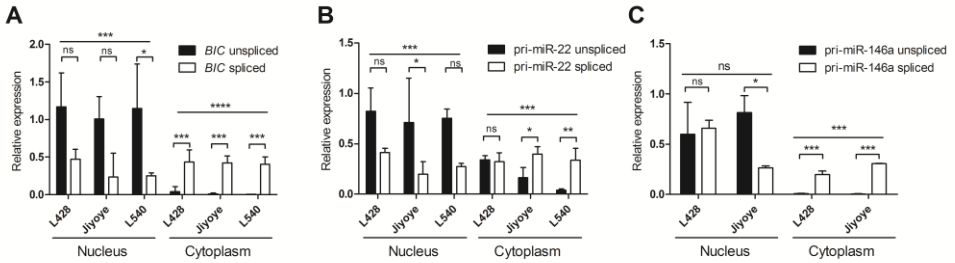

SUPPLEMENTARY FIGURE 1. Levels of unspliced and spliced pri-miRNA transcripts in the cytoplasm and in the nucleus. (A) Unspliced *BIC* transcripts showed significantly higher levels in the nucleus than spliced *BIC* transcripts and lower levels in the cytoplasm. (B) Unspliced pri-miR-22 transcripts were more abundant in the nucleus than spliced pri-miR-22 and less abundant in the cytoplasm of Jiyoye and L540 cells. (C) Unspliced pri-miR-146a transcripts showed significantly higher levels than spliced pri-miR-146a in the nucleus for Jiyoye cells. In the cytoplasm lower levels of unspliced pri-miR-146a were observed compared to levels of spliced transcript for both L428 and Jiyoye cells. Levels of pri-miRNA transcripts in the nucleus or the cytoplasm were calculated relative to their levels in the total fraction and corrected for the amount of RNA per cell. Significance was calculated using 2-way ANOVA and Bonferroni posttest (* $p<0.05$, ** $p<0.01$, *** $p<0.001$, **** $p<0.0001$, ns - not significant).

CHAPTER 4

Marked differences in the miR-17~92 miRNA expression pattern: identification of miR-19b as oncogenic miRNA in non-Hodgkin lymphoma

Izabella Slezak-Prochazka, Jan-Lukas Robertus,
Debora de Jong, Philip Kluin,
Joost Kluiver and Anke van den Berg

In preparation

ABSTRACT

The oncogenic miR-17~92 cluster contains six miRNAs (miR-17, miR-18a, miR-19a, miR-20a, miR-19b and miR-92a) that are expressed at variable levels in different normal and malignant cell types. We determined the level of the primary miR-17~92 transcript, *C13ORF25,* and the expression pattern of the six mature miRNAs in three B-cell subsets, 117 non-Hodgkin lymphoma (NHL) cases and 21 NHL cell lines. Within the normal B-cell subsets, significantly higher *C13ORF25* levels were observed for naïve B cells compared to germinal center B cells. In the NHL cases and cell lines, BL showed the highest *C13ORF25* levels. Among mature miRNAs, miR-92a levels were most abundant in the B-cell subsets, in the MCL, BL and CLL cases and all NHL cell lines. In DLBCL cases the miR-19b levels were much higher than the miR-92a levels. Comparison of the levels of the six mature miR-17~92 miRNAs between the NHL cases and their normal B-cell counterparts indicated the highest induction of miR-19b in cases and cell lines of the four NHL subtypes. We conclude that in normal B cells, CLL, MCL and BL cases miR-92a is the most abundant miRNA of the *C13ORF25* transcript, whereas in DLBCL miR-19b showed the highest expression levels. The highest induction in NHL was observed for miR-19b consistent with its known oncogenic role.

INTRODUCTION

MicroRNAs (miRNA) are a class of noncoding RNAs that are processed from longer endogenous primary transcripts (pri-miRNA). Each mature miRNA can target multiple protein-coding transcripts based on limited sequence homology, which can lead to a block in translation or to mRNA degradation. Targeting depends on the degree of sequence complementarity between the miRNA and target gene. Especially the seed region, i.e. nucleotide 2-7 at the 5'end of the miRNA, has been reported to be crucial for effective targeting. Several miRNAs are organized into so-called polycistrons that contain multiple miRNA stem loop structures in a single primary transcript. Individual miRNAs within such polycistronic transcripts contain the same or highly similar seed sequences in a proportion of miRNAs. Moreover, shared seed homology can also be observed between miRNAs of different or related polycistronic miRNAs (Lewis et al., 2005). These miRNA seed family members are thought to target overlapping sets of genes.

Altered expression of miRNAs has been shown in many cancer types and miRNAs are located within genomic regions that show recurrent chromosomal aberrations in cancer (Klein et al., 2010). Moreover, several animal models support a crucial role for miRNAs in tumorigenesis (Li et al., 2012). A rapidly increasing number of miRNAs that are involved in many cancer related cellular processes, e.g. cell growth, cell death and angiogenesis, have been identified supporting a role for miRNAs in tumorigenesis (O'Donnell et al., 2005).

One well-known oncogenic polycistron is the miR-17~92 host gene, also known as *C13ORF25* or Oncomir-1. *C13ORF25* is located at 13q31-32 and contains six miRNAs (miR-17, miR-18a, miR-19a, miR-20a, miR-19b and miR-92a). Each of these miRNAs has one or more seed family member in the *C13ORF25* gene or in one of the two other homologous miRNA clusters (Tanzer and Stadler, 2004), i.e. the miR-106a~363 cluster on chromosome X and the miR-106b~25 cluster on chromosome 7. Individual miRNAs from the miR-17~92 cluster have been shown to play a role in various cellular processes such as proliferation (Hayashita et al., 2005) and angiogenesis (Dews et al., 2006) and

indicate a role in cancer development. Several members of the miR-17~92 cluster are overexpressed in B-cell lymphoma (Humphreys et al., 2012; Tsuchida et al., 2011) and miR-17~92 has been shown to be the target of the 13q31-32 amplification in diffuse large B-cell lymphoma (DLBCL) (Ota et al., 2004) and mantle cell lymphoma (MCL) (Salaverria et al., 2007). Further proof that members of the miR-17~92 cluster have oncogenic potential was obtained from studies in a MYC mouse model in which expression of miR-17~92 accelerated lymphomagenesis (He et al., 2005). Besides overexpression induced by amplification of the 13q31-32 region, *C13ORF25* was also shown to be upregulated by MYC (Chang et al., 2008). E2F1, a well known MYC target (Matsumura et al., 2003), was targeted by two of the *C13ORF25* miRNAs, i.e. miR-17-5p and miR-20a (O'Donnell et al., 2005). This indicated a complex network between MYC, the E2F family, miR-17-5p and miR-20a (Ji et al., 2011). MiR-19a and miR-19b have been shown to be the major oncogenic components in the *Eμ-myc* transgenic mouse model of B-cell lymphoma, this was at least partly due to the repression of the tumor suppressor Phosphatase and tensin homolog (*PTEN*) (Mu et al., 2009)

The expression of individual members of polycistrons, including *C13ORF25*, has been studied in leukemia cell lines (Yu et al., 2006) and revealed marked differences between levels of miRNAs derived from the same polycistrons, suggesting variation in processing and/or stability of the individual miRNAs. Remarkably, in solid tumors (Li et al., 2012; Tsuchida et al., 2011) as well as in lymphoma (Li et al., 2012; Venturini et al., 2007), often only a single miRNA or a subset of the miRNAs of the miR-17~92 cluster are differentially expressed.

In this study, we determined the relative abundance of the six miRNAs of the *C13ORF25* polycistron in a NHL cohort (n=117) including Burkitt lymphoma (BL), chronic lymphocytic leukemia (CLL), mantle cell lymphoma (MCL) and diffuse large B-cell lymphoma (DLBCL). The aim of this study is to analyze the expression patterns and to determine possible differences in these patterns in B-cell lymphoma in comparison to normal B-cell subsets and between NHL subtypes.

RESULTS

Levels of *C13ORF25* vary in B-cell NHL

C13ORF25 levels were determined by qRT-PCR in normal B-cell subsets, in 117 B-cell NHL samples, including 20 MCL, 19 BL, 50 DLBCL and 28 CLL cases, and in 21 B-cell NHL-derived cell lines. Within the normal B-cell subsets, a significantly higher *C13ORF25* level was observed for naïve B cells compared to GC B cells ($p<0.05$) (Fig. 1A). *C13ORF25* expression within the 117 NHL subtypes revealed marked differences between the four NHL subtypes (Fig. 1B). The levels were the highest in BL and the lowest in CLL (9 fold difference) with marked differences in expression levels between individual cases of each NHL subtype. The BL cases showed a significantly higher *C13ORF25* level compared to CLL ($p<0.001$) and MCL ($p<0.01$). We also observed a significant difference between DLBCL and CLL ($p<0.001$). The overall pattern observed in the NHL cell lines was similar to the NHL cases, but the differences between NHL subtypes were not significant (Fig. 1C) probably due to smaller group sizes. The BL cell lines showed the highest levels of *C13ORF25*, followed by MCL and CLL cell lines, whereas DLBCL cell lines had the lowest levels.

Different levels of the miR-17~92 cluster members in B-cell NHL

We next studied the levels of the six individual members of the *C13ORF25* cluster, i.e. miR-17, miR-18a, miR-19a, miR-20a, miR-19b and miR-92a. Each B-cell subset showed a similar pattern with the highest level observed for miR-92a (up to 60% of the total of all miR-17~92 members together) and the lowest levels for miR-18a and miR-19b (less than 1%) (Fig. 2A). In all three B-cell subsets miR-92a levels were significantly higher than the levels of the other miRNAs ($p< 0.01$). The NHL cases also had significant differences in the levels of each of the six miR-17~92 cluster members. For MCL, BL and CLL, miR-92a was the most abundant miRNA (60-80%) followed by miR-19b (10-30%). In DLBCL, miR-19b was most abundant (~60%), whereas miR-92a levels were much lower (<20%), in the same range as miR-20a and miR-19a.

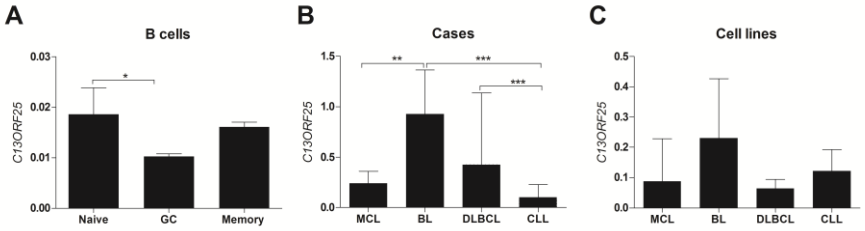

FIGURE 1. Expression levels of *C13ORF25* in normal and malignant B cells. (A) The normal B-cell subsets showed a significant difference in the primary miR-17~92 transcript levels only between naïve and GC B-cell subsets. (B) The B-cell malignancies showed significantly different *C13ORF25* levels that were the highest in BL and the lowest in CLL. *C13ORF25* levels were normalized to an external common calibrator using a comparative threshold cycle method to allow comparison of the levels between the four B-cell malignancies. (C) In the BL cell lines, the levels of *C13ORF25* were significantly higher compared to the DLBCL cell lines. P values were determined using a Kruskal-Wallis test. (*p<0.05, **p<0.01, ***p<0.001)

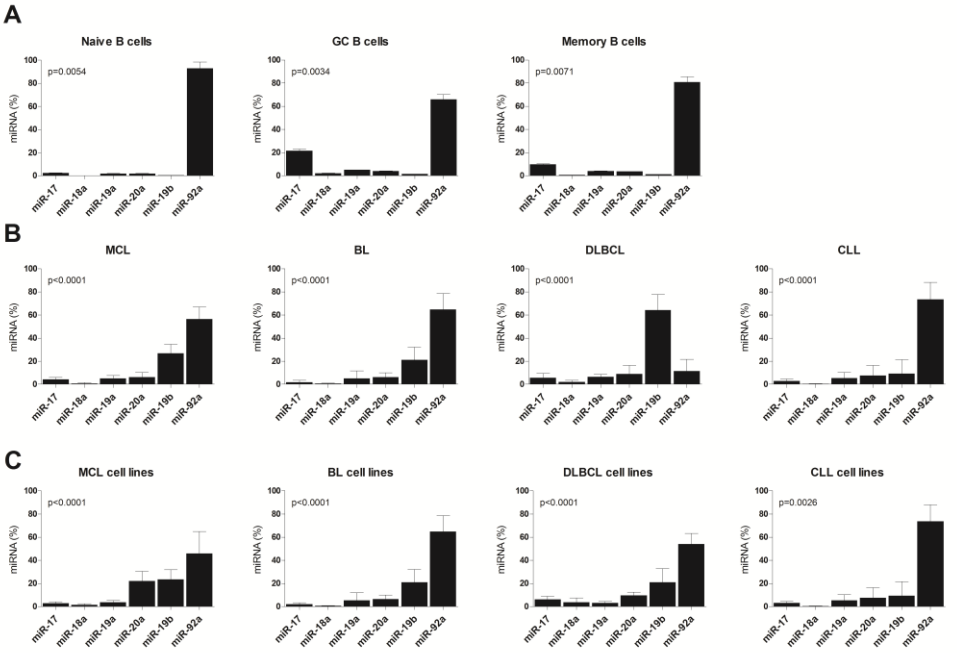

FIGURE 2. Expression patterns of miR-17~92 miRNAs in B cells and NHL. (A) In the normal B-cell subsets miR-92a levels are significantly higher as compared to the levels of the five other miRNAs. (B) The B-cell malignancies MCL, BL and CLL showed the highest levels of miR-92a, whereas in DLBCL a higher level was observed for miR-19b. (C) The cell lines also showed significant differences within the miR-17~92 cluster with the highest levels for miR-92a. P values were determined using a Kruskal-Wallis test.

The cell lines derived from the four NHL subsets showed similar expression patterns, with miR-92a being the most abundant cluster member (45-73%). MiR-19b was the second most abundant in BL and DLBCL (~21%). In MCL, miR-19b and miR-20a levels were similar (~22%) and were the second/third most abundant miRNAs in MCL. In CLL, four of the five remaining miRNAs showed similar low levels (3-8%).

We next studied the correlation between the levels of the six mature miRNAs and the *C13ORF25* levels for all NHL cases and cell lines. In the NHL cases (Fig. 3A), BL cases showed a significant correlation for five of the six miRNAs, i.e. miR-18a ($r=0.50$, $p=0.03$), miR-19a ($r=0.50$, $p=0.03$), miR-20a ($r=0.55$, $p=0.01$), miR-19b ($r=0,92$; $p<0.0001$) and miR-92a ($r=0.70$, $p=0.0008$). Correlations for the other NHL subtypes were less pronounced, with a significant association observed for miR-92a in MCL, miR-20a in DLBCL, miR-17 and miR-19a in CLL. In the NHL cell lines (Fig. 3B) only two significant associations were observed, which is probably due to the lower number of cell lines studied. Both significant associations were observed in BL cell lines, i.e. miR-19b ($r=0.93$, $p=0.007$) and miR-92a ($r=0.82$, $p=0.003$).

A possible explanation for the marked differences in expression of individual cluster members might be caused by differences in efficiency of the qRT-PCR procedure. Therefore, we tested the efficiency of the Taqman miRNA assays on serial dilutions of cDNA from the BL-derived CA46 cell line that had a relative high expression level of all six cluster members. The efficiency ranged from 103% to 109% (Supplementary Fig. 1), with the highest efficiency for miR-17 and the lowest efficiency for both miR-18a and miR-92a. Thus, based on these efficiencies it is highly unlikely that the high miR-92a levels are caused by efficiency differences in the qRT-PCR.

A second explanation for the observed differences might be a high or variable expression of the homologous pri-miR-106a~363 transcript that contains two precursor sequences that are highly homologous to the C13ORF25 precursors of miR-92a and miR-19b and result in identical mature miR-92a and miR-19b. To compare both transcripts, qRT-PCR was performed on 7 MCL, 7 BL, 7 DLBCL and 5 CLL cases. In comparison to the high expression levels of

C13ORF25, the levels of pri-miR-106a~363 were much lower (range 4 to 20 fold) (Supplementary Fig. 2). This indicates that it is unlikely that the high levels of miR-92a and miR-19b in comparison to the other members of the *C13ORF25* cluster can be explained by expression of the homologous pri-miR-106~363 cluster.

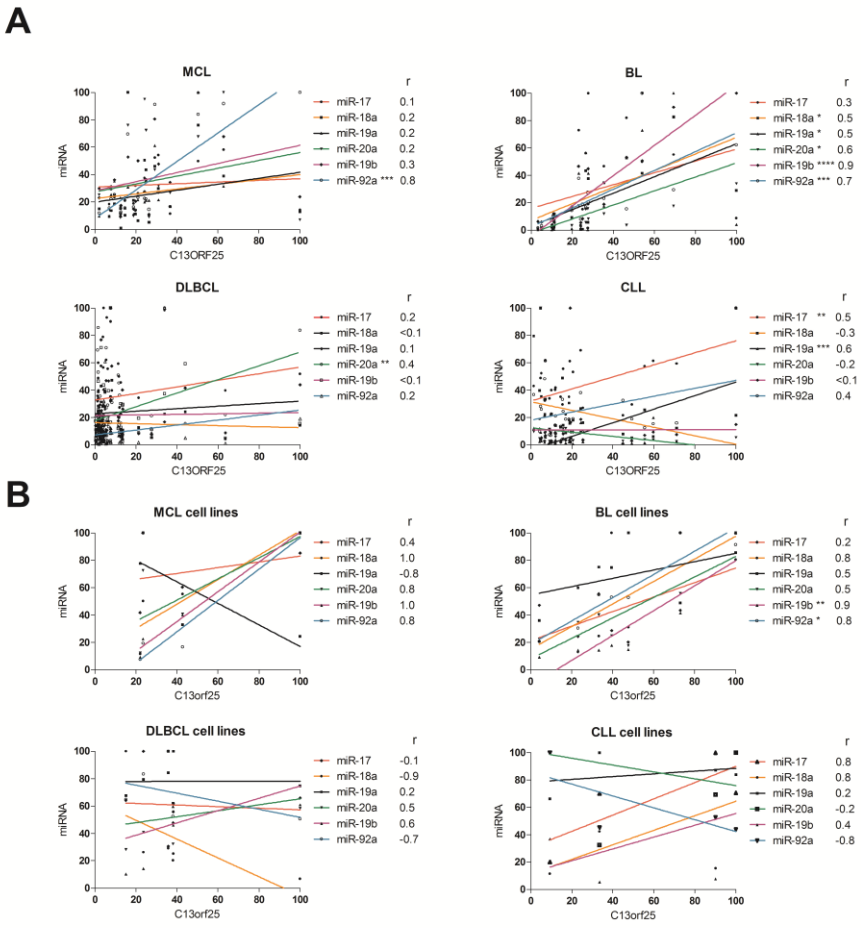

FIGURE 3. Correlation of *C13ORF25* levels with the levels of the six individual miRNAs. (A) In the NHL cases correlations were seen in each of the four NHL subtypes. In MCL and DLBCL, miR-92a showed a significant correlation with *C13ORF25* levels. In BL a significant correlation was seen for five out of the six miRNAs whereas in CLL miR-17 and miR-19a levels showed significant correlations with *C13ORF25* levels. (B) In the NHL cell lines only two significant correlations were observed, i.e. for miR-19b and miR-92a in the BL cell lines. *p<0.05, **p<0.01, ***p<0.001, ****p<0.0001.

A third possibility is that factors influencing the processing efficiency or stability of the individual miRNAs cause differences in mature miRNA levels. KH-type splicing regulatory protein (KSRP) and the RNA binding protein heterogeneous nuclear ribonucleoprotein A1 (HnRNP A1) have been reported to regulate processing of miR-20a and miR-18a, respectively. To identify a possible relation between KSRP levels and the levels of miR-20a, we performed qRT-PCR on 3 MCL, 12 DLBCL, 6 BL, 9 CLL. No relation was observed between KSRP levels and the mature miR-20a levels (data not shown). Immunohistochemical staining of HnRNP A1 in NHL cases showed no difference in expression between tumors with high or low miR-18a levels (data not shown).

Fold induction levels in NHL subtypes

To determine whether the levels of the members of the miR-17~92 cluster are deregulated in NHL we studied the fold induction of the miR-17~92 cluster members for each NHL subtype in relation to their normal B-cell counterparts (Fig. 4). The levels of all miR-17~92 cluster members were increased compared to their normal counter parts albeit at variable levels. The strongest fold increases were observed for miR-19b in all four NHL subtypes. For NHL cases the fold induction for miR-19b ranged from 10-fold for CLL compared to memory B cells to 415-fold for MCL compared to naïve B cells. For the cell lines the fold increase ranged from 746-fold for CLL compared to memory B cells, to 1344-fold for DLBCL compared to GC B cells. For the five other members of the miR-17~92 cluster the fold increase in comparison to normal B cells ranged from 1 to 21 fold for the NHL cases and from 5 to 643 fold for the cell lines. Despite the marked high levels of miR-92a, there was no apparent fold increase as compared to normal B cell subsets. Thus, miR-19b is the most pronounced upregulated member of the miR-17~92 cluster in NHL.

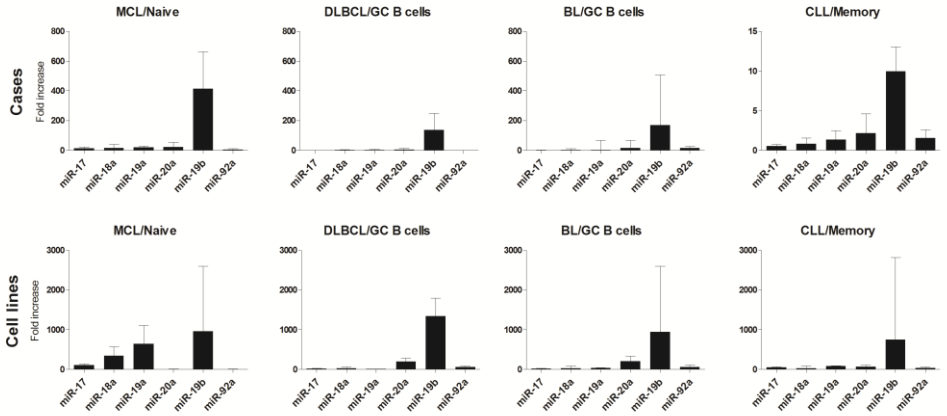

FIGURE 4. Fold induction levels in NHL subtypes. Levels of the mature miRNAs in the NHL cases are given relative to the levels of the mature miRNAs in their bormal B-cell counterparts. The cases all showed a significant fold increase in the expression levels of miR-19b ($p<0.001$). The cell lines also showed a significant fold increase in the expression of miR-19b ($p<0.05$). P values were determined using a Kruskal-Wallis test.

DISCUSSION

In this study we analyzed the expression pattern of the 6 miRNAs that are processed from the noncoding *C13ORF25* transcript in NHL. We showed that normal B cells and each of the four NHL subtypes have a distinct expression pattern for the six miRNAs. MiR-92a was the most abundant miRNA in the normal B-cell subsets and three of the four NHL subtypes, whereas miR-19b was the most abundant cluster member in DLBCL. In comparison to their normal B cell counterparts, all NHL subtypes showed the strongest fold increase for the oncogenic miR-19b.

MYC and 13q31-32 amplification are two well known mechanisms to induce *C13ORF25* in NHL (Navarro et al., 2009; O'Donnell et al., 2005; Ota et al., 2004; Tagawa et al., 2007). We observed significantly different *C13ORF25* levels in each of the four NHL subtypes. BL cases showed the highest *C13ORF25* levels, which is consistent with the genetic hallmark of BL; a translocation of the MYC locus to one of the immunoglobulin loci. The variations in *C13ORF25* levels observed between and within each NHL subtype are most likely caused by

differences in MYC levels and/or the presence of 13q31-32 amplifications in individual cases.

The most abundant miR-17~92 cluster members in B cells and NHL were miR-92a and miR-19b. The miR-106a~363 cluster contains miRNAs that are identical to miR-19b and miR-92a derived from the miR-17~92 cluster (Landais et al., 2007). In the NHL cases the level of *C13ORF25* was always much higher than the level of pri-miR-106a~363. Thus, despite the presence of a homologue cluster that also contains miR-19b and miR-92a, it is unlikely that the higher miR-92a and miR-19b levels in comparison to the four other *C13ORF25* members can be explained by co-expression of the *pri-miR-106a~363* cluster. We next examined the correlation between the primary miRNA transcript and the mature miRNAs to assess possible differences in the biogenesis or stability of individual miRNAs. BL showed a good correlation between C13ORF25 and five of the six cluster members, in the other NHL subtypes the correlation was less obvious. A poor correlation between primary transcript and mature miRNAs has been reported for miR-138 in murine brain and murine neuroblastoma cell line N2A (Obernosterer et al., 2006), let-7 in neural cell specification (Wulczyn et al., 2007) and miR-143 and miR-145 in colorectal adenocarcionoma (Michael et al., 2003). These studies indicate that the levels of primary transcripts do not necessarily correlate with the levels of mature miRNAs.

Two RNA binding proteins, i.e. KSRP and hnRNP A1, have been shown to be involved in biogenesis of certain members of the miR-17~92 cluster. HnRNP A1 facilitates processing of miRNA-18a (Guil and Caceres, 2007) and KSRP enhances biogenesis of a group of miRNAs including miR-20a and miR-106a (Garcia-Mayoral et al., 2007; Trabucchi et al., 2009). We observed no difference in hnRNP A1 staining intensity between tumors with high and low miR-18a levels, indicating that differences in miR-18a levels are not likely due to differences in hnRNP A1 expression. This might in part be caused by the overall low miR-18a levels observed in NHL. Since there was no antibody available that showed a good staining pattern on FFPE tissue sections, we analyzed KRSP by qRT-PCR. KRSP levels showed no relationship to miR-20a expression on a selection of the NHL cases with variable miR-20a levels. There are currently no

known factors that affect biogenesis of miR-19a, miR-19b or miR-92a. Chaulk et al. showed that the tertiary structure of the miR-17~92 transcript *in vitro* is organized in such a way that the miR-92a and miR-19b stem-loops are internalized making them less accessible and thus less efficiently processed (Chaulk et al., 2011). It would be interesting to analyze the structure of this primary transcript in B cells or in NHL cell lines to establish if in this cell type the miR-92a and miR-19b stem-loops are more accessible for processing. Moreover, it may be speculated that despite lower pri-miR-106a~363 levels, accessibility of miR-19b and miR-92a is much better in this transcript, and that a substantial proportion of the mature miR-19b and miR-92a miRNAs are derived from this transcript despite its lower levels.

We observed that miR-92a was the most abundant miRNA in the B-cell subsets, the MCL, BL and CLL cases and in the NHL cell lines. MiR-19b usually was the second most abundant miRNA in the NHL cases and cell lines. In contrast to the MCL, BL and CLL cases, the DLBCL cases showed the highest levels for miR-19b. Analysis of the individual DLBCL cases showed that in 49 of the 50 cases the miR-19b levels were indeed higher than the miR-92a levels (Supplementary Fig. 3). MiR-92a has been shown to be involved in carcinogenesis by suppression of angiogenesis by targeting Integrin α5 (ITGA5) (Bonauer et al., 2009) and by affecting cellular proliferation in colon and hepatocellular carcinoma cell lines (Tsuchida et al., 2011). MiR-92a is overexpressed in a wide variety of cancers, but a role in B-cell lymphomagenesis is less evident. MiR-92a is usually not among the consistently overexpressed miRNAs in profiling studies in NHL (Lawrie et al., 2009; Malumbres et al., 2009; Roehle et al., 2008). He et al. demonstrated that overexpression of a truncated miR-17~19b cluster, thus without miR-92a, cooperates with MYC to promote lymphomagenesis in mouse models (He et al., 2005). This indicates that miR-92a is not essential for the oncogenic effect of the miR-17~92 cluster. We observed no specific induction of miR-92a in comparison to their normal B cell counterparts, despite the high miR-92a levels observed in the majority of the NHL cases. Thus, it is unlikely that miR-92a plays a main role in NHL lymphomagenesis.

Finally, we assessed the putative oncogenic changes of the mature miRNA levels in relation to their normal counterparts. For all four NHL subtypes, miR-19b showed the highest fold increase ranging from 10- to ~1300-fold. It is unclear why only miR-19b and not the closely related miR-19a is induced in the NHL cases and cell lines. This might indicate that targets specific for miR-19b play a role in lymphomagenesis. MiR-19b, together with miR-19a, accelerated the MYC-induced lymphomagenesis in transgenic mice models (Mu et al., 2009; Olive et al., 2009). MiR-19a and miR-19b have also been shown to be significantly upregulated in Cyclin D1-positive MCL patients (Iqbal et al., 2012). Proven targets of miR-19b include protein kinase, AMP-activated, alpha 1 catalytic subunit (Prkaa1), protein phosphatase 2 (PP2a), Bcl-2-like protein 11 (Bim) (Mavrakis et al., 2010), pro-angiogenic protein FGFR2 (Yin et al., 2012) and the tumor suppressor gene *PTEN* (Takakura et al., 2008). PTEN negatively regulates the phosphatidylinosiol-3-kinase (PI3K) pathway (Takakura et al., 2008) and activation of the PI3K pathway is a key element for the malignant transformation of MYC expressing germinal center B cells in a BL mouse model (Sander et al., 2012). Overall, there is strong evidence that miR-19a and miR-19b are important oncogenic miRNAs in NHL pathogenesis. The mechanism of specific upregulation of miR-19b and not the other members of the miR-17-92 cluster in NHL compared to normal B cells is not yet known. It is possible that miR-19b processing is regulated by an unknown regulatory protein that is differential expressed in NHL in comparison to B cells.

In conclusion, we showed that miR-92a is the most abundant miRNA of the miR-17~92 cluster, in normal B cells, CLL, MCL and BL cases. In DLBCL, miR-19b showed the highest levels, and miR-92a was the second most abundant miRNA. Despite high miR-92a levels, we observed the highest fold induction for miR-19b in all four NHL subtypes in comparison to their normal B-cell counterparts, consistent with its known oncogenic role.

MATERIALS AND METHODS

B-cell subsets. B cells were purified from human tonsils obtained from children undergoing routine tonsillectomy as previously described (Koopman et al.,

1994). Briefly, mononuclear cells were isolated by Ficoll-Isopaque density gradient centrifugation. Monocytes and T cells were depleted by plastic adherence and sheep red blood cell (SRBC) rosetting, respectively. The total B cell subset was >97% pure as determined by FACS analyses. To sort the different B cell sub populations (naive B cells, memory B cells and GC B cells), cells were stained with FITC-conjugated anti-human IgD, PE-conjugated anti-human CD20, and allophycocyanin-conjugated anti-CD38 and sorted using a FACS aria (BD Biosciences): naive B cells (CD20+IgD+,CD38-), germinal center B cells (CD20+IgD-CD38+) and memory B cells (CD20+IgD-CD38-).

Patient samples. Formaldehyde Fixed-Paraffin Embedded (FFPE) tissue was obtained from 20 cases of MCL, 19 cases of BL, 50 cases of primary stage I and II nodal and extranodal DLBCL and 28 cases of CLL from the tissue bank at the Department of Pathology, University Medical Center Groningen and the tissue bank at the Department of Pathology, The Netherlands Cancer Institute, Amsterdam (a gift from Dr. D. de Jong). Each case history was reviewed by a hematopathologist and diagnoses were established according to the criteria of the World Health Organization classification. Only cases containing a tumor cell percentage of >80% were used for RNA isolation and qRT-PCR. All protocols for obtaining and studying human tissues and cells were approved by the institution's review board for human subject research.

Cell lines. 21 cell lines were used for the analysis, including 4 MCL cell lines (HBL-2, JEKO-1, GRANTA-519 and UPN-1), 7 BL cell lines (Raji, CA46, BL65, NAMALWA, DG75, Jiyoye and Ramos), 6 DLBCL cell lines (ROSE, VER, SUDHL6, SUDHL4, OCI-Ly3 and SCHI) and 4 CLL cell lines (EHEB, MEC-1, MEC-2 and JVM3). The mantle cell lines UPN-1 and HBL-2 were obtained from Dr. W. Klapper (Kiel, Germany); JEKO-1, Granta-519 and CLL cell lines JVM-3, MEC-1 and MEC-2 were obtained from Deutsche Sammlung von Mikroorganismen und Zellkulturen GmbH (DSMZ, Branschweig, Germany). The Burkitt cell lines DG75 and CA46 were obtained from the American type culture collection (ATCC) (LGC

standards, Middlesex, UK). The DLBCL cell lines SU-DHL-4 and SU-DHL-6 were obtained from A. Epstein (UCLA, Los Angeles, CA).

Cell lines were propagated in DMEM medium containing 10% FBS (Granta-519), IMDM medium containing 20% (OCI-Ly3) or 10% (MEC-1, MEC-2) FBS or RPMI-1640 medium containing 10% FBS (other cell lines) (Cambrex Biosciences, Walkersville, USA) supplemented with ultraglutamine (2mM), penicillin (100U/ml), streptomycin (0.1 mg/ml; Cambrex Biosciences). Cell lines were cultured at 37°C under an atmosphere containing 5% CO2.

Quantitative RT-PCR. RNA isolation from FFPE material of DLBCL, CLL, BL and MCL cases was performed as described previously (Robertus et al., 2009). All samples were DNAse treated using Turbo DNA free kit (Ambion, USA) according to the manufacturer's instructions. Efficiency of the DNase procedure was checked using a multiplex PCR with 5 primer sets specific for different genomic DNA loci and subsequent analysis on a 1.5% agarose gel. No PCR products were seen confirming the effectiveness of the DNAse treatment. RNA concentrations were measured on a NanoDrop® ND-1000 Spectrophotometer (Nano Drop Technologies, Wilmington, Delaware, USA).

For miRNA-specific cDNA synthesis we used 5ng total RNA, the Taqman MicroRNA Reverse Transcription Kit and Taqman miRNA assays for six mature miRNAs of the C13ORF25 cluster. The qPCR reaction was carried out on 0.44ng cDNA using miRNA specific primers in accordance with the instructions supplied by the manufacturer (Applied Biosystems, Foster City, CA, USA). The cDNA synthesis for mRNA was primed with random hexamer primers using Superscript II (Invitrogen, USA) on 200ng of total RNA. SYBR green (Applied Biosystems) was used for the relative quantification of *C13ORF25*, KSRP with 2ng of cDNA input in a 20µl reaction. PCR reactions were performed in triplicate, positive and negative controls were included in each run. Primer sequences used for PCR were as follows, *C13ORF25* forward primer 5'-TGTGATGTTTTGTTGTGGGTTTG-3'; reverse primer 5'-AGTGCTTTCTTTCCAAATATAGGC-3'. Pri-miR-106~363 forward primer 5'-CAGGGATGAATGGGCAGAG-3'; reverse primer 5'-TGCTTCCTACGTCTGTGTGAACA-3'. KSRP: forward primer 5'-

CAGAATACGAATGTGGACAAA-3'; reverse primer; 5'-TCACGTTCCCGGAGGATGT-3'. Quantification was performed using Taqman MicroRNA together with the 7900HT ABI Fast Real-Time PCR system (Applied Biosystems, USA). Fluorescence was quantified with the sequence detection system software SDS (version 2.1, Applied Biosystems, USA). Mean cycle threshold values (Ct) and standard deviations (SD) were calculated for all miRNAs and genes. *U6* was selected as a housekeeping gene to normalize the mRNA and miRNA levels as it showed a uniform expression level in all samples and a sufficiently low threshold Ct value. Cases with a Ct value for *U6* > 30 were regarded to have bad RNA quality and therefore excluded from further analysis. The relative expression levels were expressed as $2^{-\Delta Ct}$.

Given the large number of NHL samples (n=119), qRT-PCR of the NHL cases was performed in separate runs for each of the four subtypes. The comparative threshold cycle method was applied using RNA isolated from a pediatric tonsil obtained during routine tonsillectomy as endogenous reference using the formula $2^{-\Delta\Delta Ct}$ ($\Delta\Delta Ct = (Ct_{\text{sample}} - Ct_{\text{U6 sample}}) - (\Delta Ct_{\text{Tonsil}} - \Delta Ct_{\text{U6 Tonsil}})$). To allow comparison of the levels of the individual members of the miR-17~92 cluster the sum of the $2^{-\Delta Ct}$ values were set at 100%.

To determine the efficiency of the miRNA qPCR, a 2x serial dilution of cDNA of a cell line with relatively high expression of each of the miRNAs was used in a qPCR reaction. The amplification efficiency was calculated based on the dependence of the Ct value on the cDNA dilution using the following equation:

$$\text{Efficiency}(\%) = 2^{-\frac{1}{\text{slope}}-1} \cdot 100 .$$

Immunohistochemistry. HnRNP A1 was stained using ab50492 (Abcam, Cambridge, UK) with tris/EDTA pre-treatment and a 1:100 antibody dilution followed by detection with labeled GaRPO followed by RaGPO and DAB substrate chromagen solution. Slides were lightly counter-stained with hematoxylin before imaging.

Data analysis. To determine significant differences in C13ORF25 and individual miRNAs levels within each NHL subtype a Kruskal-Wallis test was performed with a Dunn's Multiple Comparison Test and a p-value <0.05 was considered significant (GraphPad Prism software, version 5.04). To determine the association between the primary transcript and mature miRNA, Pearson and Spearman's rank correlations together with univariate linear regression were used. A p-value <0.05 was considered significant.

REFERENCES

Bonauer, A., Carmona, G., Iwasaki, M., Mione, M., Koyanagi, M., Fischer, A., Burchfield, J., Fox, H., Doebele, C., Ohtani, K. et al. 2009. MicroRNA-92a controls angiogenesis and functional recovery of ischemic tissues in mice. *Science* **324**: 1710-1713.

Chang, T.C., Yu, D., Lee, Y.S., Wentzel, E.A., Arking, D.E., West, K.M., Dang, C.V., Thomas-Tikhonenko, A. and Mendell, J.T. 2008. Widespread microRNA repression by Myc contributes to tumorigenesis. *Nat. Genet.* **40**: 43-50.

Chaulk, S.G., Thede, G.L., Kent, O.A., Xu, Z., Gesner, E.M., Veldhoen, R.A., Khanna, S.K., Goping, I.S., MacMillan, A.M., Mendell, J.T. et al. 2011. Role of pri-miRNA tertiary structure in miR-17~92 miRNA biogenesis. *RNA Biol.* **8**: 1105-1114.

Dews, M., Homayouni, A., Yu, D., Murphy, D., Sevignani, C., Wentzel, E., Furth, E.E., Lee, W.M., Enders, G.H., Mendell, J.T. et al. 2006. Augmentation of tumor angiogenesis by a Myc-activated microRNA cluster. *Nat. Genet.* **38**: 1060-1065.

Garcia-Mayoral, M.F., Hollingworth, D., Masino, L., Diaz-Moreno, I., Kelly, G., Gherzi, R., Chou, C.F., Chen, C.Y. and Ramos, A. 2007. The structure of the C-terminal KH domains of KSRP reveals a noncanonical motif important for mRNA degradation. *Structure* **15**: 485-498.

Guil, S. and Caceres, J.F. 2007. The multifunctional RNA-binding protein hnRNP A1 is required for processing of miR-18a. *Nat. Struct. Mol. Biol.* **14**: 591-596.

Hayashita, Y., Osada, H., Tatematsu, Y., Yamada, H., Yanagisawa, K., Tomida, S., Yatabe, Y., Kawahara, K., Sekido, Y. and Takahashi, T. 2005. A polycistronic microRNA cluster, miR-17-92, is overexpressed in human lung cancers and enhances cell proliferation. *Cancer Res.* **65**: 9628-9632.

He, L., Thomson, J.M., Hemann, M.T., Hernando-Monge, E., Mu, D., Goodson, S., Powers, S., Cordon-Cardo, C., Lowe, S.W., Hannon, G.J. et al. 2005. A microRNA polycistron as a potential human oncogene. *Nature* **435**: 828-833.

Humphreys, K.J., Cobiac, L., Le Leu, R.K., Van der Hoek, M.B. and Michael, M.Z. 2012. Histone deacetylase inhibition in colorectal cancer cells reveals competing roles for members of the oncogenic miR-17-92 cluster. *Mol. Carcinog.*

Iqbal, J., Shen, Y., Liu, Y., Fu, K., Jaffe, E.S., Liu, C., Liu, Z., Lachel, C.M., Deffenbacher, K., Greiner, T.C. et al. 2012. Genome-wide miRNA profiling of mantle cell lymphoma reveals a distinct subgroup with poor prognosis. *Blood* **119**: 4939-4948.

Ji, M., Rao, E., Ramachandrareddy, H., Shen, Y., Jiang, C., Chen, J., Hu, Y., Rizzino, A., Chan, W.C., Fu, K. et al. 2011. The miR-17-92 microRNA cluster is regulated by multiple mechanisms in B-cell malignancies. *Am. J. Pathol.* **179**: 1645-1656.

Klein, U., Lia, M., Crespo, M., Siegel, R., Shen, Q., Mo, T., Ambesi-Impiombato, A., Califano, A., Migliazza, A., Bhagat, G. et al. 2010. The DLEU2/miR-15a/16-1 cluster controls B cell proliferation and its deletion leads to chronic lymphocytic leukemia. *Cancer. Cell.* **17**: 28-40.

Kluiver, J., van den Berg, A., de Jong, D., Blokzijl, T., Harms, G., Bouwman, E., Jacobs, S., Poppema, S. and Kroesen, B.J. 2007. Regulation of pri-microRNA BIC transcription and processing in Burkitt lymphoma. *Oncogene* **26**: 3769-3776.

Koopman, G., Keehnen, R.M., Lindhout, E., Newman, W., Shimizu, Y., van Seventer, G.A., de Groot, C. and Pals, S.T. 1994. Adhesion through the LFA-1 (CD11a/CD18)-ICAM-1 (CD54) and the VLA-4 (CD49d)-VCAM-1 (CD106) pathways prevents apoptosis of germinal center B cells. *J. Immunol.* **152**: 3760-3767.

Landais, S., Landry, S., Legault, P. and Rassart, E. 2007. Oncogenic potential of the miR-106-363 cluster and its implication in human T-cell leukemia. *Cancer Res.* **67**: 5699-5707.

Lawrie, C.H., Chi, J., Taylor, S., Tramonti, D., Ballabio, E., Palazzo, S., Saunders, N.J., Pezzella, F., Boultwood, J., Wainscoat, J.S. et al. 2009. Expression of microRNAs in diffuse large B cell lymphoma is associated with immunophenotype, survival and transformation from follicular lymphoma. *J. Cell. Mol. Med.* **13**: 1248-1260.

Lewis, B.P., Burge, C.B. and Bartel, D.P. 2005. Conserved seed pairing, often flanked by adenosines, indicates that thousands of human genes are microRNA targets. *Cell* **120**: 15-20.

Li, Y., Vecchiarelli-Federico, L.M., Li, Y.J., Egan, S.E., Spaner, D., Hough, M.R. and Ben-David, Y. 2012. The miR-17-92 cluster expands multipotent hematopoietic progenitors whereas imbalanced expression of its individual oncogenic miRNAs promotes leukemia in mice. *Blood* **119**: 4486-4498.

Malumbres, R., Sarosiek, K.A., Cubedo, E., Ruiz, J.W., Jiang, X., Gascoyne, R.D., Tibshirani, R. and Lossos, I.S. 2009. Differentiation stage-specific expression of microRNAs in B lymphocytes and diffuse large B-cell lymphomas. *Blood* **113**: 3754-3764.

Matsumura, I., Tanaka, H. and Kanakura, Y. 2003. E2F1 and c-Myc in cell growth and death. *Cell. Cycle* **2**: 333-338.

Mavrakis, K.J., Wolfe, A.L., Oricchio, E., Palomero, T., de Keersmaecker, K., McJunkin, K., Zuber, J., James, T., Khan, A.A., Leslie, C.S. et al. 2010. Genome-wide RNA-mediated interference screen identifies miR-19 targets in Notch-induced T-cell acute lymphoblastic leukaemia. *Nat. Cell Biol.* **12**: 372-379.

Michael, M.Z., O'Connor, S.M., van Holst Pellekaan, N.G., Young, G.P. and James, R.J. 2003. Reduced accumulation of specific microRNAs in colorectal neoplasia. *Mol. Cancer. Res.* **1**: 882-891.

Mu, P., Han, Y.C., Betel, D., Yao, E., Squatrito, M., Ogrodowski, P., de Stanchina, E., D'Andrea, A., Sander, C. and Ventura, A. 2009. Genetic dissection of the miR-17~92 cluster of microRNAs in Myc-induced B-cell lymphomas. *Genes Dev.* **23**: 2806-2811.

Navarro, A., Bea, S., Fernandez, V., Prieto, M., Salaverria, I., Jares, P., Hartmann, E., Mozos, A., Lopez-Guillermo, A., Villamor, N. et al. 2009. MicroRNA expression, chromosomal alterations, and immunoglobulin variable heavy chain hypermutations in Mantle cell lymphomas. *Cancer Res.* **69**: 7071-7078.

Obernosterer, G., Leuschner, P.J., Alenius, M. and Martinez, J. 2006. Post-transcriptional regulation of microRNA expression. *RNA* **12**: 1161-1167.

O'Donnell, K.A., Wentzel, E.A., Zeller, K.I., Dang, C.V. and Mendell, J.T. 2005. c-Myc-regulated microRNAs modulate E2F1 expression. *Nature* **435**: 839-843.

Olive, V., Bennett, M.J., Walker, J.C., Ma, C., Jiang, I., Cordon-Cardo, C., Li, Q.J., Lowe, S.W., Hannon, G.J. and He, L. 2009. miR-19 is a key oncogenic component of mir-17-92. *Genes Dev.* **23**: 2839-2849.

Ota, A., Tagawa, H., Karnan, S., Tsuzuki, S., Karpas, A., Kira, S., Yoshida, Y. and Seto, M. 2004. Identification and characterization of a novel gene, C13orf25, as a target for 13q31-q32 amplification in malignant lymphoma. *Cancer Res.* **64**: 3087-3095.

Robertus, J.L., Harms, G., Blokzijl, T., Booman, M., de Jong, D., van Imhoff, G., Rosati, S., Schuuring, E., Kluin, P. and van den Berg, A. 2009. Specific expression of miR-17-5p and miR-127 in testicular and central nervous system diffuse large B-cell lymphoma. *Mod. Pathol.* **22**: 547-555.

Roehle, A., Hoefig, K.P., Repsilber, D., Thorns, C., Ziepert, M., Wesche, K.O., Thiere, M., Loeffler, M., Klapper, W., Pfreundschuh, M. et al. 2008. MicroRNA signatures characterize diffuse large B-cell lymphomas and follicular lymphomas. *Br. J. Haematol.* **142**: 732-744.

Salaverria, I., Zettl, A., Bea, S., Moreno, V., Valls, J., Hartmann, E., Ott, G., Wright, G., Lopez-Guillermo, A., Chan, W.C. et al. 2007. Specific secondary genetic alterations in mantle cell lymphoma provide prognostic information independent of the gene expression-based proliferation signature. *J. Clin. Oncol.* **25**: 1216-1222.

Sander, S., Calado, D.P., Srinivasan, L., Kochert, K., Zhang, B., Rosolowski, M., Rodig, S.J., Holzmann, K., Stilgenbauer, S., Siebert, R. et al. 2012. Synergy between PI3K Signaling and MYC in Burkitt Lymphomagenesis. *Cancer. Cell.* **22**: 167-179.

Tagawa, H., Karube, K., Tsuzuki, S., Ohshima, K. and Seto, M. 2007. Synergistic action of the microRNA-17 polycistron and Myc in aggressive cancer development. *Cancer. Sci.* **98**: 1482-1490.

Takakura, S., Mitsutake, N., Nakashima, M., Namba, H., Saenko, V.A., Rogounovitch, T.I., Nakazawa, Y., Hayashi, T., Ohtsuru, A. and Yamashita, S. 2008. Oncogenic role of miR-17-92 cluster in anaplastic thyroid cancer cells. *Cancer. Sci.* **99**: 1147-1154.

Tanzer, A. and Stadler, P.F. 2004. Molecular evolution of a microRNA cluster. *J. Mol. Biol.* **339**: 327-335.

Trabucchi, M., Briata, P., Garcia-Mayoral, M., Haase, A.D., Filipowicz, W., Ramos, A., Gherzi, R. and Rosenfeld, M.G. 2009. The RNA-binding protein KSRP promotes the biogenesis of a subset of microRNAs. *Nature* **459**: 1010-1014.

Tsuchida, A., Ohno, S., Wu, W., Borjigin, N., Fujita, K., Aoki, T., Ueda, S., Takanashi, M. and Kuroda, M. 2011. miR-92 is a key oncogenic component of the miR-17-92 cluster in colon cancer. *Cancer. Sci.* **102**: 2264-2271.

Venturini, L., Battmer, K., Castoldi, M., Schultheis, B., Hochhaus, A., Muckenthaler, M.U., Ganser, A., Eder, M. and Scherr, M. 2007. Expression of the miR-17-92 polycistron in chronic myeloid leukemia (CML) CD34+ cells. *Blood* **109**: 4399-4405.

Wulczyn, F.G., Smirnova, L., Rybak, A., Brandt, C., Kwidzinski, E., Ninnemann, O., Strehle, M., Seiler, A., Schumacher, S. and Nitsch, R. 2007. Post-transcriptional regulation of the let-7 microRNA during neural cell specification. *FASEB J.* **21**: 415-426.

Yin, R., Bao, W., Xing, Y., Xi, T. and Gou, S. 2012. MiR-19b-1 inhibits angiogenesis by blocking cell cycle progression of endothelial cells. *Biochem. Biophys. Res. Commun.* **417**: 771-776.

Yu, J., Wang, F., Yang, G.H., Wang, F.L., Ma, Y.N., Du, Z.W. and Zhang, J.W. 2006. Human microRNA clusters: genomic organization and expression profile in leukemia cell lines. *Biochem. Biophys. Res. Commun.* **349**: 59-68.

SUPPLEMENTARY FIGURES

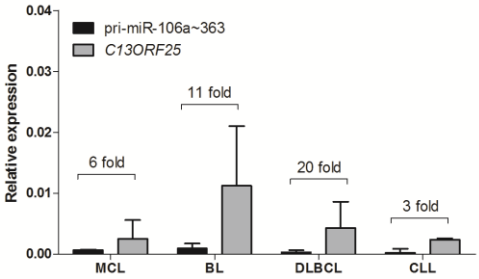

SUPPLEMENTARY FIGURE 1. Relative expression of *C13ORF25* and pri-miR-106a~363. In the four NHL subtypes *C13ORF25* levels were higher than the levels of the homolog pri-miR-106a~363 cluster.

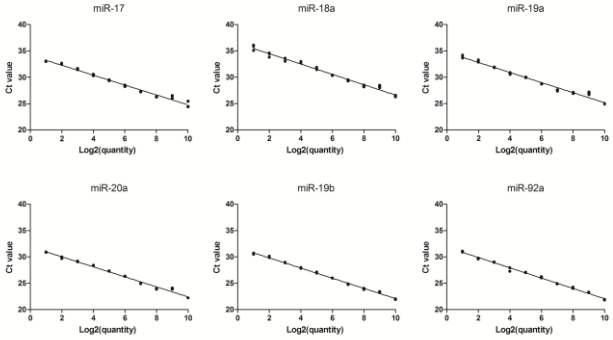

	Ct value (Log2=10)	Efficiency (%)
miR-17	24.8	109
miR-18a	26.4	103
miR-19a	25.0	106
miR-20a	22.2	107
miR-19b	22.0	105
miR-92a	21.8	103

SUPPLEMENTARY FIGURE 2. Efficiency of qRT-PCR procedure. Using a sample with relative high levels of all six cluster members the PCR efficiency was determined. The efficiencies ranged from 103% for miR-92a to 109% for miR-17.

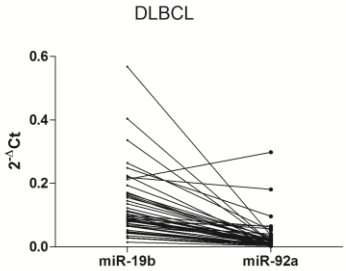

SUPPLEMENTARY FIGURE 3. Expression levels of miR-19b and miR-92a in individual DLBCL cases. To determine if the relative high expression of miR-19b in contrast to miR-92a is due to extreme outliers, the levels of both miRNAs were compared separately for each DLBCL case. Only one DLBCL case showed a higher level of miR-92a compared to miR-19b.

CHAPTER 5

Generation of miRNA sponge constructs

Joost Kluiver, Izabella Slezak-Prochazka,
Katarzyna Smigielska-Czepiel, Nancy Halsema,
Bart-Jan Kroesen and Anke van den Berg

Methods. 2012 Jul; 58: 113–7

ABSTRACT

MicroRNA (miRNA) sponges are RNA molecules with repeated miRNA antisense sequences that can sequester miRNAs from their endogenous targets and thus serve as a decoy. Stably expressed miRNA sponges are especially valuable for long-term loss-of-function studies and can be used *in vitro* and *in vivo*. We describe here a straightforward method to generate retroviral miRNA sponge constructs using a single directional ligation reaction. This approach allows generation of sponges containing more than 20 miRNA binding sites. We provide a basis for the design of the sponge constructs with respect to the sequence of the miRNA binding site and the sequences flanking the miRNA binding sites. *In silico* validation approaches are presented to test the predicted efficiencies of the sponges in comparison to known target genes. In addition, we describe *in vitro* validation experiments to confirm the effectiveness of the miRNA sponges. Finally, we describe how the described procedure can be adapted to easily generate sponges that target multiple miRNAs simultaneously. In summary, our approach allows rapid generation of single or combination miRNA sponges that can be used for long-term miRNA loss-of-function studies.

INTRODUCTION

Several approaches have been described to study the effect of miRNA loss-of-function in a specific cell type of interest, e.g. using microRNA (miRNA) antisense inhibitor oligonucleotides, knockout animal models and miRNA sponges or decoys (Brown and Naldini, 2009; Ebert et al., 2007; Kloosterman et al., 2007; Krutzfeldt et al., 2005; Park et al., 2010). Inhibitor oligonucleotides are effective for short-term (24h – 72h) experiments. However, these synthetic oligonucleotides are expensive and not very suitable for long-term experiments due to degradation and dilution caused by cell proliferation. MiRNA knockout animal models that are the method of choice for functional *in vivo* studies and conditional models allow studying the effect of miRNA knockout in specific cell types or at specific time points during development. An important disadvantage is the time-consuming procedures and costs to generate knockout animals. Moreover, generation of miRNA knockout animals may be technically challenging as a large percentage of miRNAs are located within protein-coding genes, are part of a miRNA cluster or have multiple copies on the genome. MiRNA sponges or decoys are *in vivo* expressed transcripts that contain multiple high affinity miRNA antisense binding sites (MBS). These transcripts can efficiently sequester specific miRNAs and, thereby, prevent their binding to endogenous target genes (Ebert and Sharp, 2010; Kumar et al., 2008; Papapetrou et al., 2010). The experimental application of miRNA sponge technology has met increasing interest for *in vitro* and *in vivo* applications, indicating that this approach can greatly aid to the understanding of miRNA functioning (Chaudhuri et al., 2012; Liu et al., 2012; Ma et al., 2011; Otaegi et al., 2011; Zhu et al., 2011).

Besides the strategy described by us, two different approaches have been described for the generation of miRNA sponges with multiple MBS. The first approach is based on the non-directional concatemerization of oligonucleotide duplexes followed by a ligation of 5’ and 3’ adapters and ligation into the vector of choice (Ebert et al., 2007). This method is relatively inefficient due to the non-directional cloning and multiple ligation steps. The second approach uses long oligonucleotides with two (~50-mers) or four MBS (~100-mers) that are

designed with appropriate restriction enzyme overhangs to allow direct directional cloning into a vector (Brown et al., 2007; Papapetrou et al., 2010). A disadvantage of this method is that only a limited number of MBS can be cloned, which may not be sufficient to sequester all endogenous miRNAs. We have developed a novel approach that allows rapid and efficient generation of miRNA sponges with varying sizes using a single ligation reaction (Kluiver et al., 2012). Effectiveness of the sponges was shown by demonstrating effects on cell growth in GFP proliferation assays, modulation of luciferase activity in luciferase reporter assays and presence of the sponge transcripts in the Ago2 immunoprecipitation fraction of cell lines that overexpress the sponge constructs. Here, we provide a detailed description of the design and cloning strategy to generate miRNA sponge constructs and to validate their effectiveness *in vitro*.

MATERIALS

MiRNA sponge design

Sense and antisense oligonucleotides containing two miRNA binding sites separated by a short sequence ("spacer") and 5'phosphates are ordered PAGE purified at a 100nmol scale (IDT, Coralville, IO, USA). The oligonucleotide duplexes are designed with overhangs that are compatible with the restriction endonuclease SanDI (Fermentas, St. Leon-Rot, Germany) to enable directional cloning of multiple oligonucleotide duplexes (Fig. 1a). As a negative control, a sponge with a similar design but a scrambled seed sequence (i.e. nucleotide 2-8) can be used. Combination sponges (combi-sponges) for the simultaneous inhibition of multiple miRNAs of interest can be ordered as minigenes (IDT). PITA (http://genie.weizmann.ac.il/pubs/mir07/mir07_prediction.html, Kertesz et al., 2007); and STarMir (http://sfold.wadsworth.org/cgi-bin/STarMir.pl, Long et al., 2007) software applications are used to predict RNA folding and accessibility of the miRNA binding site, as well as the specificity and binding capacity of the sponge transcripts.

MiRNA sponge cloning

For the construction of miRNA sponges starting with oligonucleotide duplexes, we use the compatible ends of the interrupted palindromic SanDI restriction site. To allow cloning and subsequent studies, we adapted the pMSCV-PIG vector (Addgene, www.addgene.org, plasmid 21654) by inserting a SanDI restriction site containing linker between the XhoI and EcoRI restriction sites yielding pMSCV-PIG-sp (Fig. 1b).

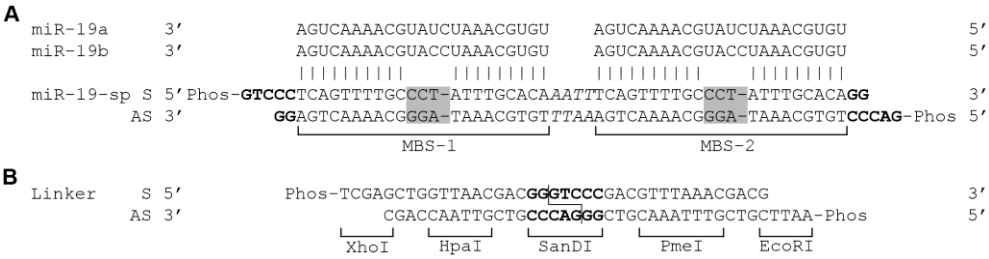

FIGURE 1. Example of a MBS oligonucleotide duplex design and a SanDI linker (A) Oligonucleotide design used to generate a miR-19 bulged sponge. Shown are the sense and antisense sequences of the miR-19 sponge and how the sense strand can bind to miR-19a and miR-19b. SanDI compatible ends are depicted in bold, the grey box indicates the bulge in the miRNA binding site, and the spacer sequence is depicted in italic. (B) The linker design used to introduce a SanDI restriction enzyme recognition site in the pMSCV-PIG vector. A 5′ Xho-I site and a 3′ EcoRI site were added to the ends of the linker for efficient subcloning. Besides a SanDI site (bold) for the generation of miRNA sponges, two other restriction sites were added to allow flexibility for potential further subcloning. Sp = sponge, S = sense, AS = antisense, MBS = miRNA binding site and Phos = phosphate group

The pMSCV-PIG-sp vector is prepared for oligonucleotide duplex ligation by digestion with SanDI and dephosphorylation with CIAP (1 U/ul, Invitrogen, Carlsbad, CA, USA). For ligation of minigenes, the vector should be restricted with EcoRI and XhoI (NEB, Ipswich, MA, USA). Digested vectors are gel purified using a DNA gel extraction kit (Zymoclean Gel DNA recovery kit, Zymo Research, Irvine, CA, USA). For the ligation reaction, T4 DNA ligase is used (Invitrogen). Additional material needed for transformation of the ligation reaction and screening of colonies include competent E. coli cells, SOC medium, waterbath, agar plates with appropriate antibiotic (ampicillin for pMSCV-PIG-sp), incubator, PCR reagents (for colony PCR using pMSCV-PIG-sp: forward primer =

5'-TTTATCCAGCCCTCACTCC-3', reverse primer = 5'-TTGTGTAGCGCCAAGTGCC-3') and PCR machine to screen for insert-containing colonies and a plasmid isolation kit.

In vitro validation of sponge efficiency

Luciferase assay

MicroRNA sponge sequences are subcloned into the 3'UTR of the Renilla luciferase gene in the psiCHECK2 vector (Promega, Madison, USA). For transfection of HEK293 cells, the Amaxa nucleofector I device (Amaxa, Gaithersburg, USA) is used with solution V, program Q-01. MiRNA inhibitor oligonucleotides are designed as previously described (Kluiver et al., 2012) (Exiqon, Vedbaek, Denmark). MiRNA precursors are purchased from Ambion (Life technologies, Grand Island, NY, USA). For assessment of Renilla and Firefly activity the Dual-luciferase Reporter assay (Promega) is used. Luciferase activity is measured on a Luminoskan luminometer (Thermo scientific, Asheville, NC, USA).

Ago2-IP

Ago2-IP procedure and material details were fully described previously (Tan et al., 2009; Tan et al., 2011). The anti-Ago2 antibody clone 2E12-1C9 (Abnova, Taipei, Taiwan) is used for the IP procedure.

METHODS

MiRNA sponge design

Oligonucleotide and minigenes composition

The method of choice for the generation of miRNA sponges may depend on number of miRNAs that need to be targeted simultaneously with a single sponge construct. For the generation of sponges that target one or two miRNAs, the oligonucleotide duplex approach can be used. For the generation of sponges

targeting more than two miRNAs, the minigene approach is more efficient (Fig. 2). As an appropriate negative control for both approaches, one may generate the sponge sequence harboring a scrambled miRNA seed-binding region.

For the oligonucleotide duplex approach, oligonucleotides are designed with two identical MBS, in case one miRNA is inhibited, or two different MBS, in case two miRNAs are inhibited simultaneously (Fig. 1A). Each MBS is the antisense sequence of the miRNA to be studied, with a central mismatch at position 9-12 of the miRNA sequence ("bulge"). This bulge is created by deletion of one nucleotide and changing the remaining three nucleotides in such a way that chance of base paring (including G-U wobbling) is minimal. The two MBS are separated by a short 4-6nt sequence ("spacer"). The 5′ and 3′ ends of the oligonucleotide duplex consist of overhangs that are compatible with the SanDI restriction endonuclease. This enzyme recognizes a 7-bp interrupted palindromic sequence, i.e. 5′-GGGWCCC-3′ (W = A or T), and produces 3nt long 5′ protruding ends that will enable directional ligation of the oligonucleotide duplexes.

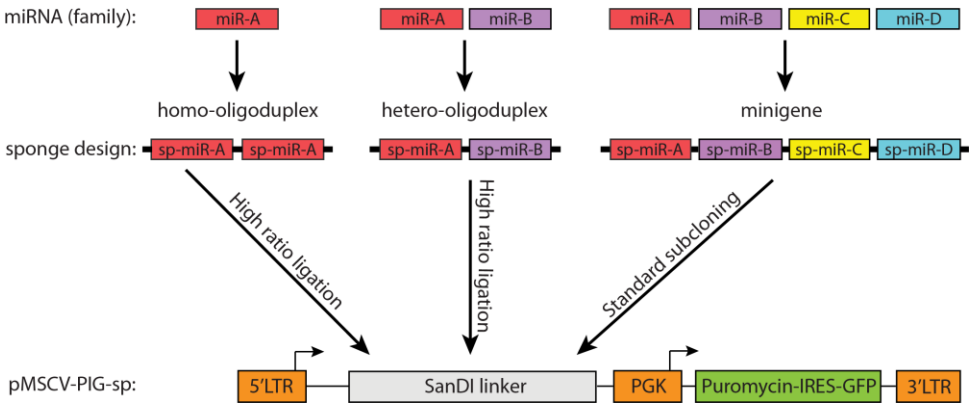

FIGURE 2. Scheme for the selection of the most appropriate cloning strategy for generation of sponges with MBS for one, two, or more than two miRNAs. Sp = sponge, LTR = long terminal repeat, PGK = phosphoglycerate kinase, IRES = internal ribosome entry site, GFP = green fluorescent protein.

For the cloning of minigenes, the same approach is applied. For directional cloning, 5'-XhoI and 3'-EcoRI sites are added to the minigene design. A pre-selected number of MBS for each miRNA can be included (see also hints section 4.4). Increase in the total number of MBS will increase the size and thus also the cost of the minigene. Different spacers between MBS may be used and the order of MBS can be shuffled. Testing the effects of these variations using *in silico* validation will aid in maximizing the binding efficiency of the miRNA sponge to each of the selected miRNAs (see next paragraph).

In silico validation of sponge specificity and binding efficiency

To optimize the sequence of the desired sponges, two published algorithms, i.e. PITA (Kertesz et al., 2007) and STarMir are used with standard settings (Long et al., 2007). For this *in silico* analysis, the full RNA transcript as generated from the vector of interest plus the desired number of MBS is uploaded in the program. For our pMSCV-PIG-sp vector this included the end of the psi packaging signal up to the start of the PGK promoter resulting in a transcript of 466bp + the length of the sponge sequence. Based on different RNA folding computations, both algorithms predict the effectiveness of the designed MBS in the sponges by calculating the difference between the free energy gained by binding of the miRNA to the MBS and the free energy lost by unwinding of the MBS nucleotides (ΔΔG (PITA) and ΔG_{total} (STarMiR)). The PITA algorithm also provides information on all other miRNAs that can potentially bind to the sponge sequence. The binding energy of the miRNA to the sponge transcript can be compared with the binding energy of experimentally proven endogenous targets. By varying sequences within the sponge, a design that has a high free energy gain upon miRNA binding to most or all MBS and minimal off-target miRNA binding can be generated. Variations that can be tested include nucleotide composition, length of the spacer sequence and the nucleotide sequence in the bulge region (position 9-12) of the MBS. In case the oligonucleotide duplex approach is used, one can also vary the nucleotide in the middle of the SanDI restriction site (A or T). Care should be taken to ensure the SanDI site in the cloning vector is compatible with the A or T choice in the SanDI compatible

overhangs of the oligonucleotide duplex. It is important to also test the scrambled seed-binding control constructs to rule out the possibility of creation of novel off-target effects.

MiRNA sponge cloning

Oligonucleotide duplex generation

Oligonucleotides are dissolved to 50µM in STE^{-4} (100mM NaCl, 10mM Tris/HCl, 1mM EDTA, pH 8.0). Sense and antisense oligonucleotides are mixed at a 1:1 ratio resulting in a final concentration of 25µM for each oligonucleotide. Oligonucleotide mixtures are placed in boiling water for 10 minutes and slowly cooled to room temperature to allow annealing of the two oligonucleotides (let boiling water slowly cool to room temperature in approx. 30 minutes). Store oligonucleotide duplexes at -20°C.

Preparation of cloning vector

The pMSCV-PIG-sp vector is digested with SanDI according to the reaction conditions recommended by the supplier. After completion of the restriction enzyme reaction (check small aliquot on 0.7% agarose gel) add 1µl CIAP and incubate for an additional 5 minutes at 37°C to dephosphorylate the sticky ends of the vector. Enzymes are inactivated by incubation at 65°C for 10 minutes. When cloning minigenes, the pMSCV-PIG-sp vector should be digested with EcoRI and XhoI. Gel-purify the restricted and dephosphorylated vector using a DNA gel extraction kit. After purification, the DNA concentration is measured on a NanoDrop.

Ligation reaction

For ligation of sponge oligonucleotide duplexes into the vector, a vector/insert ratio of 1:300 or 1:1000 is recommended. A higher ratio results in an average longer insert size at the cost of a lower number of clones. The number of MBS we obtained varied between 2-16 (average 6) for a ratio of 1:300 and 2-22 (average 7.5) for a ratio of 1:1000 (Table 1). To calculate the amount of vector

and oligonucleotide duplexes required for the ligation the following formula is used: ng insert = { (bp insert * ng vector) / bp vector } * ratio. For efficient ligation, a minimum of 50-100ng of digested vector is recommended. Ligation reactions are performed in 10µl with 1µl 5U/µl T4 DNA ligase in the buffer supplied by the manufacturer. In addition, it is recommended to perform ligation control reactions to be able to determine whether the prepared vector is efficiently digested and dephosphorylated (see troubleshooting section, 5.1). For the minigene cloning strategy, inserts with 5'XhoI – 3'EcoR1 overhangs are ligated at a standard 1:3 ratio into the pMSCV-PIG-sp vector. The ligation reaction is performed by incubation at room temperature for 30 minutes. Approximately 10ng DNA (vector + insert) of the ligation reaction is used for standard transformation to *E. coli* and at least two different amounts of the transformed bacteria culture are plated on agar plates.

TABLE 1. Expected number of MBS per clone upon ligations with different vector/insert ratios.

Ratio vector/insert	# MBS/insert	Median # MBS/insert	Mean # MBS/insert
1:3	2-8	2	3.2
1:100	2-10	5	5.5
1:300	2-16	6	6.0
1:1000	2-22	6	7.5

Check presence and length of insert

As a rapid screen to select clones with the desired number of MBS, a colony PCR can be done. Mark the selected colonies and pick part of the colony with a sterile toothpick and re-suspend the bacteria in 100µl water. Boil samples for 10 minutes, spin tubes and use 1ul of the supernatant as template DNA for an insert PCR using primers that flank the multiple cloning site. Run PCR products on an agarose gel. The size of the PCR product indicates the number of MBS present in the selected clone (empty vector PCR product for pMSCV-PIG-sp is 144bp). Select the clones with the desired insert sizes, grow bacteria on a large scale and isolate plasmid DNA (Qiagen, Venlo, the Netherlands). These clones

are submitted for Sanger sequencing to confirm the insert sequence (LGC genomics, Berlin, Germany).

In vitro validation of sponge efficiency

Luciferase assay

To validate the effectiveness of the sponge transcript to bind to the desired miRNA, the entire sponge is subcloned into the 3'UTR of the Renilla luciferase gene of the dual-luciferase reporter vector psiCHECK2 using XhoI and PmeI restriction sites. HEK293 cells or other easy to transfect cells can be used for these experiments. One million HEK293 cells are transfected with 2µg of each construct with or without miRNA precursor (100nM) or inhibitor (20µM). Harvest cells after 24 hours and make cell lysates for luciferase measurement according to the manufacturer's protocol. Renilla and Firefly activities are measured in duplicate for each transfection and each transfection is performed at least in triplicate to obtain robust results. A decreased Renilla to Firefly luciferase ratio is expected upon transfection with the miRNA precursor, while transfection with the miRNA inhibitor should lead to an increase in the Renilla to Firefly luciferase ratio.

Ago2-IP

To confirm that the miRNA containing RISC complexes are bound to the miRNA sponge transcripts, an Ago2 immunoprecipitation can be performed. Sponge transcripts should be enriched in the IP fraction similar to endogenous miRNA targets. The immunoprecipitation of Ago2-containing protein-RNA complexes is described in detail elsewhere (Tan et al., 2011). In short, 15-30 million cells that express the miRNA and the miRNA sponge of interest are lysed. The cleared supernatant is incubated with sepharose beads coated with Ago2 or IgG control antibody at 4°C overnight. After washing, total, flow-through and immunoprecipitated fractions are harvested for protein and RNA isolation. Western blot is used to show that Ago2 is enriched in the

IP fraction and thus confirm effectiveness of the IP procedure. QRT-PCR of the sponge transcripts is performed to determine enrichment in the Ago2 IP fraction as compared to the IgG control IP, the total cell lysate and the IP flow-through fractions.

HINTS

Targeting seed-families

Several miRNAs have seed family members at different genomic loci that most likely have a large overlap in their target genes and thus have similar functions. In general, the miRNA sequences of these seed family members are highly similar and oligonucleotides may be designed in such a way that all members can be targeted simultaneously. If this is not possible, two slightly different MBS can be made within the oligonucleotide to enable optimal binding of all individual miRNA seed family members. The sponge approach thereby allows an effective loss-of-function analysis of entire seed families.

Generation of combi-sponges

For the generation of combi-sponges that target two unrelated miRNAs, a strategy similar to the single sponge procedure can be followed. The principle difference is that the oligonucleotides contain two different miRNA binding sites. For the generation of sponges with binding sites for multiple miRNAs, e.g. MBS for all miRNAs of a specific miRNA cluster; it may be more convenient to use a minigene approach. In this way the number of binding sites for each miRNA can be easily selected. Also for these constructs, the binding efficiency and availability of each binding site should be checked using the STarMir and/or PITA software.

Bulged or perfect MBS sponges

Bulged miRNA sponges are reported to be more effective for the sequestration of miRNAs than perfect antisense sponges (Ebert et al., 2007; Gentner et al.,

2009; Haraguchi et al., 2009). Consistent with these findings we also showed that miR-19 bulged MBS sponges are effective inhibitors of miR-19 driven proliferation while miR-19 perfect MBS sponges are not (Kluiver et al., 2012). This difference may be caused by degradation of the sponge transcripts due to endonucleolytic cleavage activity of the Ago2 complex upon perfect binding of the miRNA to its binding site. Thus, perfect MBS may be more suitable for the induction of degradation of a transcript upon binding of the miRNA.

Number of MBS per sponge

Several factors may influence the number of MBS in a sponge needed for maximal miRNA inhibition for a specific cell type, i.e. the miRNA expression levels, the miRNA sponge transcript levels and the miRNA binding efficiency of the MBS of endogenous targets. We showed that when comparing miR-19 sponges with 2, 6 or 12 MBS, 6 MBS appeared to be sufficient for maximal miR-19 mediated inhibition of WEHI-231 cell growth (Kluiver et al., 2012). In a study utilizing neuroblastoma cells, a miRNA sponge construct containing 12 miR-9 MBS was reported to be more effective than 6 or 24 miR-9 MBS (Otaegi et al., 2011). Thus, for each experimental setting the optimal or minimal number of MBS needed may vary and should be determined experimentally. The fact that increasing the number of MBS in the sponge construct does not, by definition, correlate with increased effectiveness of functional miRNA sequestration may be explained by increased sponge transcript degradation caused by the high number of MBS. In our experience sponges with 6-12 MBS are a good starting point for testing functional effects of long-term miRNA inhibition.

TROUBLESHOOTING

Ineffective cloning results

If no or only a few colonies are obtained, vector preparation, ligation efficiency or the transformation procedure might have failed. To check the efficiencies of each of these steps the following negative and positive controls can be performed. Transformation of digested non-ligated vector should yield no or only

a very few colonies to confirm that the vector was efficiently digested. To test the dephosphorylation step, a ligation reaction without insert can be performed which again should yield no or only a few colonies upon transformation. To test the T4-DNA-ligase, a ligation reaction with digested vector which has not been dephosphorylated can be performed. After transformation a high number of colonies (>500) should be obtained. To test transformation efficiency, a control circular plasmid vector can be transformed and this should yield a high number of colonies (>1,000). For optimal transformation, an aliquot of the ligation reaction containing a maximum of 10ng of DNA (plasmid and oligonucleotide duplex) should be used (too much DNA input is toxic and will result in a lower number of colonies). To increase the efficiency of the ligation reaction in general, the vector concentration can be increased from 50ng to 200ng per 10µl ligation reaction. To increase the number of colonies the vector/oligonucleotide duplex ratio can be lowered to 1:100. However, this will result in a decrease of the average insert size (Table1).

Sponges have no (obvious) functional effect

When there is a known functional readout for the miRNA of interest and no or little effect is observed upon overexpression of the sponge this may indicate ineffective sequestration of the miRNAs by the sponge. A sponge containing more MBS may be tested or a new sponge with an altered design of the oligonucleotide duplexes can be tested. In addition, the expression level of the sponge transcript may be checked in relation to the level of the endogenous miRNA. In case the expression levels of the sponge are low and the levels of the endogeneous miRNAs of interest are high, testing different promoters for the sponge transcript may help to achieve an optimal balance between the expression level of the sponge and the edogeneous miRNA. Suitable strong promoters include PGK, EF1α, MSCV, SFFV and CMV promoters (Hong et al., 2007). Selection of the most optimal promoter depends on the cell type of interest and the application.

In case the miRNA loss-of-function phenotype is not known, it may be difficult to determine the effectiveness of the sponge. To ensure effective

binding of the miRNAs to the sponge a luciferase reporter assay may be performed or enrichment of the sponge transcripts in the Ago2-IP fraction following Ago2 immunoprecipitation may be tested.

SUMMARY

We describe a method that allows straightforward generation of retroviral miRNA sponges with a selected number of MBS that can target one or more miRNAs simultaneously. We also provide *in silico* and *in vitro* approaches to verify the (putative) effectiveness of miRNA binding to the miRNA sponges. The practical guidelines to generate miRNA sponges described here will contribute to our understanding of the role of miRNAs in diverse biological processes.

ACKNOWLEDGEMENTS

This work was supported by the Dutch Cancer Society [RUG 2009-4279 to B.J.K. and A.v.d.B.].

REFERENCES

Brown, B.D., Gentner, B., Cantore, A., Colleoni, S., Amendola, M., Zingale, A., Baccarini, A., Lazzari, G., Galli, C. and Naldini, L. 2007. Endogenous microRNA can be broadly exploited to regulate transgene expression according to tissue, lineage and differentiation state. *Nat. Biotechnol.* **25**: 1457-1467.

Brown, B.D. and Naldini, L. 2009. Exploiting and antagonizing microRNA regulation for therapeutic and experimental applications. *Nat. Rev. Genet.* **10**: 578-585.

Chaudhuri, A.A., So, A.Y., Mehta, A., Minisandram, A., Sinha, N., Jonsson, V.D., Rao, D.S., O'Connell, R.M. and Baltimore, D. 2012. Oncomir miR-125b regulates hematopoiesis by targeting the gene Lin28A. *Proc. Natl. Acad. Sci. U. S. A.* **109**: 4233-4238.

Ebert, M.S., Neilson, J.R. and Sharp, P.A. 2007. MicroRNA sponges: competitive inhibitors of small RNAs in mammalian cells. *Nat. Methods* **4**: 721-726.

Ebert, M.S. and Sharp, P.A. 2010. MicroRNA sponges: progress and possibilities. *RNA* **16**: 2043-2050.

Gentner, B., Schira, G., Giustacchini, A., Amendola, M., Brown, B.D., Ponzoni, M. and Naldini, L. 2009. Stable knockdown of microRNA in vivo by lentiviral vectors. *Nat. Methods* **6**: 63-66.

Haraguchi, T., Ozaki, Y. and Iba, H. 2009. Vectors expressing efficient RNA decoys achieve the long-term suppression of specific microRNA activity in mammalian cells. *Nucleic Acids Res.* **37**: e43.

Hong, S., Hwang, D.Y., Yoon, S., Isacson, O., Ramezani, A., Hawley, R.G. and Kim, K.S. 2007. Functional analysis of various promoters in lentiviral vectors at different stages of in vitro differentiation of mouse embryonic stem cells. *Mol. Ther.* **15**: 1630-1639.

Kertesz, M., Iovino, N., Unnerstall, U., Gaul, U. and Segal, E. 2007. The role of site accessibility in microRNA target recognition. *Nat. Genet.* **39**: 1278-1284.

Kloosterman, W.P., Lagendijk, A.K., Ketting, R.F., Moulton, J.D. and Plasterk, R.H. 2007. Targeted inhibition of miRNA maturation with morpholinos reveals a role for miR-375 in pancreatic islet development. *PLoS Biol.* **5**: e203.

Kluiver, J., Gibcus, J.H., Hettinga, C., Adema, A., Richter, M.K., Halsema, N., Slezak-Prochazka, I., Ding, Y., Kroesen, B.J. and van den Berg, A. 2012. Rapid generation of microRNA sponges for microRNA inhibition. *PLoS One* **7**: e29275.

Krutzfeldt, J., Rajewsky, N., Braich, R., Rajeev, K.G., Tuschl, T., Manoharan, M. and Stoffel, M. 2005. Silencing of microRNAs in vivo with 'antagomirs'. *Nature* **438**: 685-689.

Kumar, M.S., Erkeland, S.J., Pester, R.E., Chen, C.Y., Ebert, M.S., Sharp, P.A. and Jacks, T. 2008. Suppression of non-small cell lung tumor development by the let-7 microRNA family. *Proc. Natl. Acad. Sci. U. S. A.* **105**: 3903-3908.

Liu, Y., Sun, R., Lin, X., Liang, D., Deng, Q. and Lan, K. 2012. Kaposi's sarcoma-associated herpesvirus-encoded microRNA miR-K12-11 attenuates transforming growth factor beta signaling through suppression of SMAD5. *J. Virol.* **86**: 1372-1381.

Long, D., Lee, R., Williams, P., Chan, C.Y., Ambros, V. and Ding, Y. 2007. Potent effect of target structure on microRNA function. *Nat. Struct. Mol. Biol.* **14**: 287-294.

Ma, F., Xu, S., Liu, X., Zhang, Q., Xu, X., Liu, M., Hua, M., Li, N., Yao, H. and Cao, X. 2011. The microRNA miR-29 controls innate and adaptive immune responses to intracellular bacterial infection by targeting interferon-gamma. *Nat. Immunol.* **12**: 861-869.

Otaegi, G., Pollock, A. and Sun, T. 2011. An Optimized Sponge for microRNA miR-9 Affects Spinal Motor Neuron Development in vivo. *Front. Neurosci.* **5**: 146.

Papapetrou, E.P., Korkola, J.E. and Sadelain, M. 2010. A genetic strategy for single and combinatorial analysis of miRNA function in mammalian hematopoietic stem cells. *Stem Cells* **28**: 287-296.

Park, C.Y., Choi, Y.S. and McManus, M.T. 2010. Analysis of microRNA knockouts in mice. *Hum. Mol. Genet.* **19**: R169-75.

Tan, L.P., Seinen, E., Duns, G., de Jong, D., Sibon, O.C., Poppema, S., Kroesen, B.J., Kok, K. and van den Berg, A. 2009. A high throughput experimental approach to identify miRNA targets in human cells. *Nucleic Acids Res.* **37**: e137.

Tan, L.P., van den Berg, A. and Kluiver, J. 2011. Application of RIP-Chip for the Identification of miRNA Targets. *Neuromethods* **58**: 159-169.

Zhu, Q., Sun, W., Okano, K., Chen, Y., Zhang, N., Maeda, T. and Palczewski, K. 2011. Sponge transgenic mouse model reveals important roles for the microRNA-183 (miR-183)/96/182 cluster in postmitotic photoreceptors of the retina. *J. Biol. Chem.* **286**: 31749-31760.

CHAPTER 6

Overexpression of miR-155 enhances cell growth by targeting the TBRG1 gene in B-cell lymphoma

Izabella Slezak-Prochazka, Joost Kluiver, Debora de Jong, Katarzyna Smigielska-Czepiel, Gertrud Kortman, Melanie Winkle, Bea Rutgers, Sibrand Poppema, Bart-Jan Kroesen and Anke van den Berg

In preparation

ABSTRACT

MiR-155 is an important regulator of B-cell development and deregulation of miR-155 contributes to B-cell lymphomagenesis. High miR-155 levels are observed in several types of lymphoma, including Hodgkin lymphoma. In contrast, Burkitt lymphoma is characterized by very low miR-155 levels. To determine the function of miR-155 in B-cell lymphoma, we studied the effect of miR-155 induction on BL cell growth and identified miR-155 target genes in BL and HL. Overexpression of miR-155 enhanced growth of ST486 BL cells but not of Ramos BL cells in a GFP competition assay. Ago2-RIP-Chip in miR-155-transduced or empty vector-transduced cells revealed 54 miR-155 target genes in ST486 and 15 in Ramos cells. Besides the higher number of targets, also the fold enrichments were much higher in miR-155-ST486 as compared to miR-155-Ramos. *In silico* validation of the 54 genes identified in ST486 cells indicated that 32% of the genes were predicted as miR-155 targets by TargetScan and 77% contained the 6-mer miR-155-binding motif in the 3'UTR. We confirmed miR-155 targeting for the 5 most enriched genes, i.e. DET1, TBRG1, TRIM32, HOMEZ and PSIP1, and a known miR-155 target, JARID2, using luciferase reporter assays in ST486 cells. Inhibition of miR-155 in KM-H2 HL cells using a sponge construct revealed that DET1, TBRG1, TRIM32, HOMEZ and JARID2 are also targeted by endogenous miR-155 in KM-H2 cells. To determine if the identified miR-155 target genes were involved in the observed enhanced growth of ST486 cells upon miR-155 overexpression, we inhibited the 6 selected genes by shRNA constructs and showed that inhibition of TBRG1 enhanced growth of ST486 cells. In conclusion, we identified novel miR-155 targets in BL and HL and showed that miR-155 promotes growth of BL cells by targeting the TBRG1 gene.

INTRODUCTION

MicroRNAs (miRNAs) constitute a subgroup of short (~22nt) single-stranded RNAs that belong to the family of noncoding RNAs (Bartel, 2004). MiRNAs are transcribed as longer primary transcripts (pri-miRNAs) that contain one or more hairpin-structures which are processed by the Microprocessor complex in the nucleus (Cai et al., 2004; Denli et al., 2004; Gregory et al., 2004). The resulting precursor miRNAs (pre-miRNAs) are transported to the cytoplasm by Exportin-5 and further processed by Dicer to the mature miRNAs (Bohnsack et al., 2004; Grishok et al., 2001; Hutvagner et al., 2001; Yi et al., 2003). Mature miRNAs are bound by one of the Argonaute (Ago) proteins and incorporated into the RNA-induced silencing complex (RISC) (Hutvagner and Zamore, 2002; Mourelatos et al., 2002). The miRNA guides the RISC to protein-coding RNA transcripts (mRNAs) based on partial sequence homology and inhibits their translation or induces RNA degradation (Eulalio et al., 2008; Filipowicz et al., 2008). MiRNAs regulate expression of more than 30% of all human genes (Bartel, 2009) including genes that play important roles in fundamental cell biological processes like differentiation, proliferation and apoptosis. In line with their obvious importance to regulate and maintain cellular and physiological homeostasis, deregulation of miRNA levels has been linked to pathological conditions such as development and progression of cancer.

The well-known oncogenic miR-155 is an important regulator of diverse aspects of the immune response including B-cell development. MiR-155 is processed from the transcript of the B-cell integration cluster (*BIC*) gene (Lagos-Quintana et al., 2002). Most germinal center (GC) B cells express *BIC* and miR-155 in the course of the GC response (Thai et al., 2007). The role of miR-155 for normal B-cell development was demonstrated in miR-155-deficient mice that have reduced numbers of germinal centre B cells, abolished antibody affinity maturation and fail to generate memory B cells (Rodriguez et al., 2007; Thai et al., 2007; Vigorito et al., 2007). Deregulation of miR-155 expression has been shown to contribute to the pathogenesis of hematological malignancies by different mechanisms. The oncogenic potential of miR-155 was shown in miR-

155 transgenic mice in which overexpression of miR-155 driven by the B-cell-specific Eμ-enhancer induced pre-B-cell lymphoma (Costinean et al., 2006). Recently, Babar *et al*. showed that induction of miR-155 in lymphoid tissues of mice caused disseminated lymphoma characterized by a clonal, transplantable pre-B-cell population (Babar et al., 2012). Withdrawal of miR-155 lead to tumor regression, partly due to increased apoptosis of the malignant cells, demonstrating that the tumor cells were dependent on miR-155. MiR-155 levels were shown to be high in GC B cell-derived lymphomas like Hodgkin lymphoma (HL), primary mediastinal and diffuse large B-cell lymphomas (Kluiver et al., 2005; van den Berg et al., 2003). In contrast, very low levels of miR-155 were observed in GC B-cell derived Burkitt lymphoma (BL) (Kluiver et al., 2006) suggesting a tumor suppressive function in this B-cell lymphoma subtype. This was supported by the finding that miR-155 targeted activation-induced cytidine deaminase (AID) and that miR-155 downregulation resulted in an increased number of AID-mediated MYC translocations in B cells (Dorsett et al., 2007). The hallmark of Burkitt lymphoma is the (8;14) translocation which involves the MYC and one of the immunoglobulin gene loci (Taub et al., 1982). Thus, low miR-155 levels may be required to drive AID-mediated formation of the MYC/Ig translocations in BL. These findings demonstrate that both high and low miR-155 levels may be beneficial for lymphomagenesis depending on the target gene repertoire and deregulation of miR-155 is a common feature in different lymphoma subtypes.

To understand the function of miR-155 in B-cell lymphomas, it is crucial to identify genes that are targeted by miR-155. In this study, we show that overexpression of miR-155 in BL derived cell lines leads to enhanced growth of the ST486 cells, whereas no effect was observed in Ramos cells. We subsequently identified miR-155 target genes in both ST486 and Ramos cells and found 54 targets in ST486 and 15 in Ramos. Six selected genes were validated as miR-155 targets and five of them, i.e. DET1, TBRG1, TRIM32, HOMEZ and JARID2, were shown to be targeted by endogenous miR-155 in Hodgkin lymphoma cells. Inhibition of TBRG1, which is a miR-155 target in

ST486 but not in Ramos, caused increased growth of ST486 cells similar to the miR-155 overexpression phenotype.

RESULTS

MiR-155 confers growth advantage in ST486 Burkitt lymphoma cells

To determine the effect of miR-155 in BL cell lines, we overexpressed miR-155 in two EBV-negative BL-derived cell lines, i.e. ST486 and Ramos. These cell lines were chosen based on their very low endogenous miR-155 levels and similar response to anti-IgM treatment. Upon miR-155 overexpression, we observed a 200-400 fold increase in miR-155 levels in both miR-155-ST486 and miR-155-Ramos compared to empty vector (EV)-transduced cells (Fig. 1A). These levels were ~3 fold lower than the endogenous miR-155 levels observed in the Hodgkin lymphoma cell line KM-H2 (Fig. 1A). Next, we determined the effect of miR-155 overexpression on growth of ST486 and Ramos cells in a GFP competition assay. We observed a growth advantage of GFP+ miR-155-ST486 cells compared to GFP- wild-type ST486 cells (Fig. 1B). In 3 weeks, the GFP+ miR-155-ST486 cell fraction increased ~2 fold over the GFP- wild-type cell fraction. In contrast, overexpression of miR-155 did not result in any difference

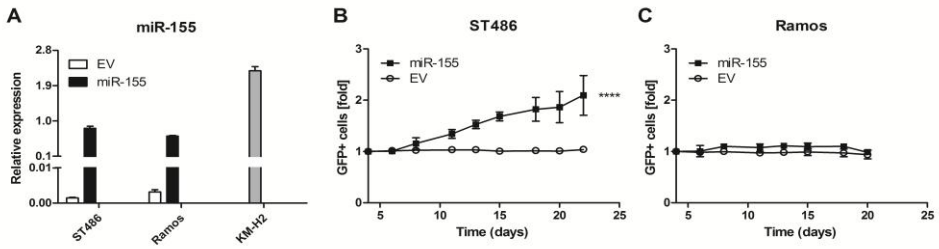

FIGURE 1. Overexpressed miR-155 enhanced growth of ST486 but not Ramos cells. (A) Levels of miR-155 were strongly increased in miR-155-ST486 and miR-155-Ramos cells compared to empty vector (EV) control. Endogenous miR-155 levels in KM-H2 HL cells were ~3 fold higher. (B) ST486 cells showed a 2 fold increase in the percentage of GFP+ cells after 22 days in comparison to GFP- cells. (C) Ramos cells showed no difference in cell growth. The GFP+ percentage in EV control remained stable in both cell lines. Changes in the percentage of GFP+ cells were calculated as the fold increase/decrease relative to the percentage of GFP+ cells at day 4. An average of three independent GFP competition assay experiments was presented. P value was determined by linear regression (**** $p<0.0001$).

in growth between GFP+ and GFP- Ramos cells (Fig. 1C). Empty vector control did not cause any difference in the percentage of GFP+ cells. Thus, these two Burkitt lymphoma cell lines respond differently to overexpression of miR-155, despite the similar high miR-155 levels.

High-throughput identification of endogenous miRNA targets

To determine the miRNAs target genes in ST486 and Ramos cells, we characterized the miRNA targetome of ST486 and Ramos cells using the RIP-Chip approach (Tan et al., 2009). We used an antibody against endogenous Ago2 to immunoprecipitate (IP) RISC together with the miRNA target transcripts. Enrichment of Ago2 in the Ago2-IP fraction and depletion of Ago2 in the flowthrough (FT) fraction was confirmed in both cell lines by Western blot (Supplementary Fig. 1A). In addition, we also showed efficiency of the IP procedure by enrichment of miR-155 and miR-19b in the Ago2-IP fraction, but not in the negative control IgG-IP fraction when compared to the total fraction (Supplementary Fig. 1B). RNA samples isolated from the total and IP fractions of ST486 and Ramos cells were analyzed on the Agilent microarray platform. The miRNA-targetome was defined by the transcripts that were more than two fold enriched in the IP fraction compared to the total fraction (Table 1). The miRNA targetome included 12,5% and 16,5% of all analyzed probes in ST486 cells and Ramos cells, respectively.

TABLE 1. Number of probes in miRNA targetome of ST486 and Ramos cells

Enrichment		ST486 (n=14,468*)	Ramos (n=11,928*)
# probes	IP/T>2	1,804 (12.5%)	1,969 (16.5%)
	IP/T>4	664 (4.6%)	743 (6.2%)
	IP/T>8	239 (1.7%)	269 (2.3%)

*Number of probes that are flag present and show consistent signals for Cy3 and Cy5

To identify miRNAs that contribute to the targetome in ST486 and Ramos cells, we performed a gene set enrichment analysis (GSEA) (Subramanian et al., 2005) comparing gene abundance levels in IP and total fractions. The most

enriched gene set for both cell lines was the miR-17 seed family binding motif (Fig. 2A). This is consistent with the high abundance of the miR-17 seed family members in ST486 and Ramos and the overall high percentage of miR-17 targets in the human genome as predicted by TargetScan. The 20 most enriched gene sets in IP vs total fraction included 14 miRNA binding motifs in ST486 and 17 in Ramos cells (Supplementary Table 1).

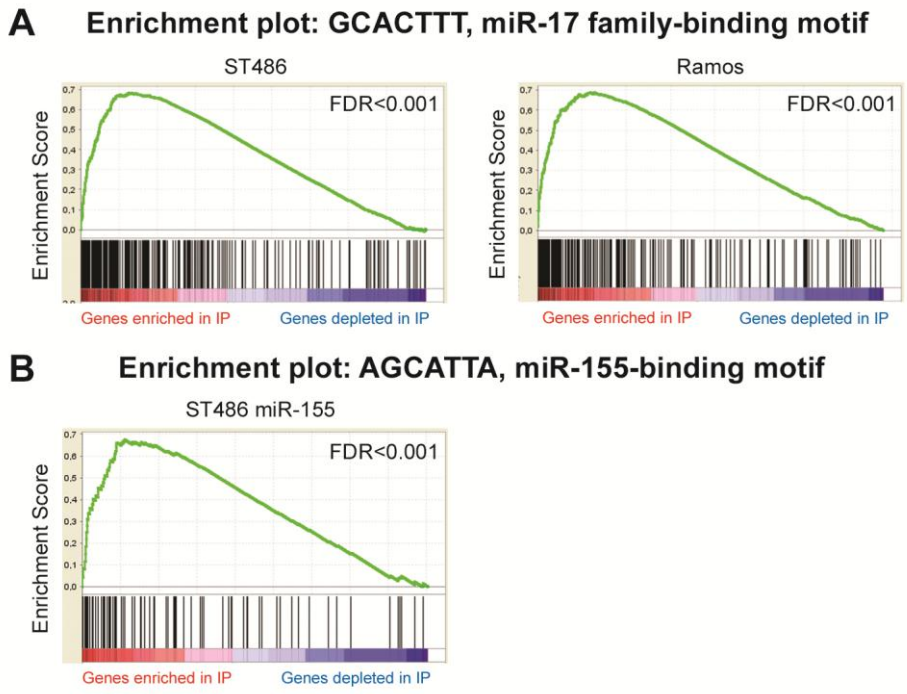

FIGURE 2. Enrichment of the miR-17 seed family and miR-155 binding motives in the Ago2-IP fraction compared to the total fraction. (A) miR-17 family binding motif was the most enriched gene set in the IP of ST486 and Ramos cells. (B) miR-155 binding motif was the 13th most enriched gene sets in miR-155-ST486. In miR-155-Ramos and the EV-transduced cells, the miR-155 binding motif was not among the top-20 most enriched gene sets. FDR- false discovery rate.

Identification of miR-155 target genes

To identify the genes that were targeted by miR-155 in miR-155-ST486 and miR-155-Ramos cells, we compared the targetomes of miR-155 and EV-transduced cells. Targetomes of miR-155-ST486 and miR-155-Ramos consisted of a similar number of probes as compared to their EV-transduced controls (Supplementary Table 2). The most enriched gene set in the IP fraction of miR-155-ST486 and miR-155-Ramos was the miR-17 seed family binding motif (Fig. 2A). EV and miR-155 transduced cells shared 16 and 17 of the top-20 most enriched gene sets in ST486 and Ramos, respectively (Supplementary Table 1). In miR-155-ST486 the miR-155-binding motif was the 13th most enriched gene set with a false discovery rate (FDR) <0.001 (Fig. 2B). In contrast, the miR-155-binding motif was not within the 20 most enriched gene sets for EV-ST486 or any of the transduced Ramos cell lines.

To identify the miR-155-specific targets we determined which probes are more than two-fold stronger enriched in the IP fraction of miR-155 compared to EV-transduced cells. We identified 64 probes that fulfilled this condition in ST486 and 18 probes in Ramos cells. Out of the 64 probes identified in ST486, 61 probes belonged to 54 genes and 3 probes did not correspond to any known gene. The fold enrichment in the targetome of miR-155-ST486 compared to EV-ST486 ranged from 2.0 to 12.6 fold. *In silico* validation indicated that 26 of the 54 identified genes (48%) contained an 8-mer miR-155 binding site (AGCATTAA) and 43 genes (80%) contained a 6-mer miR-155 binding site (GCATTA) in the 3'UTR. 18 of the 54 genes (33%) were predicted to be miR-155 targets by TargetScan (Supplementary Table 3). This percentage was strongly increased as compared to the ~1.7% predicted miR-155 targets among all expressed genes. For Ramos cells, 15 of the 18 probes were assigned to known genes. The enrichment fold in the targetome of miR-155-Ramos compared to EV-Ramos ranged from 2.0 to 2.6 fold. Two of the genes (13%) contained an 8-mer and 9 genes (60%) contained a 6-mer miR-155 binding site (Supplementary Table 4). Three of the 15 genes (20%) were predicted to be miR-155 targets by TargetScan. Five of the miR-155 target genes are identified in both ST486 and Ramos cells. Three of these genes showed similar fold

enrichment in both cell lines, whereas the fold enrichment for De-etiolated-1 (DET1) and PC4 and SF2 interacting protein 1 (PSIP1) was much higher in ST486 cells (Fig. 3A).

MiR-155 target genes validation

We selected six miR-155 target genes for validation, i.e. one known target gene, Jumonji AT rich interactive domain 2 (JARID2), and the five genes that were most enriched in the targetome of miR-155-ST486 cells, i.e. DET1, Transforming growth factor beta regulator (TBRG1), Tripartite motif-32 (TRIM32), Homeobox leucine zipper (HOMEZ) and PSIP1. Four of the six genes, TBRG1, TRIM32, HOMEZ and JARID2, were ST486-specific miR-155 target genes and two genes, DET1 and PSIP1, were found both in ST486 and in Ramos (Fig. 3A). We first compared the endogenous levels of the six selected genes in wild-type ST486 and Ramos cells (Fig. 3B). The levels of TBRG1, HOMEZ, JARID2, DET1 and PSIP1 were similar for ST486 and Ramos cells, whereas the TRIM32 level was substantially lower in Ramos cells. Thus, the lack of TRIM32 enrichment in the IP fraction of miR-155-Ramos cells can be explained by its very low expression level.

We performed luciferase reporter assay in ST486 cells to validate the six selected genes as miR-155 target genes. The 3'UTRs of TBRG1, TRIM32, JARID2, DET1 and PSIP1 genes and the coding sequence of HOMEZ contained miR-155 binding sites that were cloned into the psiCHECK2 luciferase vector (Fig. 3C). Co-transfection of the resulting luciferase constructs with a miR-155 precursor to ST486 wt cells resulted in significantly decreased relative luciferase levels, ranging from 15 to 53%, compared to co-transfection with negative control precursors (Fig. 3D). Western blot analysis for the most enriched gene in the targetome of miR-155-ST486 cells, i.e. DET1, revealed a 2 fold decrease in DET1 protein level in miR-155-ST486 compared to EV-ST486 cells (Fig. 3E, F). Thus, we confirmed that TBRG1, TRIM32, HOMEZ, JARID2, DET1 and PSIP1 are valid miR-155 target genes in ST486 cells.

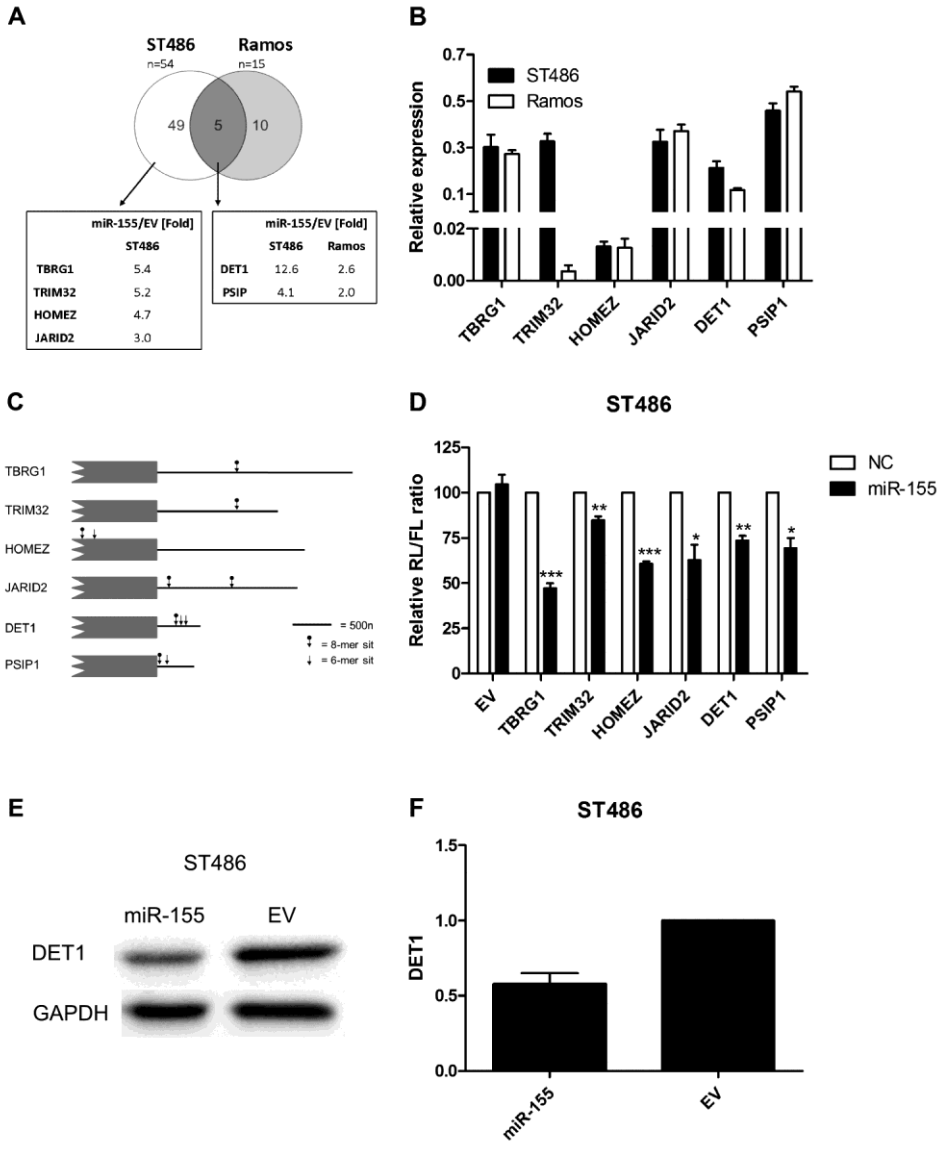
A
ST486
n=54
Ramos
n=15
49
5
10
miR-155/EV [Fold]
ST486
TBRG1 5.4
TRIM32 5.2
HOMEZ 4.7
JARID2 3.0
miR-155/EV [Fold]
ST486 Ramos
DET1 12.6 2.6
PSIP 4.1 2.0
B
Relative expression
ST486
Ramos
TBRG1
TRIM32
HOMEZ
JARID2
DET1
PSIP1
C
TBRG1
TRIM32
HOMEZ
JARID2
DET1
PSIP1
= 500n
= 8-mer sit
= 6-mer sit
D
ST486
Relative RL/FL ratio
NC
miR-155
EV
TBRG1
TRIM32
HOMEZ
JARID2
DET1
PSIP1
E
ST486
miR-155
EV
DET1
GAPDH
F
ST486
DET1
miR-155
EV

FIGURE 3. Validation of miR-155 target genes. (A) Venn diagram showing the overlap between miR-155 target genes in ST486 and Ramos cells upon overexpression of miR-155 as identified by AGO2-RIP-CHIP. Genes selected for validation are presented in the boxes. Fold enrichment in IP/T ratio in miR-155 compared to EV cells is indicated. (B) Transcript levels of TBRG1, TRIM32, HOMEZ, JARID2, DET1 and PSIP1 were measured by qRT-PCR in wild-type ST486 and Ramos cells. TRIM32 levels were much lower in Ramos compared to ST486 cells. (C) Schematic overview of 3'UTR regions with the positions of the predicted miR-155 binding sites indicated by the arrows (8-mer and 6-mer sites) in 3'UTRs. For HOMEZ, no miR-155 binding sites were predicted in the 3'UTR, but two putative sites were observed in the coding region. For TBRG1 and PSIP1, the 3'UTR of the isoforms containing the miR-155 binding sites are shown (ENST00000441174 and NM_021144, respectively). (D) Luciferase reporter assay for six selected genes in ST486 cells revealed reduced Renilla luciferase (RL) / Firefly luciferase (FL) ratios for all six genes. Thus, TBRG1, TRIM32, HOMEZ, JARID2, DET1 and PSIP1 are validated miR-155 target genes in ST486 cells. Ratios were calculated for cells co-transfected with the psiCHECK2 construct and either synthetic miR-155 precursor or a negative control (NC). Luciferase ratio for miR-155 precursor relative to negative control was calculated for each construct. P values were calculated with Student's t-test (*p<0.05, **p<0.001, ***p<0.01). (E) DET1 protein level was decreased in miR-155-ST486 compared to EV-ST486. (F) Quantification of the Western blot for DET1 relative to GAPDH. EV-ST486 was set as 1, the average of 2 experiments was shown.

TBRG1, TRIM32, HOMEZ, JARID2 and DET1 are targeted by endogenous miR-155 in Hodgkin lymphoma

We next investigated whether the six validated miR-155 target genes are also targeted by endogenous miR-155 in HL cells. We inhibited miR-155 using a retroviral vector containing a miR-155 sponge with 14 binding sites (Kluiver et al., 2012) in KM-H2 HL cells that have high endogenous miR-155 level (Fig. 1A). We performed Ago2-RIP-Chip in KM-H2 cells transduced with EV (EV-KM-H2) or miR-155 sponge (miR-155AS-KM-H2) to identify the miR-155 targets (Supplementary Table 5). The IP/T ratio for TBRG1, TRIM32, HOMEZ, JARID2 and DET1 decreased in miR-155AS-KM-H2 cells, whereas there was no difference in the IP/T ratios for PSIP1. These results indicate that TBRG1, TRIM32, HOMEZ, JARID2 and DET1 are targeted by endogenous miR-155 in KM-H2 cells. For comparison we also show the increase in IP/total ratio observed in miR-155-ST486 compared to EV-ST486 cells (Fig. 4A, B).

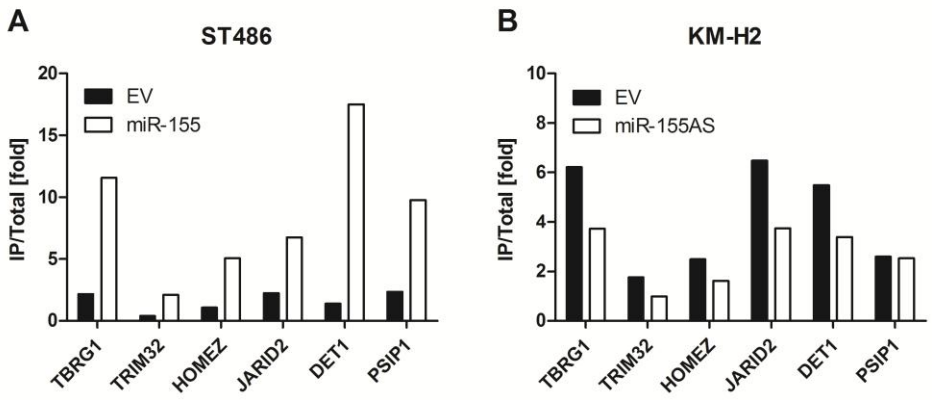

FIGURE 4. Five of the six validated miR-155 target genes are also targeted by endogenous miR-155 in HL. (A) IP/T ratio of the six miR-155 target genes was increased in miR-155-ST486 with compared to EV-ST486. (B) IP/T ratio of in five of the six genes was decreased in miR-155AS-KM-H2 compared to EV-KM-H2. IP/T ratios were calculated from expression levels as determined by the gene expression microarrays.

Inhibition of TBRG1 phenocopy miR-155 overexpression in ST486 cells

To show the relevance of these six validated miR-155 target genes we generated 12 shRNA constructs directed against these six genes. Effectiveness of the shRNA constructs was determined by qRT-PCR (Supplementary Fig. 2). Inhibition of TRIM32, HOMEZ, JARID2, DET1 and PSIP1 decreased growth of ST486 cells during GFP competition assay for at least one of the two shRNA constructs (Supplementary Fig. 2). For TBRG1, there are 11 transcript variants in the Ensemble database (Supplementary Table 6). Only 3 of the 11 variants contain the miR-155 binding site, i.e. ENST00000441174, ENST00000284290 and ENST00000529543 (Supplementary Table 6). Deng et al. assessed levels of 7 of the 11 transcripts and showed that isoforms ENST00000441174 and ENST00000473629 were most abundant in the Burkitt lymphoma cell line MutuI (Deng et al., 2011) (Fig. 5A). The Agilent platform contains two probes for TBRG1, i.e. one probe that binds to both abundant isoforms (probe 1) and one probe that is specific for the protein-coding isoform that contains the miR-155 binding site (probe 2). Consistent with the findings of Deng *et al.* (2011) we observed that probe 1 showed much higher signals than probe 2 (Fig. 5B). Probe

1 was not enriched in the IP, whereas probe 2 was 5.4 fold enriched in the IP fraction. Thus, miR-155 binds specifically to the protein coding isoform. We used three shRNAs to inhibit TBRG1, one was specific for the protein-coding isoform and the other two were targeting most TBRG1 isoforms. Inhibition of the protein-coding TBRG1 isoform resulted in enhanced growth of ST486 cells, whereas inhibition of the other isoforms revealed no change or a decrease in growth of ST486 cells (Fig. 5C). Thus, inhibition of the protein-coding isoform of TBRG1 phenocopied the growth promoting effect of miR-155 overexpression in ST486 cells.

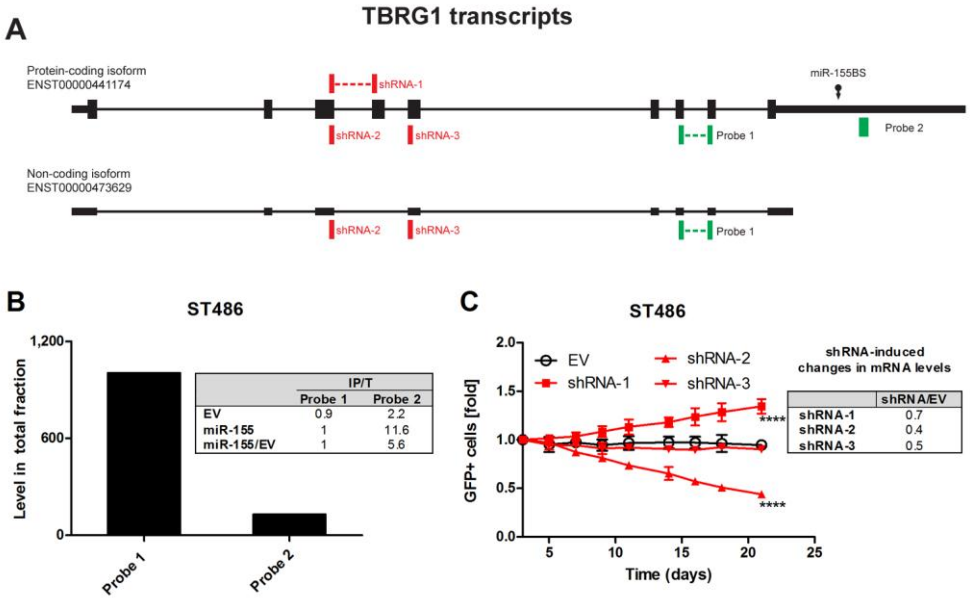

FIGURE 5. Specific inhibition of the protein-coding isoform of TBRG1 caused increase of ST486 cell growth. (A) Schematic overview of two most abundant TBRG1 isoforms. Position of the miR-155 binding site (miR-155BS), the region targeted by the shRNAs and the location of the two microarray probes were indicated. (B) Signal intensity measured by probe 1 was much higher than the signal intensity measured by probe 2. The protein-coding isoform detected specifically by probe 2 was strongly enriched in the targetome of miR-155-ST486 cells, whereas the common probe was not enriched. (C) shRNA-1 that specifically inhibits the protein-coding isoform induced a growth advantage of ST486 cells in a GFP competition assay. shRNA-2 resulted in decreased cell growth and shRNA-3 had no effect on cell growth of ST486 cells.

DISCUSSION

MiR-155 and the miR-155 primary transcript, *BIC*, are among the most studied miRNAs in B-cell lymphoma. Over the past few years many target genes involved in functioning of normal hematopoietic cells have been identified. In the context of B-cell lymphoma, it is frequently not clear which target genes are relevant for the pathogenesis of a specific B-cell lymphoma subtype. In this study we showed that upon overexpression of miR-155 in BL cells, growth of ST486 cells was enhanced, whereas growth of Ramos cells was not affected. Phenotype copy experiments revealed that TBRG1 is involved in the enhanced growth observed upon miR-155 overexpression in ST486 cells.

We selected two commonly used BL cell lines for the functional studies that have similar miRNA and gene expression profiles (data not shown) and both show very low miR-155 levels. Nevertheless, ST486 and Ramos cells responded differently to overexpression of miR-155 and Ago2-RIP-Chip analysis upon miR-155 induction resulted in the identification of a larger and more enriched set of miR-155 target genes in ST486 than in Ramos cells. The differences in targeting were not caused by differences in endogenous expression levels of the target genes, because the endogenous levels were similar for 5 out of 6 genes. For TRIM32 we observed low expression levels in Ramos cells compared to ST486 cells which might explain the absence of TRIM32 in the IP fraction of Ramos cells. Besides similar endogenous transcript levels, also the induced miR-155 levels were similar in both cell lines making it unlikely that the miR-155 levels were insufficient to target these genes in Ramos cells. However, we did see a slightly higher enrichment of miR-155 in the IP fraction of ST486 as compared to Ramos cells (Supplementary Fig. 1), which might in part explain differences in miR-155 targeting and phenotype.

We selected six miR-155 target genes for validation and confirmed effective targeting in ST486 BL cells for all. One gene, JARID2, was a known target, whereas TRIM32, DET1, HOMEZ, PSIP1 and TBRG1 were novel miR-155 targets. In contrast to the observed miR-155 effect on growth of ST486 cells, inhibition of five of the target genes revealed either no or a growth inhibitory

effect. Only inhibition of TBRG1 phenocopied the observed effect upon miR-155 overexpression in ST486 cells.

JARID2 was previously shown to inhibit apoptosis in chicken B-cell lymphoma (Bolisetty et al., 2009) and cardiomyocyte proliferation by regulating Cyclin D1, D2 and D3 (Jung et al., 2005). TRIM32 and DET1 have been shown to be involved in the ubiquitinylation pathway and the subsequent degradation of proteins. TRIM32 is a member of the ubiquitination-related tripartite motif (TRIM) family and was shown to ubiquitinylate MYC, inhibit proliferation and enhance differentiation of mouse neuronal progenitors (Schwamborn et al., 2009). Overexpression of TRIM32 in mouse embryonic fibroblast cell line, NIH 3T3, resulted in accelerated proliferation (Kano et al., 2008). Another established function of TRIM32 is enhancement of activity of certain miRNAs, including the cell differentiation-promoting miRNA let-7a. DET1 is a component of the E3 ubiquitin ligase DCX DET1-COP1 complex, which is involved in c-Jun ubiquitination and degradation. Inhibition of DET1 induced apoptosis of human osteosarcoma cells (Wertz et al., 2004). This is consistent with the growth inhibition that we observed upon DET1 inhibition in ST486 cells. HOMEZ did not have a miR-155 binding site in the 3'UTR, and consistent with this we observed no effect in the luciferase reporter construct upon cloning of this 3'UTR region (data not shown). However, the two putative miR-155 binding sites in the coding region were validated by the luciferase reporter assay. In general, the majority of the miRNA binding sites are found in the 3'UTR and the remaining binding sites are located in the 5'UTR or in the coding region (Chi et al., 2009). The cellular function of HOMEZ is not well characterized, but based on the protein domains it is predicted to function as a transcription factor (Bayarsaihan et al., 2003). Inhibition of HOMEZ decreased growth of ST486 cells, suggesting that it may be involved in regulation of genes involved in growth of Burkitt lymphoma cells. PSIP1 encodes two protein isoforms, i.e. p52 and p75, which are generated by alternative splicing. Only the Psip1/p52 has a miR-155 binding site in the 3'UTR and consistent with this we indeed observed enrichment of the probe that recognizes this isoform in the IP fraction, whereas the probe for the other isoform was not enriched (data not shown). Psip1/p52 was shown to be

involved in alternative splicing (Pradeepa et al., 2012). Tissue specific expression patterns of Psip1/p52 and Psip1/p75 are consistent with different regulation of these two proteins and support different cellular functions.

For TBRG1 only one probe detecting two out of eleven isoforms was enriched in the IP fraction, which was consistent with the putative miR-155 binding site that was present in the 3'UTR of these isoforms. These isoforms are not the dominant isoforms in our BL cells as was apparent from the lower probe signals in the microarrays. In Mutu1 BL cells, Deng et al. showed that the protein-coding isoform containing the miR-155 binding site constitutes only ~35% of all detected TBRG1 transcripts (Deng et al., 2011). In addition, the authors showed that also for some other genes a non-dominant isoform is targeted by miRNAs, which is consistent with our findings. Inhibition of the protein-coding isoforms of TBRG1 using an shRNA construct phenocopied the enhanced growth of ST486 cells as observed for miR-155 overexpression. The two other shRNA constructs, targeting most isoforms, showed either no or a growth inhibitory effect. This indicates that the protein-coding isoform of TBRG1 is involved in the growth stimulating effect of miR-155 in ST486 cells. This is consistent with growth inhibitory role of TBRG1 protein described by Tomkins et al. (Tompkins et al., 2007). They showed that TBRG1 was linked to ARF-MDM2-p53 signaling in several ways. The level of TBRG1 protein was downregulated by MDM2-mediated ubiquitination. TBRG1 in cooperation with alternative reading frame (ARF) protein induced G1-phase arrest in human osteosarcoma cells. Moreover, both TBRG1 and ARF were shown to increase p53 activity (Tompkins et al., 2007). Microarray studies indicated that TBRG1 was downregulated in various types of cancer, including diffuse large B cell lymphoma and chronic lymphocytic leukemia (Tompkins et al., 2007). This is consistent with the high miR-155 levels found in many types of cancer and supports our findings regarding to the role of TBRG1 in growth of ST486 cells.

Dorsett et al. showed that low miR-155 in B cells results in increased level of the miR-155 target gene AID and this enhanced the frequency of *MYC* translocations (Dorsett et al., 2008). Since *MYC* translocations are the hallmark of BL, it might be anticipated that low miR-155 levels are especially crucial at

the initiation step of the malignant transformation of the germinal center precursor B cells. This might explain why we do see an oncogenic effect of high miR-155 levels in an established Burkitt lymphoma cell lines. Our data show that the effect of miR-155 modulation may be different even between similar cell types such as ST486 and Ramos. It may be speculated that the balance between the target gene transcript levels and the efficiency of regulation by miR-155 and probably other miRNAs determines the final outcome of miR-155 modulation.

In conclusion, we identified six miR-155 target genes in BL cells with overexpression of miR-155 and showed that five of these genes are also targeted by endogenous miR-155 in HL cells. Induction of miR-155 enhances growth of ST486 BL cells and this phenotype involves inhibition of the TBRG1 gene.

MATERIAL AND METHODS

Cell lines. The ST486 and Ramos BL cell lines and the KM-H2 HL cell line were cultured at 37°C under an atmosphere containing 5% CO_2 in RPMI-1640 medium (Cambrex Biosciences, Walkersville, USA) supplemented with ultraglutamine (2mM), penicillin (100U/ml), streptomycin (0.1mg/ml; Cambrex Biosciences), and 20% (ST486) or 10% (Ramos, KM-H2) fetal calf serum (Cambrex Biosciences). Cell lines were purchased from ATCC (ST486) or DSMZ (Ramos, KM-H2).

DNA constructs. To overexpress miR-155, the pre-miR-155 and ~150ntflanking sequences were amplified from genomic DNA using Taq polymerase and primers listed in Supplementary Table 7. A XhoI restriction site was added to the forward and an EcoRI site to the reverse primer to allow directional cloning to the retroviral MXW-PGK-IRES-GFP vector (Mao and Chen, 2007) using standard laboratory procedures. The MXW-PGK-IRES-GFP vector was a kind gift from C-Z. Chen (Stanford University, CA). To inhibit miR-155, a miR-155 sponge construct was generated as previously described (Kluiver et al., 2012). Briefly, we cloned 14 bulged miR-155 binding sites to the retroviral

pMSCV-PIG vector (Addgene). The 3' UTR of DET1, TRIM32, JARID2, PSIP1, TBRG1 and the ~300nt fragment of HOMEZ in the coding sequence containing the potential miR-155-binding sites were amplified from genomic DNA using the primers listed in Supplementary Table 7. A NotI restriction site was added to the forward and a SstI to the reverse primers to enable cloning of the PCR products in the psiCHECK2 vector (Promega, Madison, WI). To inhibit DET1, TRIM32, JARID2, PSIP1, TBRG1 and HOMEZ, shRNA sequences were selected from shRNA library (TRC, Broad Institute, http://www.broadinstitute.org/rnai/trc/lib). Sequences of the shRNA oligo's are listed in Supplementary Table 8. XhoI and EcoRI sites were added to enable cloning to the retroviral pMDH1-PGK-GFP 2.0 vector (Mao and Chen, 2007). The pMDH1-PGK-GFP 2.0 vector was a kind gift from C-Z. Chen (Stanford University, CA). All inserts were verified by sequencing.

Retroviral transductions. To generate retroviral particles, Phoenix-Ampho packaging cells (Swift et al., 2001) were $CaPO_4$ transfected using 37,5µg of retroviral vector in T75 flasks. Viral particles were harvested after two days and concentrated with Retro-X concentrator (Clontech, Saint-Germain-en-Laye, France) according to the manufacturer's protocol. Target cells were transduced with the virus by spinning at 2,000rpm for 2hrs. Cells transduced with retroviral vectors were sorted for GFP+ cells using MoFlo sorter (Dako cytomation).

Quantitative RT-PCR. Total RNA from total, FT and IP fractions was isolated using miRNeasy kit (Qiagen, Carlsbad, USA). Total RNA from other samples was isolated using Trizol (Invitrogen, Carlsbad, USA) according to the manufacturer's protocol for the cell lines. The RNA concentration was measured with a NanoDropTM 1000 Spectrophotometer (Thermo Fisher Scientific Inc., Waltham, USA) and RNA integrity was evaluated by 1% agarose electrophoresis. qRT-PCR for miR-155, miR-19b and RNU48 (control) was performed using miRNA qRT-PCR assays (Applied Biosystems, Foster City, USA) as described previously (Gibcus et al., 2009). Reverse transcription (RT) primers specific for a miR-155, miR-19b and RNU48 were multiplexed in 15µl RT reactions containing 1µl of each RT primer. MiR-155 and miR-19b levels were normalized to the RNU48

levels. To determine the levels of TBRG1, TRIM32, HOMEZ, JARID2, DET1, PSIP1, cDNA was synthesized using 500ng input RNA, SuperScript II and random primers according to the manufacturer's protocol (Invitrogen). The qPCR reaction contained a final concentration of 1x qPCR MasterMix Plus (Eurogentec, Liege, Belgium), 1x Gene expression assay (Applied Biosystems, Foster City, USA), and 1ng of cDNA in a total volume of 10µl. The following gene expression assays were used: Hs00262345_m1 (TBRG1), Hs00705875_s1 (TRIM32), Hs01866743_s1 (HOMEZ), Hs01004460_m1 (JARID2), Hs00894490_m1 (DET1), Hs01045711_g1 (PSIP1) (All Applied Biosystems). Gene expression levels were normalized to HPRT levels. Mean cycle threshold (Ct) values were determined with the SDS software (version 2.1). Relative expression levels were calculated as $2^{-\Delta Ct}$.

Transfection of cell lines and luciferase assay. Luciferase assay was performed using Promega Dual-Luciferase Reporter Assay System (Promega, Madison, WI) as described previously (Gibcus et al., 2009). Briefly, two million ST486 cells were transfected with 4µg of each psiCHECK2 construct and co-transfected with 100nM miR-155 precursor (Ambion) or negative control #1 (Ambion) using Amaxa nucleofector device, program A23 (Amaxa, Gaithersburg, MD). Cell lysates were made 24 hours after transfection. For each transfection, the Renilla and Firefly luciferase activities were measured in duplicate, the Renilla over Firefly (R/L) luciferase ratio for miR-155 precursor was calculated and compared to negative control (set at 100%). Transfections were performed in triplicate and standard deviations were calculated. To determine significance of difference in the R/F ratio between miR-155 precursor and negative control #1 a Student's t-test was performed.

Western Blot. Cell lysates were prepared, separated on polyacrylamide gels and transferred onto nitrocellulose membranes using standard protocols. Mouse anti-DET1 antibody (clone 3G5, Genentech, San Francisco, CA) was diluted to a concentration of 1µg/ml in 5% milk in Tris-buffered saline with Tween-20 (TBST). Immunoblots were incubated with primary anti-DET1 antibody at 4ºC overnight. Secondary rabbit anti-mouse antibody conjugated with horseradish

peroxidase was used. Chemiluminescence was detected with the ChemiDoc MP scanner and protein bands were visualized and quantified with Image Lab 4.0.1 software (both BioRad, Veenendaal, NL). To detect protein levels of TBRG1, TRIM32 and JARID2, we tested the following antibodies: anti-TBRG1, clone 11E12, kindly provided by D. Quelle (The University of Iowa, Iowa) and clone 18951-1-AP purchased from Proteintech Manchester, UK; anti-TRIM32, clone 10326-1-AP (Proteintech); anti- JARID2, antibody was kindly provided by D. Reinberg (NYU School of Medicine Smilow Research Center, NY). However, we were not able to obtain reliable immunoblot results for these three proteins.

FACS analysis. For GFP competition assays, ST486 and Ramos cells were transduced with the MXW-PGK-IRES-GFP empty vector or miR-155 containing construct. For GFP competition assays with shRNAs, ST486 cells were transduced with the pMDH1-PGK-GFP 2.0 empty vector of shRNA containing construct (Supplementary Table 8). GFP expression was measured on a FACS Calibur flow cytometer (BD PharMingen) at day 3 or 4 post-transduction and monitored for three weeks tri-weekly. The percentage of GFP positive cells at day 3 or 4 was set to 1 and a fold difference per measurement was calculated.

Ago2-RIP-Chip procedure. Immunoprecipitation of Ago2-containing RISC complexes was performed as described previously (Tan et al., 2009). Briefly, cleared lysate of 10-20 million cells was incubated with protein G Sepharose beads (GE Healthcare) coated with anti-Ago2 antibody (Clone 2E12-1C9, Abnova, Taiwan) at 4°C overnight. Anti-IgG antibody was used as a negative control (Millipore BV, Amsterdam, The Netherlands). After washing the beads, RNA was harvested for microarray and qRT-PCR analysis and protein lysates were prepared for Western blot. Western blot for Ago2 was performed as described previously (Tan et al., 2009). Total RNA was isolated with miRNeasy Kit (Qiagen) according to manufacturer's protocol. RNA from total and Ago2-IP fractions of miR-155-ST486, EV-ST486, miR-155-Ramos, EV-Ramos, miR-155AS-KMH2 and EV-KMH2 cells was used for microarray analysis. Labelling and hybridization was performed using two-color Quick Amp Labeling Kit (ST486 and Ramos) and Low Input Quick Amp Labeling Kit (KM-H2), according to

manufacturer's protocol (Agilent, Santa Clara, USA). Briefly, 60-100ng of RNA from total and Ago2-IP samples was used for cDNA synthesis, followed by cRNA amplification and Cy3 and Cy5 labelling. cRNA was purified with RNeasy Kit (Qiagen) and quantified on NanoDropTM 1000 Spectrophotometer (Thermo Fisher Scientific Inc.). Equal amounts of Cy3 and Cy5-labelled cRNA were combined and hybridized at 65°C overnight on the 44k Human Whole Genome Oligo Microarray. Next, slides were washed and scanned with GenePix 4000B (Agilent). Scanned images were used for Agilent Feature Extraction software version 10.5., converted into Linear and Lowess normalized data. Quality control report was generated for each microarray. Using GeneSpring GX version 9.0 (Agilent), quantile normalization of the signals was performed separately for Ramos, ST486 and KM-H2 samples. Next, probes not detected in more than half of the samples and probes that were inconsistent (more than 2 fold different) in Cy3 and Cy5 replicates of the same sample were filtered out. The averaged signals for Cy3 and Cy5 replicates were used to calculate the IP/T ratio for each sample.

Gene Set Enrichment Analysis. To determine which genes sets are significantly enriched in the Ago2-IP in comparison to the total fraction in miR-155-ST486, EV-ST486, miR-155-Ramos and EV-Ramos, we performed a Gene Set Enrichment Analysis using The Molecular Signatures Database (GSEA; http://www.broad.mit.edu/gsea, Subramanian et al., 2005). If more than one probe was assigned for a certain gene, we selected the probe with the highest fold enrichment in the IP/T ratio in miR-155-ST486 or miR-155-Ramos compared to EV controls. This selection resulted in 9,047 genes submitted for analysis for ST486 and 7,809 genes for Ramos.

ACKNOWLEDGMENTS

This study was supported by a grant from the Dutch Cancer Society (RUG 2009-4279) and by a grant from the Ubbo Emmius Foundation. We thank Ann-Christin Lüdiger her help with constructing psiCHECK2-3'UTR vectors and Geert Mesander and Henk Moes for technical assistance during cell sorting.

REFERENCES

Babar, I.A., Cheng, C.J., Booth, C.J., Liang, X., Weidhaas, J.B., Saltzman, W.M. and Slack, F.J. 2012. Nanoparticle-based therapy in an in vivo microRNA-155 (miR-155)-dependent mouse model of lymphoma. *Proc. Natl. Acad. Sci. U. S. A.* **109**: E1695-704.

Bartel, D.P. 2004. MicroRNAs: genomics, biogenesis, mechanism, and function. *Cell* **116**: 281-297.

Bartel, D.P. 2009. MicroRNAs: target recognition and regulatory functions. *Cell* **136**: 215-233.

Bayarsaihan, D., Enkhmandakh, B., Makeyev, A., Greally, J.M., Leckman, J.F. and Ruddle, F.H. 2003. Homez, a homeobox leucine zipper gene specific to the vertebrate lineage. *Proc. Natl. Acad. Sci. U. S. A.* **100**: 10358-10363.

Bohnsack, M.T., Czaplinski, K. and Gorlich, D. 2004. Exportin 5 is a RanGTP-dependent dsRNA-binding protein that mediates nuclear export of pre-miRNAs. *RNA* **10**: 185-191.

Bolisetty, M.T., Dy, G., Tam, W. and Beemon, K.L. 2009. Reticuloendotheliosis virus strain T induces miR-155, which targets JARID2 and promotes cell survival. *J. Virol.* **83**: 12009-12017.

Cai, X., Hagedorn, C.H. and Cullen, B.R. 2004. Human microRNAs are processed from capped, polyadenylated transcripts that can also function as mRNAs. *RNA* **10**: 1957-1966.

Chi, S.W., Zang, J.B., Mele, A. and Darnell, R.B. 2009. Argonaute HITS-CLIP decodes microRNA-mRNA interaction maps. *Nature* **460**: 479-486.

Costinean, S., Zanesi, N., Pekarsky, Y., Tili, E., Volinia, S., Heerema, N. and Croce, C.M. 2006. Pre-B cell proliferation and lymphoblastic leukemia/high-grade lymphoma in E(mu)-miR155 transgenic mice. *Proc. Natl. Acad. Sci. U. S. A.* **103**: 7024-7029.

Deng, N., Puetter, A., Zhang, K., Johnson, K., Zhao, Z., Taylor, C., Flemington, E.K. and Zhu, D. 2011. Isoform-level microRNA-155 target prediction using RNA-seq. *Nucleic Acids Res.* **39**: e61.

Denli, A.M., Tops, B.B., Plasterk, R.H., Ketting, R.F. and Hannon, G.J. 2004. Processing of primary microRNAs by the Microprocessor complex. *Nature* **432**: 231-235.

Dorsett, Y., McBride, K.M., Jankovic, M., Gazumyan, A., Thai, T.H., Robbiani, D.F., Di Virgilio, M., Reina San-Martin, B., Heidkamp, G., Schwickert, T.A. et al. 2008. MicroRNA-155 suppresses activation-induced cytidine deaminase-mediated Myc-Igh translocation. *Immunity* **28**: 630-638.

Dorsett, Y., Robbiani, D.F., Jankovic, M., Reina-San-Martin, B., Eisenreich, T.R. and Nussenzweig, M.C. 2007. A role for AID in chromosome translocations between c-myc and the IgH variable region. *J. Exp. Med.* **204**: 2225-2232.

Eulalio, A., Huntzinger, E. and Izaurralde, E. 2008. Getting to the root of miRNA-mediated gene silencing. *Cell* **132**: 9-14.

Filipowicz, W., Bhattacharyya, S.N. and Sonenberg, N. 2008. Mechanisms of post-transcriptional regulation by microRNAs: are the answers in sight? *Nat. Rev. Genet.* **9**: 102-114.

Gibcus, J.H., Tan, L.P., Harms, G., Schakel, R.N., de Jong, D., Blokzijl, T., Moller, P., Poppema, S., Kroesen, B.J. and van den Berg, A. 2009. Hodgkin lymphoma cell lines are characterized by a specific miRNA expression profile. *Neoplasia* **11**: 167-176.

Gregory, R.I., Yan, K.P., Amuthan, G., Chendrimada, T., Doratotaj, B., Cooch, N. and Shiekhattar, R. 2004. The Microprocessor complex mediates the genesis of microRNAs. *Nature* **432**: 235-240.

Grishok, A., Pasquinelli, A.E., Conte, D., Li, N., Parrish, S., Ha, I., Baillie, D.L., Fire, A., Ruvkun, G. and Mello, C.C. 2001. Genes and mechanisms related to RNA interference regulate expression of the small temporal RNAs that control C. elegans developmental timing. *Cell* **106**: 23-34.

Hutvagner, G., McLachlan, J., Pasquinelli, A.E., Balint, E., Tuschl, T. and Zamore, P.D. 2001. A cellular function for the RNA-interference enzyme Dicer in the maturation of the let-7 small temporal RNA. *Science* **293**: 834-838.

Hutvagner, G. and Zamore, P.D. 2002. A microRNA in a multiple-turnover RNAi enzyme complex. *Science* **297**: 2056-2060.

Jung, J., Kim, T.G., Lyons, G.E., Kim, H.R. and Lee, Y. 2005. Jumonji regulates cardiomyocyte proliferation via interaction with retinoblastoma protein. *J. Biol. Chem.* **280**: 30916-30923.

Kano, S., Miyajima, N., Fukuda, S. and Hatakeyama, S. 2008. Tripartite motif protein 32 facilitates cell growth and migration via degradation of Abl-interactor 2. *Cancer Res.* **68**: 5572-5580.

Kluiver, J., Gibcus, J.H., Hettinga, C., Adema, A., Richter, M.K., Halsema, N., Slezak-Prochazka, I., Ding, Y., Kroesen, B.J. and van den Berg, A. 2012. Rapid generation of microRNA sponges for microRNA inhibition. *PLoS One* **7**: e29275.

Kluiver, J., Haralambieva, E., de Jong, D., Blokzijl, T., Jacobs, S., Kroesen, B.J., Poppema, S. and van den Berg, A. 2006. Lack of BIC and microRNA miR-155 expression in primary cases of Burkitt lymphoma. *Genes Chromosomes Cancer* **45**: 147-153.

Kluiver, J., Poppema, S., de Jong, D., Blokzijl, T., Harms, G., Jacobs, S., Kroesen, B.J. and van den Berg, A. 2005. BIC and miR-155 are highly expressed in Hodgkin, primary mediastinal and diffuse large B cell lymphomas. *J. Pathol.* **207**: 243-249.

Lagos-Quintana, M., Rauhut, R., Yalcin, A., Meyer, J., Lendeckel, W. and Tuschl, T. 2002. Identification of tissue-specific microRNAs from mouse. *Curr. Biol.* **12**: 735-739.

Mao, T.K. and Chen, C.Z. 2007. Dissecting microRNA-mediated gene regulation and function in T-cell development. *Methods Enzymol.* **427**: 171-189.

Mourelatos, Z., Dostie, J., Paushkin, S., Sharma, A., Charroux, B., Abel, L., Rappsilber, J., Mann, M. and Dreyfuss, G. 2002. miRNPs: a novel class of ribonucleoproteins containing numerous microRNAs. *Genes Dev.* **16**: 720-728.

Pradeepa, M.M., Sutherland, H.G., Ule, J., Grimes, G.R. and Bickmore, W.A. 2012. Psip1/Ledgf p52 binds methylated histone H3K36 and splicing factors and contributes to the regulation of alternative splicing. *PLoS Genet.* **8**: e1002717.

Rodriguez, A., Vigorito, E., Clare, S., Warren, M.V., Couttet, P., Soond, D.R., van Dongen, S., Grocock, R.J., Das, P.P., Miska, E.A. et al. 2007. Requirement of bic/microRNA-155 for normal immune function. *Science* **316**: 608-611.

Schwamborn, J.C., Berezikov, E. and Knoblich, J.A. 2009. The TRIM-NHL protein TRIM32 activates microRNAs and prevents self-renewal in mouse neural progenitors. *Cell* **136**: 913-925.

Subramanian, A., Tamayo, P., Mootha, V.K., Mukherjee, S., Ebert, B.L., Gillette, M.A., Paulovich, A., Pomeroy, S.L., Golub, T.R., Lander, E.S. et al. 2005. Gene set enrichment analysis: a knowledge-based approach for interpreting genome-wide expression profiles. *Proc. Natl. Acad. Sci. U. S. A.* **102**: 15545-15550.

Swift, S., Lorens, J., Achacoso, P. and Nolan, G.P. 2001. Rapid production of retroviruses for efficient gene delivery to mammalian cells using 293T cell-based systems. *Curr. Protoc. Immunol.* **Chapter 10**: Unit 10.17C.

Tan, L.P., Seinen, E., Duns, G., de Jong, D., Sibon, O.C., Poppema, S., Kroesen, B.J., Kok, K. and van den Berg, A. 2009. A high throughput experimental approach to identify miRNA targets in human cells. *Nucleic Acids Res.* **37**: e137.

Taub, R., Kirsch, I., Morton, C., Lenoir, G., Swan, D., Tronick, S., Aaronson, S. and Leder, P. 1982. Translocation of the c-myc gene into the immunoglobulin heavy chain locus in human Burkitt lymphoma and murine plasmacytoma cells. *Proc. Natl. Acad. Sci. U. S. A.* **79**: 7837-7841.

Thai, T.H., Calado, D.P., Casola, S., Ansel, K.M., Xiao, C., Xue, Y., Murphy, A., Frendewey, D., Valenzuela, D., Kutok, J.L. et al. 2007. Regulation of the germinal center response by microRNA-155. *Science* **316**: 604-608.

Tompkins, V.S., Hagen, J., Frazier, A.A., Lushnikova, T., Fitzgerald, M.P., di Tommaso, A., Ladeveze, V., Domann, F.E., Eischen, C.M. and Quelle, D.E. 2007. A novel nuclear interactor of ARF and MDM2 (NIAM) that maintains chromosomal stability. *J. Biol. Chem.* **282**: 1322-1333.

van den Berg, A., Kroesen, B.J., Kooistra, K., de Jong, D., Briggs, J., Blokzijl, T., Jacobs, S., Kluiver, J., Diepstra, A., Maggio, E. et al. 2003. High expression of B-cell receptor inducible gene BIC in all subtypes of Hodgkin lymphoma. *Genes Chromosomes Cancer* **37**: 20-28.

Vigorito, E., Perks, K.L., Abreu-Goodger, C., Bunting, S., Xiang, Z., Kohlhaas, S., Das, P.P., Miska, E.A., Rodriguez, A., Bradley, A. et al. 2007. microRNA-155 regulates the generation of immunoglobulin class-switched plasma cells. *Immunity* **27**: 847-859.

Wertz, I.E., O'Rourke, K.M., Zhang, Z., Dornan, D., Arnott, D., Deshaies, R.J. and Dixit, V.M. 2004. Human De-etiolated-1 regulates c-Jun by assembling a CUL4A ubiquitin ligase. *Science* **303**: 1371-1374.

Yi, R., Qin, Y., Macara, I.G. and Cullen, B.R. 2003. Exportin-5 mediates the nuclear export of pre-microRNAs and short hairpin RNAs. *Genes Dev.* **17**: 3011-3016.

SUPPLEMENTARY DATA

SUPPLEMENTARY TABLE 1. 20 most enriched gene sets in EV-ST486, miR-155-ST486, EV-Ramos and miR-155-Ramos

Gene set	Position in GSEA			
	ST486		Ramos	
	EV	miR-155	EV	miR-155
GCACTTT,MIR-17-5P,MIR-20A,MIR-106A,MIR-106B,MIR-20B,MIR-519D	1	1	1	1
ACACTAC,MIR-142-3P	2	3	11	12
AGCACTT,MIR-93,MIR-302A,MIR-302B,MIR-302C,MIR-302D,MIR-372,MIR-373,MIR-520E,MIR-520A,MIR-526B,MIR-520B,MIR-520C,MIR-520D	3	2	4	4
CTACTGT,MIR-199A	4	8	10	9
GTGCAAT,MIR-25,MIR-32,MIR-92,MIR-363,MIR-367	5	4	3	3
TGAATGT,MIR-181A,MIR-181B,MIR-181C,MIR-181D	6	6	7	7
TTTGCAC,MIR-19A,MIR-19B	7	7	5	5
AAGCACT,MIR-520F	8	10	16	15
ACTTTAT,MIR-142-5P	9	11	6	6
NAGASHIMA_NRG1_SIGNALING_UP	10	9		
TGCACTT,MIR-519C,MIR-519B,MIR-519A	11	5	2	2
KIM_WT1_TARGETS_UP	12	14		
TTGCCAA,MIR-182	13			
BONCI_TARGETS_OF_MIR15A_AND_MIR16_1	14			
TGCACTG,MIR-148A,MIR-152,MIR-148B	15	12	8	10
TGTTTAC,MIR-30A-5P,MIR-30C,MIR-30D,MIR-30B,MIR-30E-5P	16	20		
PICCALUGA_ANGIOIMMUNOBLASTIC_LYMPHOMA_DN	17	18		
ATAAGCT,MIR-21	18			
TACTTGA,MIR-26A,MIR-26B	19	15	18	18
AMIT_EGF_RESPONSE_40_HELA	20			
AGCATTA,MIR-155		13		
NAGASHIMA_EGF_SIGNALING_UP		16		
ACATATC,MIR-190		17		
TONKS_TARGETS_OF_RUNX1_RUNX1T1_FUSION_HSC_UP		19		
DAZARD_RESPONSE_TO_UV_NHEK_DN			9	8
TTGCACT,MIR-130A,MIR-301,MIR-130B			12	11
DACOSTA_UV_RESPONSE_VIA_ERCC3_COMMON_DN			13	16
CACTTTG,MIR-520G,MIR-520H			14	
DACOSTA_UV_RESPONSE_VIA_ERCC3_DN			15	13
GARGALOVIC_RESPONSE_TO_OXIDIZED_PHOSPHOLIPIDS_TURQUOISE_UP			17	
ATTACAT,MIR-380-3P			19	
TGCTGCT,MIR-15A,MIR-16,MIR-15B,MIR-195,MIR-424,MIR-497			20	19
ATGCTGC,MIR-103,MIR-107				14
GTACTGT,MIR-101				17
CTTTGCA,MIR-527				20

SUPPLEMENTARY TABLE 2. Similar numbers of probes were identified in the miRNA-targetomes of EV and miR-155-transduced ST486 and Ramos cells.

Enrichment		ST486 (n=14,468*)		Ramos (n=11,928*)	
		EV	miR-155	EV	miR-155
# probes	IP/T>2	1,804 (12.5%)	1,833 (12.7%)	1,969 (16.5%)	1,927 (16.2%)
	IP/T>4	664 (4.6%)	701 (4.8%)	743 (6.2%)	751 (6.3%)
	IP/T>8	239 (1.7%)	226 (1.6%)	269 (2.3%)	263 (2.2%)

*Number of probes that were flag present and showed consistent signals in Cy3 and Cy5 signals.

SUPPLEMENTARY TABLE 3. MiR-155 target genes in miR-155-ST486 cells identified with Ago2-RIP-Chip.

Gene		ProbeName	miR-155 IP/T	EV IP/T	miR-155/ EV	TS[1]	# 8-mer[2] in 3'UTR	# 6-mer[3] in 3'UTR
DET1*	NM_017996	A_23_P26184	17.5	1.4	12.6	+	1	3
TBRG1	NM_032811	A_23_P98463	11.6	2.2	5.4	+	1	2
TRIM32	NM_012210	A_23_P112311	2.1	0.4	5.2	+	1	1
HOMEZ	NM_020834	A_23_P76829	5.1	1.1	4.7		0[4]	0[4]
PSIP1*	NM_021144	A_23_P256384	9.8	2.4	4.1	+	1	2
C14orf159	BC009182	A_24_P58177	2.0	0.6	3.7		0	1
CCDC126	NM_138771	A_23_P168592	4.0	1.1	3.7		1	3
MAX	NM_145114	A_23_P436138	2.1	0.6	3.7		0	0
PSKH1	NM_006742	A_23_P390596	11.7	3.3	3.5	+	1	1
BRWD1	NM_018963	A_24_P190541	3.5	1.1	3.3	+	0	2
ZNF578	NM_001099694	A_23_P339601	5.0	1.5	3.3		1	1
IER5	NM_016545	A_23_P86330	3.4	1.1	3.1		0	1
TCF4	NM_003199	A_23_P27332	3.1	1.0	3.1	+	2	4
SAR1A	NM_020150	A_23_P127175	4.6	1.5	3.0		0	0
KLHL5	NM_015990	A_23_P121527	3.9	1.3	3.0		1	3
TBC1D14	NM_020773	A_24_P120352	2.3	0.8	3.0		1	1
JARID2	NM_004973	A_23_P214876	6.8	2.2	3.0	+	2	2
PRDM15	AY063456	A_32_P145989	2.8	1.0	3.0		1	2
ZNF845	NM_138374	A_32_P207428	6.2	2.1	2.9		1	2
USPL1*	NM_005800	A_24_P338757	6.4	2.2	2.9		0	1
DPY19L1	NM_015283	A_23_P358628	3.4	1.2	2.8		1	3
ARRDC2	NM_001025604	A_23_P130965	2.1	0.7	2.8		0	1
FAM119A	NM_145280	A_23_P209337	2.6	1.0	2.7		0	0
PHKB	NM_001031835	A_23_P206532	2.2	0.8	2.7		0	1
TAB2	NM_015093	A_23_P19702	7.1	2.7	2.6	+	1	2
ERI2	NM_080663	A_23_P129717	6.6	2.5	2.6		0	0
PICALM	NM_007166	A_23_P147995	2.2	0.9	2.6		0	4
ZFP36*	NM_003407	A_23_P39237	19.4	7.6	2.6		0	1

SUPPLEMENTARY TABLE 3 continued

VAMP3*	NM_004781	A_24_P370887	20.2	7.9	2.5		0	3
CENPI	NM_006733	A_23_P252292	2.1	0.8	2.5		0	0
BACH1	NM_206866	A_23_P211047	14.5	5.8	2.5	+	1	3
RHEB	NM_005614	A_23_P134247	3.8	1.5	2.5	+	0	1
PHC2	NM_198040	A_23_P423864	2.6	1.1	2.4	+	1	1
ZNF320	NM_207333	A_32_P540407	6.1	2.5	2.4		1	2
PLEKHB2	NM_001100623	A_24_P873414	4.6	1.9	2.4		1	1
C5orf15	NM_020199	A_23_P81650	3.2	1.3	2.4		0	0
ARFIP1	NM_001025595	A_24_P166094	2.3	1.0	2.4		0	1
CLUAP1	NM_024793	A_23_P77714	2.6	1.1	2.3		1	1
RNF26	NM_032015	A_23_P64630	2.2	1.0	2.3		1	1
PPA2	NM_176869	A_24_P214625	3.0	1.3	2.2		0	0
PANK1	NM_148977	A_23_P127054	3.7	1.7	2.2	+	0	1
GALT	NM_000155	A_24_P12865	2.4	1.1	2.1		1	1
TPD52	NM_001025252	A_23_P216257	2.6	1.2	2.1		0	1
ZNF137	NR_023311	A_23_P208238	3.1	1.5	2.1		0	0
CD58	NM_001779	A_23_P138308	3.8	1.9	2.1		0	2
CSRP2	NM_001321	A_23_P44724	10.8	5.2	2.0		1	2
LIN9	NM_173083	A_23_P301995	2.2	1.1	2.0		0	1
DCTN6	NM_006571	A_23_P43049	8.8	4.3	2.0		0	0
FGF7	NM_002009	A_23_P14612	10.7	5.3	2.0	+	1	2
KIAA1715	CR936742	A_32_P127248	2.6	1.3	2.0	+	0	2
MARK2	NM_004954	A_24_P914495	3.3	1.6	2.0	+	0	1
CSNK1G2	NM_001319	A_24_P99963	3.2	1.6	2.0	+	1	1
MFSD5	NM_032889	A_23_P72850	5.0	2.5	2.0		0	0
LNX2	NM_153371	A_23_P402287	3.4	1.7	2.0	+	1	1

*present on miR-155-Ramos miR-155 target list,[1]TS-miR-155 target predicted by TargetScan 6.2, [2]8-mer sequence – AGCATTAA, [3]6-mer sequence – GCATTA, [4]8-mer and 6-mer in CDS

SUPPLEMENTARY TABLE 4. MiR-155 target genes in miR-155-Ramos cells identified with Ago2-RIP-Chip.

Gene		Probe	miR-155 IP/T	EV IP/T	miR-155/ EV	TS[1]	# 8-mer[2] in 3'UTR	# 6-mer[3] in 3'UTR
MCM3APAS	NR_002776	A_24_P117301	13.5	5.1	2.6		NA[4]	NA
DET1*	NM_017996	A_23_P26184	4.1	1.5	2.6	+	1	3
SLC23A2	NM_203327	A_24_P254278	3.3	1.3	2.6		0	0
VAMP3*	NM_004781	A_24_P370887	9.0	3.6	2.5		0	3
USPL1*	NM_005800	A_24_P338757	5.0	2.0	2.5		0	1
ZFP36*	NM_003407	A_23_P39237	11.1	4.6	2.4		0	1
AKTIP	NM_001012398	A_32_P224840	7.2	3.0	2.4		0	1
ZBTB4	NM_020899	A_23_P100654	34.4	15.1	2.3		0	0
SNAP23	NM_003825	A_23_P206177	3.3	1.5	2.2		0	0
SETD7	NM_030648	A_24_P251841	2.5	1.2	2.1	+	0	4
STK38	NM_007271	A_24_P63727	2.8	1.4	2.0		0	1
FAM82A2	NM_018145	A_24_P296280	3.9	1.9	2.0		0	0
RC3H2	NM_018835	A_23_P94636	2.8	1.4	2.0		0	3
PSIP1*	NM_021144	A_23_P256384	4.6	2.3	2.0	+	1	2
OAZ3	NM_016178	A_23_P432583	5.3	2.7	2.0		0	0

*present on miR-155-ST486 miR-155 target list,[1]TS-miR-155 target predicted by TargetScan 6.2, [2]8-mer sequence – AGCATTAA, [3]6-mer sequence – GCATTA, [4]Antisense RNA

SUPPLEMENTARY TABLE 5. MiR-155 target genes in KM-H2 cells (Ago2-RIP-Chip).

Gene		Probe	miR-155 AS IP/T	EV IP/T	miR-155 AS/ EV	TS[1]	# 8-mer[2] in 3'UTR	# 6-mer[3] in 3'UTR
RICTOR	NM_152756	A_32_P193322	7.2	17.0	0.42	+	1	3
OOEP	NM_001080507	A_32_P14762	1.0	2.3	0.42		1	1
SMC4	NM_005496	A_23_P91900	1.4	3.1	0.47		0	0
ASPH	NM_032466	A_24_P18105	5.3	10.9	0.49		0	2
TMTC3	NM_181783	A_24_P141804	4.9	9.9	0.49		0	1
EPG5	NM_020964	A_24_P392146	5.5	11.2	0.49		0	0
RBBP6	NM_032626	A_23_P342053	1.0	2.0	0.51		0	3
SLC25A25	NM_001006641	A_23_P9435	1.7	3.3	0.52		0	0
PDE4B	NM_001037341	A_24_P325333	4.1	7.7	0.53		0	0
GCNT2	NM_001491	A_24_P397489	6.8	12.6	0.54		0	0
ISCA1	NM_030940	A_24_P387609	2.2	3.9	0.56		0	0
DNA2	NM_001080449	A_24_P366107	4.6	8.2	0.57		0	0
PKN2	NM_006256	A_24_P387869	40.3	70.0	0.58	+	1	1
JARID2*	NM_004973	A_23_P214876	3.7	6.5	0.58	+	2	2
HIF1AN	NM_017902	A_23_P46964	1.4	2.5	0.58		0	0
ZNF174	NM_003450	A_24_P193600	1.3	2.3	0.58		0	0
SETD8	NM_020382	A_32_P82807	2.2	3.8	0.59		0	0
SLC30A1	U68494	A_24_P937095	3.5	5.8	0.60		0	1
TBRG1*	NM_032811	A_23_P98463	3.7	6.2	0.60	+	1	2
AKAP11	NM_016248	A_23_P204929	11.3	18.7	0.60		0	0
ZNF776	AK095607	A_23_P378499	2.5	4.1	0.60		0	1
SYNJ1	NM_203446	A_23_P324718	9.5	15.6	0.61		0	1
FAM108C1	NM_021214	A_23_P369701	3.1	5.0	0.61		0	0
BET1	NM_005868	A_23_P59700	1.3	2.1	0.62		0	1
DET1*	NM_017996	A_23_P26184	3.4	5.5	0.62	+	1	3
MORF4L1	NM_206839	A_32_P164314	1.5	2.4	0.62		0	0
PANK3	CR612518	A_24_P311845	14.5	23.1	0.63		0	1
SLC2A3	NM_006931	A_24_P81900	7.8	12.3	0.63		0	0
POLK	NM_016218	A_23_P386450	2.9	4.7	0.63		0	0
HDAC4	NM_006037	A_23_P210048	2.1	3.3	0.63	+	1	2
C6orf204	NM_001042475	A_32_P49832	5.1	8.1	0.64		0	0
DCAF8	NM_015726	A_23_P200143	1.5	2.3	0.64		0	0
BICD1	BC010091	A_24_P916586	1.3	2.0	0.64		0	0
ABCC5	NM_005688	A_23_P212665	7.7	11.9	0.64		0	0
RB1CC1	NM_014781	A_23_P9056	2.4	3.7	0.64		0	0
HOMEZ*	NM_020834	A_23_P76829	1.6	2.5	0.64		0	0
BRWD1	NM_001007246	A_24_P861009	1.8	2.7	0.65		0	0
TCF7L2	NM_001198525	A_24_P921823	5.3	8.2	0.65	+	1	2
UBE2D1	NM_003338	A_24_P364025	2.7	4.2	0.65		0	0
ZNF729	NM_001242680	A_24_P161696	20.9	32.1	0.65		0	0
TMEM127	NM_017849	A_24_P80181	1.9	2.9	0.65		0	0
TBC1D20	NM_144628	A_23_P354193	2.6	4.0	0.65		0	1

*present on miR-155-ST486 miR-155 target list,[1]TS-miR-155 target predicted by TargetScan 6.2, [2]8-mer sequence – AGCATTAA, [3]6-mer sequence – GCATTA

SUPPLEMENTARY TABLE 6. TBRG1 transcript isoforms deposited in the Ensemble database.

Name TBRG1	Transcript ID ENST	Length (bp)	Biotype	miR-155BS in 3'UTR	shRNA-1	shRNA-2	shRNA-3
001	00000441174*	4004	Protein coding	Yes	Yes	Yes	Yes
011	00000531667	552	Protein coding	No	No	No	Yes
201	00000375005	1483	Protein coding	No	No	Yes	Yes
003	00000284290	4461	Nonsense mediated decay	Yes	No	Yes	Yes
004	00000452080	730	Nonsense mediated decay	No	No	Yes	No
005	00000529543	2142	Nonsense mediated decay	Yes	No	No	Yes
009	00000530731	1571	Nonsense mediated decay	No	No	Yes	Yes
007	00000438907	842	Processed transcript	No	No	Yes	Yes
002	00000473629	1634	Retained intron	No	No	Yes	Yes
006	00000491010	2308	Retained intron	No	No	No	Yes
008	00000531033	1809	Retained intron	No	No	No	No

***** CCDS8448

SUPPLEMENTARY TABLE 7. Primer sequences used for cloning.

Gene	Forward primer (5'-3')	Reverse primer (5'-3')
miR-155	TGTCACCTCCAGCTTTATAACC	GGCTTTATCATTTTTCAATCT
DET1	GTGCCTCACCAGAGCCAGAT	CACTTAGTTCTCCCAGGAACAG
TRIM32	GAGAAATTATCAGTTTCTTCTGC	GTTCAACATCATTTTAATGACC
JARID2	AACGCCCGTGGTCGATTTAT	TATTATTAAACCTTGTAGTACAAAC
TBRG1	ACAAGAAGGGATCAGATGCCACATCG	GAAAGAGGCCTTCAGTGTTTG
PSIP	TTGGGCTCAAAGCATTAATC	TTTGGTTACAGTTTCATTCTT
HOMEZ	ATGGCATAGGTACTGCTTCC	GAGTTATGCCGTAGCCCTTG
TBRG1	CTCCATGTTCCATGCAACTG	GGGTAACTAAGGCATCCCAC

SUPPLEMENTATY TABLE 8. shRNA sequences.

shRNA	Sequence (5'-3')
shTRIM32-1-S*	TCGAGATAACTCCCTCAAGGTATATACTCGAGTATATACCTTGAGGGAGTTATTTTTTG
shTRIM32-1-AS*	AATTCAAAAAATAACTCCCTCAAGGTATATACTCGAGTATATACCTTGAGGGAGTTATC
shTRIM32-2-S	TCGAGGCCACTTCTTCTCGGAGAATGCTCGAGCATTCTCCGAGAAGAAGTGGCTTTTTG
shTRIM32-2-AS	AATTCAAAAAGCCACTTCTTCTCGGAGAATGCTCGAGCATTCTCCGAGAAGAAGTGGCC
shHOMEZ-1-S	TCGAGAGGCACCATGCCTCCTAATAACTCGAGTTATTAGGAGGCATGGTGCCTTTTTTG
shHOMEZ-1-AS	AATTCAAAAAAGGCACCATGCCTCCTAATAACTCGAGTTATTAGGAGGCATGGTGCCTC
shHOMEZ-2-S	TCGAGTACCTCGGCCTGAGATCATTCCTCGAGGAATGATCTCAGGCCGAGGTATTTTTG
shHOMEZ-2-AS	AATTCAAAAATACCTCGGCCTGAGATCATTCCTCGAGGAATGATCTCAGGCCGAGGTAC
shJARID2-1-S	TCGAGGAAACAGGTTTCTAAGGTAAACTCGAGTTTACCTTAGAAACCTGTTTCTTTTTG
shJARID2-1-AS	AATTCAAAAAGAAACAGGTTTCTAAGGTAAACTCGAGTTTACCTTAGAAACCTGTTTCC
shJARID2-2-S	TCGAGGCCCAACAGCATGGTGTATTTCTCGAGAAATACACCATGCTGTTGGGCTTTTTG
shJARID2-2-AS	AATTCAAAAAGCCCAACAGCATGGTGTATTTCTCGAGAAATACACCATGCTGTTGGGCC
shDET1-1-S	TCGAGAACGTTGAAAAGCCTCCTTGTCTCGAGACAAGGAGGCTTTTCAACGTTTTTTTG
shDET1-1-AS	AATTCAAAAAAACGTTGAAAAGCCTCCTTGTCTCGAGACAAGGAGGCTTTTCAACGTTC
shDET1-2-S	TCGAGAAGACTATTCCCTCCATATCACTCGAGTGATATGGAGGGAATAGTCTTTTTTTG
shDET1-2-AS	AATTCAAAAAAAGACTATTCCCTCCATATCACTCGAGTGATATGGAGGGAATAGTCTTC
shPSIP1-1-S	TCGAGGCAGCAACTAAACAATCAAATCTCGAGATTTGATTGTTTAGTTGCTGCTTTTTG
shPSIP1-1-AS	AATTCAAAAAGCAGCAACTAAACAATCAAATCTCGAGATTTGATTGTTTAGTTGCTGCC
shTBRG1-1 -S	TCGAGACTGGAAGTTCTGAAGAAACTCGAGTTTCTTCAGAACTTCCAGTTTTTTG
shTBRG1-1 -AS	AATTCAAAAAACTGGAAGTTCTGAAGAAACTCGAGTTTCTTCAGAACTTCCAGTC
shTBRG1-2-S	TCGAGGAGAACAACAAACTGGAAGATCTCGAGATCTTCCAGTTTGTTGTTCTCTTTTTG
shTBRG1-2-AS	AATTCAAAAAGAGAACAACAAACTGGAAGATCTCGAGATCTTCCAGTTTGTTGTTCTCC
shTBRG1-3-S	TCGAGCCAGACCAGAAGTGTCTATATCTCGAGATATAGACACTTCTGGTCTGGTTTTTG
shTBRG1-3-AS	AATTCAAAAACCAGACCAGAAGTGTCTATATCTCGAGATATAGACACTTCTGGTCTGGC

*S-sense strand, AS-antisense strand

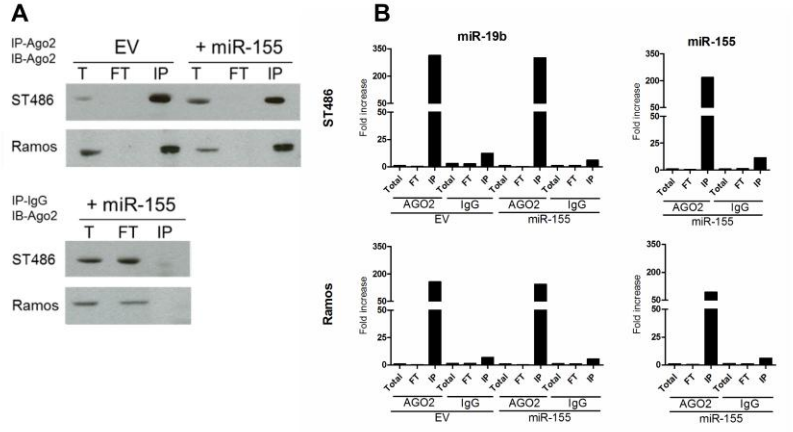

SUPPLEMENTARY FIGURE 1. Ago2, miR-19b and miR-155 are enriched in Ago2-IP fraction in ST486 and Ramos cells. (A) Analysis of the IP efficiency by Western blotting for Ago2 protein. Ago2 was pulled down when anti-Ago2 antibody was used and not when IgG1 negative control antibody was used. (B) IP efficiency of the Ago2-RISC complex analyzed by qRT-PCR for miR-19b and miR-155. Both miRNAs were pulled down with anti-Ago2 antibody and not with IgG1 negative control antibody. MiRNA levels were normalized to RNU48. MiR-155 levels could only be measured in miR-155-transduced samples, since the levels in EV-transduced samples were not detectable.

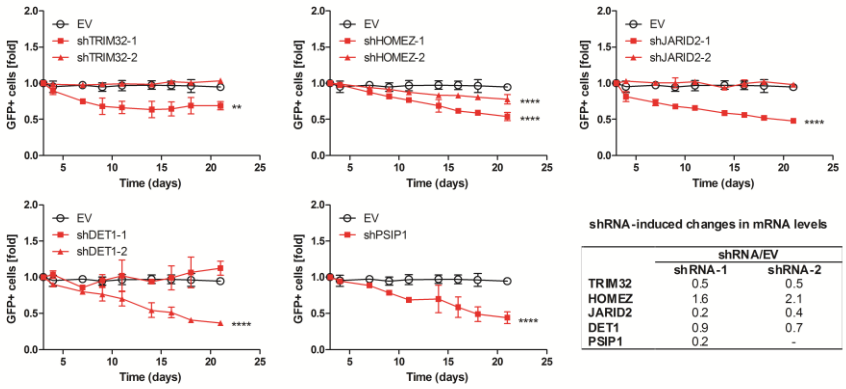

SUPPLEMENTARY FIGURE 2. GFP competition assay of cells transduced with shRNAs against five validated miR-155 target genes. Percentage of GFP+ cells was normalized to day 3 and fold increase or decrease within 21 days was shown. For TRIM32, JARID and DET1, one shRNAs caused decrease in percentage of GFP+ ST486 cells, whereas the other shRNA construct had no effect. For HOMEZ, both shRNAs showed an growth inhibitory effect. For PSIP1 the shRNA construct also resulted in growth inhibition of ST486 cells. The average of 2 or 3 experiments was presented. P value was determined by linear regression (**p<0.01, **** p<0.0001). Decrease in mRNA level of selected genes upon shRNA presented in a table as a ratio between mRNA level in GFP+ cells with shRNA compared to GFP+ cells with EV. None of the shRNAs induced a phenotype similar to that observed for miR-155.

CHAPTER 7

Summary and Discussion
Future Perspectives

Izabella Ślęzak-Prochazka

SUMMARY AND DISCUSSION

MiRNAs are effective gene expression regulators that play crucial roles in many cellular processes, such as apoptosis, proliferation and differentiation. Deregulated miRNA levels are observed in many diseases including cancer and have been causatively implicated in the cancer pathogenesis. The mechanisms causing altered miRNA levels or the genes affected by miRNA deregulation are often unknown. The aim of the research project presented in this thesis was to elucidate key aspects of the regulation of miRNA biogenesis (chapter 2-4) and consequences of altered miR-155 levels (chapter 5-6) in B-cell lymphoma.

Regulation of miRNA biogenesis

MiRNA levels are regulated at the transcriptional and post-transcriptional level. At the transcriptional level, the regulation of expression is often similar to that of protein-coding genes and includes regulation of expression by transcription factors, methylation, etc. A very important additional step in the regulation of miRNA expression is the processing from the primary transcript to the mature miRNA. In chapter 2, we discuss currently known mechanisms involved in regulation of miRNAs processing and we indicate that most regulatory factors are specific for individual miRNAs or for a subgroup of the miRNAs. Several tissue-specific mechanisms have been identified that result in either enhanced or inhibited miRNA processing. Regulatory mechanisms, as currently known from the literature, are described for a group of ~30 miRNAs. We speculate that in addition to the miRNAs specifically addressed in this chapter, many more miRNAs are being regulated during processing.

MiR-155 is one of the most studied oncogenic miRNAs that has a presumed regulated processing in B-cell lymphoma, although no regulating factors have been identified so far. MiR-155 belongs to a small group of exonic miRNAs that are characterized by location of the stem-loop structure in exons of non-protein-coding genes. Processing of miR-155 and two additional exonic miRNAs was investigated in chapter 3.

We assessed levels and subcellular localization of unspliced and spliced primary transcripts in B-cell lymphoma cell lines. We showed that unspliced transcripts are predominantly nuclear, whereas spliced transcripts are partly transported to the cytoplasm and are, as such, unavailable for processing by the Microprocessor complex. These results indicate that splicing and nuclear export can serve as a mechanism to prevent processing of exonic miRNAs. Upon stimulation of B-cell lymphoma cells the unspliced/spliced transcript ratio of *BIC* (pri-miR-155) decreased, indicating that external stimuli may affect the efficiency of pri-miRNA splicing and nuclear export, and thereby regulate the levels of exonic miRNAs.

A second oncogenic miRNA cluster that is frequently deregulated in B-cell lymphoma is the miR-17~92 cluster that consists of six miRNAs, i.e. miR-17, miR-18a, miR-19a, miR-20a, miR-19b and miR-92a. In chapter 4, we investigated the expression pattern of these six miRNAs in 117 non-Hodgkin lymphoma (NHL) cases and in 21 NHL cell lines. We show that miR-92a is the most abundant miRNA in three of the four subtypes of the NHL cases, all NHL cell lines and in the normal B-cell subsets. Only in diffuse large B-cell lymphoma, miR-19b levels were higher than the miR-92a levels. Comparison of the individual miRNA levels in NHL as compared to their normal counterparts showed that miR-19b is the most significantly induced miR-17~92 cluster member. This suggests that either the processing efficiency or the stability of miR-19b is increased in NHL. The observed miR-19b induction is consistent with the known oncogenic role of miR-19b in lymphomagenesis.

Identification of microRNA-155 target genes

Studying the cellular function of specific miRNAs often includes their inhibition or overexpression in the cell type of interest. Transfection of small precursor-like molecules or anti-sense oligo's is effective only for short-term experiments. To achieve long-term induction or inhibition of specific miRNAs, viral vectors are commonly used. For overexpression of miRNAs, cloning of the stem-loop region with the 100-150nt 3' and 5' flanking region is generally effective to induce the miRNA of interest. Effective strategies for inhibition of highly abundant miRNAs

or all members of a specific seed family are technically more challenging. In chapter 5, we describe a straightforward and rapid method to generate constructs with antisense miRNA sequences against single miRNAs, multiple miRNAs or seed families. These so-called miRNA sponges were generated starting from short oligo's that were ligated to concatamers of variable sizes and cloned in a selected vector. We demonstrate that these miRNA sponges efficiently sequester miRNAs, inhibit their function and, as such, can be used for *in vitro* or *in vivo* loss-of-function studies.

To study the role of miR-155 and identify its target genes, we overexpressed miR-155 in two Burkitt lymphoma cell lines, ST486 and Ramos (chapter 6). Both cell lines have very low endogenous miR-155 levels compared to the levels in germinal center B cells. Interestingly, we observed an enhanced growth of ST486 cells upon miR-155 overexpression, but not of Ramos cells. Using Ago2-RIP-Chip we identified 54 and 15 miR-155 target genes in ST486 and Ramos cells, respectively. The lower number of target genes and the lower fold enrichment of the miR-155 targets in the Ago2-IP fraction observed for miR-155-transduced Ramos cells suggest a differential targeting efficiency in these two cell lines. We selected four ST486-specific miR-155 targets, TBRG1, TRIM32, HOMEZ, JARID2, and two common targets, DET1 and PSIP1, for further validation. All six genes were confirmed as miR-155 targets in a luciferase reporter assay. Next, we investigated whether these miR-155 targets were also targeted in Hodgkin lymphoma cells with high endogenous miR-155 levels. Five of the six selected target genes showed diminished abundance in the miRNA targetome of cells transduced with miR-155 sponge compared to cells transduced with empty vector. This suggests that these five genes are also targeted by endogenous miR-155 in Hodgkin lymphoma cells. To determine if we can copy the growth promoting phenotype observed in ST486 cells upon miR-155 overexpression, we inhibited TBRG1, TRIM32, HOMEZ, JARID2, DET1 and PSIP1 using shRNA constructs. Inhibition of TBRG1 resulted in growth enhancement suggesting that TBRG1 is involved in growth promoting phenotype observed upon miR-155 overexpression in ST486 cells.

In conclusion, in this thesis we investigated mechanisms involved in regulation of miRNA processing and proposed a novel mechanism to regulate processing of exonic miRNAs by nuclear export of spliced pri-miRNA transcripts. We also showed differential processing of miR-17~92 cluster members and specific upregulation of miR-19b in NHL. In the second part, we investigated the effect of miRNA modulation on B-cell lymphoma cells and we described method to inhibit miRNAs by miRNA sponges. Finally, we identified novel miR-155 targets in B-cell lymphoma and showed that miR-155 induced cell growth by targeting the TBRG1 gene.

FUTURE PERSPECTIVES

In the past 10 years, the miRNA research field has greatly expanded and knowledge regarding miRNA processing, target gene recognition and functioning has been gained. Despite these developments it is also clear that there are still many questions that need to be answered to fully understand miRNA biology.

Identification of miRNAs with (de)regulated processing

In this thesis we discussed miRNAs that undergo regulated processing. Specifically, we investigated processing of miR-155 and the miR-17~92 cluster. The group of miRNAs regulated at the processing level is likely to be much larger than currently described in the literature. An indication for regulated processing is an inconsistency between primary and mature miRNA levels. We started analysis of pri-miRNAs and mature miRNAs levels in 12 samples of normal B cells and B-cell lymphoma to gain a global insight in the number of miRNAs that are potentially regulated at the processing level.

The incomplete characterization of a significant subset of the primary miRNA transcripts makes it challenging to reliably analyze their expression levels. Many miRNAs are localized in introns of protein coding genes and commercially available probes that mostly detect spliced transcripts are not suitable for detection of such pri-miRNAs. Potential problems that may affect detection of primary miRNA transcripts of miRNAs are that (1) the exact length

and transcriptional start site of intergenic pri-miRNAs transcripts is frequently unknown; (2) it is unknown if the spliced or unspliced transcripts serve as templates for the biogenesis of exonic miRNA; (3) many intronic miRNAs are transcribed from a promoter that is different from the promoter used by the protein-coding host gene and this might lead to different transcript sizes; (4) some mature miRNAs can be transcribed from multiple loci on the genome. All these aspects complicate the design of a good platform to determine the expression levels of pri-miRNA transcripts. To address these putative complicating factors we designed a custom gene expression array containing probes that cover the stem-loop region and sequences flanking the stem-loop regions of all pri-miRNA transcripts (Fig. 1A). For data analysis we selected the probe that showed the highest signal for each stem-loop region. Probes corresponding to 974 miRNAs were present on both the mature and the pri-miRNA arrays and were detectable for the pri-miRNA and/or mature miRNA in at least 1 of the 12 samples. Comparison of the levels of pri-miRNAs and mature miRNAs revealed a significant positive correlation for only 39 miRNAs, whereas a significant inversed correlation was observed for 35 miRNAs (Table 1).

The group of miRNAs with a positive correlation contained all six members of the miR-17~92 cluster with a Pearson correlation coefficient that ranged from 0.77 to 0.92 ($p < 0.01$). This was consistent with the positive correlation observed for these six miRNAs and the *C13ORF25* transcript levels in

TABLE 1. Correlation between pri-miRNA and mature miRNA.

	#miRNAs	Pearson correlation	p-value
Significant positive correlation	39	0.57- 0.92	<0.05
Positive correlation	121	0-0.56	>0.05
Significant negative correlation	35	-0.94- -0.58	<0.05
Negative correlation	99	-0.57-0	>0.05
Only pri-miRNA detected*	629	-	-
Only mature miRNA detected*	51	-	-
Total	**974**		

*Detected at least in 1 of 12 samples

NHL cases and cell lines (chapter 4). MiR-155 levels were also positively correlated with *BIC* transcript levels and showed a Pearson correlation coefficient of 0.56 (p=0.055). This is in accordance with the positive miR-155 - *BIC* correlation observed in B-cell lymphoma cell lines (chapter 3). For the vast majority of the analyzed miRNAs, i.e. 629 (65%), we only detected the pri-miRNA transcripts and not the mature miRNAs. This suggests that most of the primary transcripts are expressed, but not processed to mature miRNAs in B cells or B-cell lymphoma. Another explanation might be that the mature miRNAs are unstable or actively degraded.

DGCR8 is an essential component of the Microprocessor complex and therefore required for miRNA processing (Han et al., 2006; Landthaler et al., 2004). Inhibition of DGCR8 should prevent miRNA biogenesis and thus result in an increase of pri-miRNA levels. In our initial experiment with an shRNA against DGCR8 in HL cell line we observed enhanced levels for only a small fraction (n=53) of the pri-miRNA transcripts (Fig. 1B). The lack of enhanced pri-miRNA levels for the vast majority of the transcripts is not caused by a global shift in pri-miRNA levels during normalization procedures, since we observed no difference for the protein-coding transcript levels that were also present on the array. The efficiency of DGCR8 inhibition was shown by 2.4 fold decrease in DGCR8 transcript levels (Fig. 1C) and 3 fold decrease in miR-155 levels (Fig. 1D).

There was a striking overlap, i.e. 33 of the 53 (62%), between the miRNAs that showed enhanced pri-miRNA levels upon DGCR8 inhibition and the miRNAs that showed a positive correlation between the mature and primary transcript levels. Probes for all six members of the miR-17~92 cluster as well as miR-155 showed 15 to 65 fold higher transcript levels upon shDGCR8 and were among the top ten most affected probes.

At present, we cannot explain why the correlation between primary and mature miRNA levels is so poor and why the levels of most pri-miRNA transcripts are not enhanced upon DGCR8 inhibition. This poor correlation might represent a mechanism for the cells to achieve tissue-specific miRNA expression patterns. This would mean that pri-miRNAs are abundantly expressed, but need auxiliary

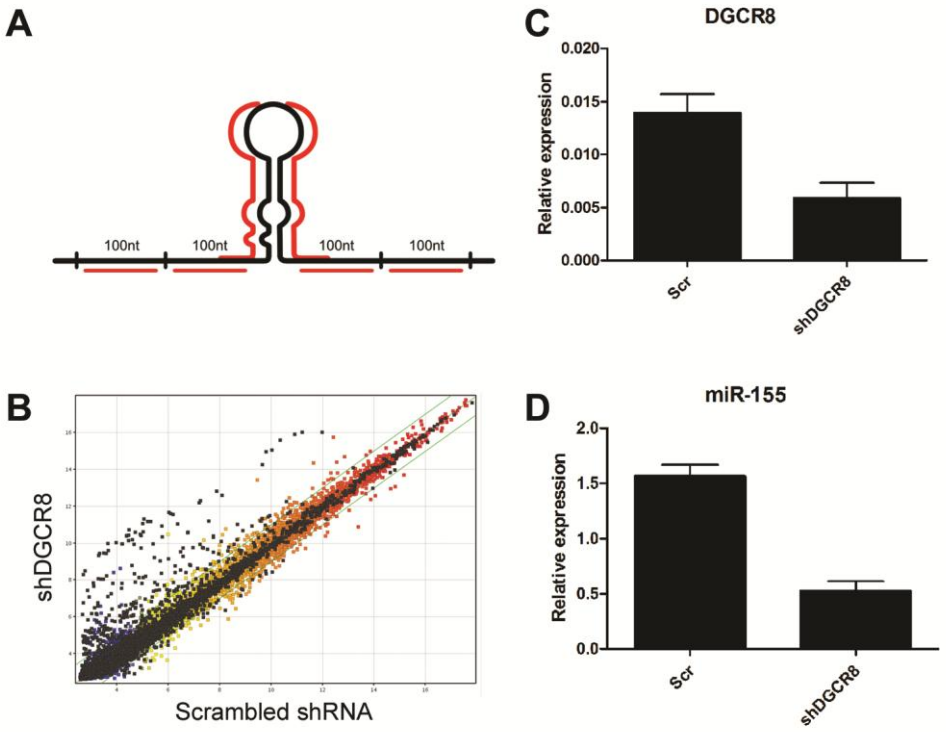

FIGURE 1. Inhibition of DGCR8 affect only fraction of pri-miRNAs. (A) Up to 6 probes were designed for each miRNA stem-loop (indicated in red), i.e. 2 probes that cover stem-loop region, 2 probes located within 100nt stem-loop flanking sequence and 2 probes located in the region 100-200nt from stem-loop structure. (B) Comparison of levels of pri-miRNAs (indicated in black) in L1236 cells transduced with lentiviral vector containing shDGCR8 versus scrambled control. Correlation of protein-coding gene levels was indicated in color. All transcripts were detected by Agilent custom gene expression array. Levels of DGCR8 (C) and miR-155 (D) were decresed upon DGCR8 inhibition measured by qRT-PCR relative to HPRT and RNU48 levels, respectively.

tissue-specific proteins to regulate processing by the Microprocessor complex. To identify the proteins that are bound to specific pri-miRNAs, immunoprecipitation of the Microprocessor complex and the subsequent identification of the proteins in different cell types need to be performed. On the other hand, it might be that a 2.4 fold inhibition of DGCR8 is not sufficient to effectively inhibit biogenesis of pri-miRNA transcripts. It would be interesting to investigate whether the same set of pri-miRNAs is affected in different tissue types and whether the correlation between specific pri-miRNAs and mature miRNAs is tissue-specific. Based on

these preliminary findings it is tempting to speculate that only a minority of the actively transcribed pri-miRNAs is processed to mature miRNAs. This implies that regulation of miRNA biogenesis might be a much more general phenomenon than currently anticipated.

Identification of miRNA target genes in B-cell lymphoma

In the studies described in this thesis, a clear phenotype of enhanced miR-155 levels was observed in one of two BL cell lines. One of the identified miR-155 targets, TBRG1, phenocopied this effect. To further study the relevance of TBRG1 in the pathogenesis of B-cell lymphoma it would be interesting to determine TBRG1 protein expression patterns in B-cell lymphoma cases with high and low miR-155 levels. In addition, it would be of interest to study the effect of enhanced TBRG1 expression in HL cell lines and study the effect of TBRG1 shRNA constructs in the Ramos BL cell line that did not show a phenotype upon miR-155 induction. It is clear that miR-155 modulation may have different effects in various subtypes of B-cell malignancies. To unravel these cell type-specific miR-155 functions the miR-155 targetomes should be studied in different stages of B-cell development and in different B-cell lymphoma subtypes. It is intriguing, why some genes are very efficiently targeted by specific miRNAs in one cell type, whereas they are not regulated by the same miRNAs in other cell types despite being expressed at high levels. Comparison of the miRNA targetomes of normal B cells to that of malignant B cells will allow indentification of the target genes that are related to the malignant transformation. However, it is challenging to obtain enough normal GC B cells for efficient immunoprecipitation of endogenous Ago2. Analogous to miR-155 and the previously analyzed miR-17 family target genes, several other miRNAs that are important for lymphomagenesis, such as miR-150, miR-21 and miR181b (Kotani et al., 2010), should be modulated in B-cell lymphoma cells and subjected to Ago2-RIP-Chip.

In this thesis we used anti-Ago2 antibody for immunoprecipitation of the RISC and the subsequent identification of miRNA target genes. However, Ago1, 3 and 4 can also be a part of the RISC complex and the four isoforms are

generally redundant (Azuma-Mukai et al., 2008; Liu et al., 2004; Meister et al., 2004). In B-cell lymphoma, we showed that Ago1 and Ago2 are expressed at high levels, whereas Ago3 and Ago4 are much less abundant (Tan et al., 2009). Nevertheless, it would be of interest to investigate the miRNA targetome using antibodies for all Ago isoforms separately or use a pan-Ago antibody for the RIP-Chip.

Studies described in this thesis have been performed with miRNA and gene expression microarray analysis using the Agilent platform. In future studies, it would be advisable to use RNA-sequencing instead of gene expression arrays. For identification of miRNA target sequence by Ago2-RIP-Chip, RNA-seq analysis will allow specific identification of alternative splice isoforms that may be differentially regulated by miRNAs as shown for targeting of TBRG1 by miR-155. Targeting of specific transcript isoforms by a miRNA has been suggested to represent a more common phenomenon (Deng et al., 2011). Also for miRNA profiling studies small-RNA-seq should be implemented to allow identification of novel miRNAs that are important for B-cell lymphoma. In addition, this will provide specific information concerning sequence variations of the miRNAs. Moreover, small-RNA-seq of the RIP-Chip fraction, also allows to specifically identify the miRNAs that are indeed loaded into the RISC and this may facilitate discrimination of true novel miRNAs from RNA degradation products. Recent technical developments such as HITS-CLIP, PAR-CLIP and CLASH attempt to improve methods to experimentally link miRNAs to their cellular target genes (Chi et al., 2009; Hafner et al., 2010; Kudla et al., 2011). This will facilitate identification of cell type-specific miRNA-target gene combinations, without modulation of miRNA levels.

At present, the only antisense miRNA-based therapy which is a subject of clinical trials is directed against miR-122 and aims to block hepatitis C virus replication and viremia (Elmen et al., 2008; Jopling et al., 2005; Sarasin-Filipowicz et al., 2009). Modulation of miRNA levels also has a great potential in anti-cancer therapy. Mice overexpressing miR-155 and miR-21 develop miRNA-dependent lymphomas, and removal or inhibition of these miRNAs leads to reduced tumor sizes indicating that the tumor cells are "addicted" to these

oncogenic miRNAs (Babar et al., 2012; Medina et al., 2010). Therefore, these miRNAs present promising candidates for antisense therapy to treat B-cell lymphoma patients. In this respect, it would be valuable to study the potential of miRNA sponges described in chapter 5 to inhibit miRNAs *in vivo*. Tightly controlled modulation of miRNA levels in combination with predictable outcome of such modulations, i.e. the affected miRNA target genes, will enable the application of miRNA modulating agents in anti-cancer therapy in future studies.

REFERENCES

Azuma-Mukai, A., Oguri, H., Mituyama, T., Qian, Z.R., Asai, K., Siomi, H. and Siomi, M.C. 2008. Characterization of endogenous human Argonautes and their miRNA partners in RNA silencing. *Proc. Natl. Acad. Sci. U. S. A.* **105**: 7964-7969.

Babar, I.A., Cheng, C.J., Booth, C.J., Liang, X., Weidhaas, J.B., Saltzman, W.M. and Slack, F.J. 2012. Nanoparticle-based therapy in an in vivo microRNA-155 (miR-155)-dependent mouse model of lymphoma. *Proc. Natl. Acad. Sci. U. S. A.* **109**: E1695-704.

Chi, S.W., Zang, J.B., Mele, A. and Darnell, R.B. 2009. Argonaute HITS-CLIP decodes microRNA-mRNA interaction maps. *Nature* **460**: 479-486.

Deng, N., Puetter, A., Zhang, K., Johnson, K., Zhao, Z., Taylor, C., Flemington, E.K. and Zhu, D. 2011. Isoform-level microRNA-155 target prediction using RNA-seq. *Nucleic Acids Res.* **39**: e61.

Elmen, J., Lindow, M., Silahtaroglu, A., Bak, M., Christensen, M., Lind-Thomsen, A., Hedtjarn, M., Hansen, J.B., Hansen, H.F., Straarup, E.M. et al. 2008. Antagonism of microRNA-122 in mice by systemically administered LNA-antimiR leads to up-regulation of a large set of predicted target mRNAs in the liver. *Nucleic Acids Res.* **36**: 1153-1162.

Hafner, M., Landthaler, M., Burger, L., Khorshid, M., Hausser, J., Berninger, P., Rothballer, A., Ascano, M.,Jr, Jungkamp, A.C., Munschauer, M. et al. 2010. Transcriptome-wide identification of RNA-binding protein and microRNA target sites by PAR-CLIP. *Cell* **141**: 129-141.

Han, J., Lee, Y., Yeom, K.H., Nam, J.W., Heo, I., Rhee, J.K., Sohn, S.Y., Cho, Y., Zhang, B.T. and Kim, V.N. 2006. Molecular basis for the recognition of primary microRNAs by the Drosha-DGCR8 complex. *Cell* **125**: 887-901.

Jopling, C.L., Yi, M., Lancaster, A.M., Lemon, S.M. and Sarnow, P. 2005. Modulation of hepatitis C virus RNA abundance by a liver-specific MicroRNA. *Science* **309**: 1577-1581.

Kotani, A., Harnprasopwat, R., Toyoshima, T., Kawamata, T. and Tojo, A. 2010. miRNAs in normal and malignant B cells. *Int. J. Hematol.* **92**: 255-261.

Kudla, G., Granneman, S., Hahn, D., Beggs, J.D. and Tollervey, D. 2011. Cross-linking, ligation, and sequencing of hybrids reveals RNA-RNA interactions in yeast. *Proc. Natl. Acad. Sci. U. S. A.* **108**: 10010-10015.

Landthaler, M., Yalcin, A. and Tuschl, T. 2004. The human DiGeorge syndrome critical region gene 8 and Its D. melanogaster homolog are required for miRNA biogenesis. *Curr. Biol.* **14**: 2162-2167.

Liu, J., Carmell, M.A., Rivas, F.V., Marsden, C.G., Thomson, J.M., Song, J.J., Hammond, S.M., Joshua-Tor, L. and Hannon, G.J. 2004. Argonaute2 is the catalytic engine of mammalian RNAi. *Science* **305**: 1437-1441.

Medina, P.P., Nolde, M. and Slack, F.J. 2010. OncomiR addiction in an in vivo model of microRNA-21-induced pre-B-cell lymphoma. *Nature* **467**: 86-90.

Meister, G., Landthaler, M., Patkaniowska, A., Dorsett, Y., Teng, G. and Tuschl, T. 2004. Human Argonaute2 mediates RNA cleavage targeted by miRNAs and siRNAs. *Mol. Cell* **15**: 185-197.

Sarasin-Filipowicz, M., Krol, J., Markiewicz, I., Heim, M.H. and Filipowicz, W. 2009. Decreased levels of microRNA miR-122 in individuals with hepatitis C responding poorly to interferon therapy. *Nat. Med.* **15**: 31-33.

Tan, L.P., Seinen, E., Duns, G., de Jong, D., Sibon, O.C., Poppema, S., Kroesen, B.J., Kok, K. and van den Berg, A. 2009. A high throughput experimental approach to identify miRNA targets in human cells. *Nucleic Acids Res.* **37**: e137.

NEDERLANDSE SAMENVATTING

MicroRNAs (miRNAs) zijn korte, ~22 nucleotiden (nt), RNA moleculen die betrokken zijn bij de regulatie van genexpressie en daarmee een cruciale rol spelen in een groot aantal cellulaire processen, zoals apoptose, proliferatie en differentiatie. Veranderingen in het expressie patroon van miRNAs zijn kenmerkend voor allerlei ziektebeelden en ook tumoren worden gekenmerkt door een afwijkend miRNA expressiepatroon. Functionele *in vitro* en *in vivo* studies hebben aangetoond dat deze afwijkende miRNA expressie patronen causaal geassocieerd zijn met het ontstaan van kanker. Echter, de mechanismen die betrokken zijn bij de veranderingen in het miRNA expressie patroon en de genen die daardoor worden gereguleerd zijn vaak nog niet bekend. Het doel van deze promotie studie was om factoren betrokken bij de regulatie van de miRNA biogenese te onderzoeken (hoofdstuk 2-4) en om de effecten van een miRNA dat frequent verhoogd tot expressie komt in B-cel lymfomen, miR-155, te onderzoeken (hoofdstuk 5-6).

Regulatie van de miRNA biogenese

De expressie van miRNAs in de cel kan op transcriptioneel en post-transcriptioneel niveau gereguleerd worden. Op het niveau van transcriptie zijn de regulerende mechanismen gelijk aan de mechanismen die ook de expressie van eiwit coderende genen reguleren, waarbij transcriptiefactoren en methylatie een belangrijke rol spelen. Post-transcriptioneel wordt de expressie van miRNAs in belangrijke mate gereguleerd door de biogenese van de functionele mature miRNAs uit de langere primaire transcripten. In hoofdstuk 2 wordt een overzicht gegeven van de factoren waarvan bekend is dat ze de biogenese van mature miRNAs kunnen beïnvloeden. Deze factoren oefenen direct of indirect invloed uit op de activiteit / specificiteit van de twee enzym complexen die betrokken zijn bij de biogenese. Ook kunnen ze door binding aan de "stem" of aan de "loop" van het primaire of precursor miRNA transcript de biogenese beïnvloeden. Tot op heden zijn er voor in totaal zo'n 30 verschillende miRNAs verschillende weefsel specifieke factoren gepubliceerd.

In hoofdstuk 3 hebben we de biogenese onderzocht van een relatief kleine groep van miRNAs die in exonen van niet coderende genen liggen. Voor deze groep van miRNAs kan het transcript met of zonder intronen dienen als template voor de biogenese van de mature miRNAs. Voor miRNAs die in de intronen liggen van coderende of niet coderende genen kunnen splicing en de eerste stappen van de miRNA biogenese tegelijkertijd plaats vinden. We hebben ons onderzoek gericht op drie miRNAs: miR-22, miR-146a en miR-155, die in exonen liggen van niet coderende genen. We hebben eerst gekeken naar de intracellulaire locatie van de primaire (pri-)miRNA transcripten met en zonder intronen. Hieruit bleek dat de intron houdende pri-miRNA transcripten bijna exclusief in de kern gelokaliseerd zijn, terwijl de pri-miRNA transcripten na splicing van de intronen gedeeltelijk in de kern zitten en gedeeltelijk in het cytoplasma. Aangezien de 1e stap voor de biogenese uitsluitend in de kern plaats vindt, is het aannemelijk dat de intron-houdende pri-miRNA transcripten de belangrijkste bron voor de miRNA biogenese zijn. De verhouding tussen de hoeveelheid transcript voor en na splicing kan variëren onder invloed van stimulatie, wat er op kan duiden dat de miRNA biogenese gereguleerd kan worden door het veranderen van de balans tussen splicing in combinatie met het nucleair export of miRNA biogenese. Overexpressie van een transcript zonder intronen resulteerde echter wel in een duidelijk toename van de hoeveelheid mature miRNA. Dit betekent dat het transcript zonder intronen wel degelijk gebruikt kan worden voor de miRNA biogenese mits in voldoende mate aanwezig in de kern.

In hoofdstuk 4 hebben we een aantal karakteristieken van het miR-17~92 transcript in B-cel lymfomen onderzocht. Dit oncogene miRNA cluster bevat de "stem-loop" structuren voor 6 miRNAs, miR-17, miR-18a, miR-19a, miR-20a, miR-19b and miR-92a. Er zijn twee iso-vormen van dit transcript, waarbij de stem-loop structuren zich kunnen bevinden in het exon van de ene iso-vorm en in het intron van de andere iso-vorm. Opmerkelijk is dat de expressie van de mature miRNAs in de cel sterk kan verschillen, terwijl ze allen afkomstig zijn van hetzelfde primaire transcript. We hebben de hoeveelheid van de zes miRNAs bepaald in drie B cel maturatie stadia, 117 B cel lymfomen en in 21 B cel

lymfoom cellijnen. In normale B cel subsets en drie B cel lymfoom subtypen was de expressie van miR-92 10 tot 100x hoger dan de 5 andere miRNAs. Alleen bij het diffuus groot cellig B cel lymfoom was de expressie van miR-19b het hoogst. In vergelijking met de normale voorloper cellen lieten alle lymfoom subtypen een sterke toename zien van met name miR-19b, terwijl geen toename werd gezien van miR-92. Ook voor de andere vier miRNAs werden geen verhoogde expressie niveaus gevonden ten opzichte van de normale B cellen. De sterke inductie van miR-19b is consistent met de oncogene effecten van dit miRNA zoals aangetoond in muis modellen. Onze data duiden erop dat er een sterke regulatie is van de hoeveelheid mature miRNAs, dit kan bereikt worden door verschillen in de processing efficiency van de zes precursor miRNAs en/of door verschillen in de stabiliteit van de mature miRNAs.

miRNA-155 target genen

In hoofdstuk 5 beschrijven we een methode waarmee we op een efficiënte manier de functie van miRNAs kunnen remmen door productie van antisense transcripten met meerdere bindingsplaatsen voor de miRNA(s) van interesse. De antisense transcripten worden op een zodanige manier ontwikkeld dat ze een variabel aantal bindingsplaatsen gericht tegen een of meerdere miRNAs kunnen bevatten. De antisense transcripten worden tot overexpressie gebracht door klonering in een virale vector en infectie in het celtype van interesse. We laten op verschillende manieren, waaronder reporter testen en functionele testen, zien dat deze zogenaamde spons vectoren effectief zijn in B cel lymfoom cellijnen. De methode is gebaseerd op concatemerisatie van dubbelstrengs oligo's die twee miRNA bindingsplaatsen bevatten met daar tussen een korte willekeurige sequentie. De 1-staps ligatie reactie met een oligo-vector ratio variërend van 1:10 tot 1:1000 resulteert in constructen met een variabel aantal oligo's en dus ook een variabel aantal miRNA bindingsplaatsen. De spons vectoren kunnen op deze manier efficiënt gemaakt worden gebruikt worden om het effect van miRNA inhibitie in een specifiek celtype te bestuderen.

Om de oncogene rol van miR-155 verder te bestuderen hebben we in hoofdstuk 6 dit miRNA tot overexpressie gebracht in twee Burkitt lymfoom cellijnen, ST486 and Ramos. Deze twee cellijnen hebben een lage endogene miR-155 expressie in vergelijking met de normale voorloper cellen. In een cel proliferatie test toonden we aan dat in ST486 cellen miR-155 een groei voordeel opleverde, terwijl in Ramos cellen geen effect werd gezien op de groei snelheid. Door immuunprecipitatie van het RNA-induced silencing complex in cellen met overexpressie van miR-155, en de daarop volgende gen expressie profiling konden we 54 miR-155 target genen in ST485 en 15 in Ramos aan tonen. Voor zes genen hebben we vervolgens aanvullende functionele studies uitgevoerd om te kijken of een van deze genen betrokken was bij het miR-155 fenotype in ST486. TBRG1, TRIM32, HOMEZ en JARID2 werden alleen in ST486 gevonden als zijnde miR-155 targets, terwijl DET1 en PSIP1, in zowel ST486 als ook in Ramos als target genen voor miR-155 werden geïdentificeerd. Voor zes geselecteerde genen hebben we middels een luciferase test binding door miR-155 bevestigd. Voor DET1 konden we ook op eiwit niveau aantonen dat er regulatie door miR-155 plaats vond. Remming van miR-155 in een Hodgkin lymfoom cellijn met hoge endogene miR-155 niveaus, bevestigde binding van miR-155 voor vijf van de zes genen. Cel proliferatie testen met shRNAs tegen alle zes genen in ST486 lieten voor vijf genen geen effect of geen groei remming zien. Voor TBRG1 zagen we groei stimulerend effect, vergelijkbaar met het effect zoals gevonden voor miR-155. Dit onderzoek toont aan dat het groei stimulerende effect van miR-155 op zijn minst gedeeltelijk kan worden toegeschreven aan het remmen van TBRG1 in ST486 cellen.

Samenvattend, laten we in dit proefschrift zien hoe de miRNA biogenese gereguleerd kan worden voor een specifieke groep van miRNAs die gelokaliseerd zijn in exonen van niet voor eiwit coderende genen. Verder laten we zien dat er in B cel lymfomen een sterke regulatie is van de miRNA expressie niveaus van miRNAs die afkomstig zijn van hetzelfde primaire miR-17~92 miRNA transcript. in alle B cel lymfoom subtypen werd overexpressie van het oncogene miR-19b gevonden. In het tweede deel van dit proefschrift hebben we een methode

ontwikkeld om op een effectieve manier miRNAs te kunnen remmen. Daarnaast hebben we de rol van miR-155 onderzocht in B cel lymfomen en aangetoond dat TBRG1 een belangrijk target gen is voor de oncogene rol van miR-155.

Translated by Anke van den Berg

PUBLICATIONS

Slezak-Prochazka I, Kluiver J, de Jong D, Halsema N, Poppema S, Kroesen BJ, van den Berg A. 2012. Cellular localization and processing of primary transcripts of exonic microRNAs. *PLoS One, provisionally accepted*.

Kluiver J, **Slezak-Prochazka I**, van den Berg A. 2012. Studying MicroRNAs in Lymphoma. *Methods in Molecular Biology* 971, *in press.*

Kluiver J, **Slezak-Prochazka I**, Smigielska-Czepiel K, Halsema N, Kroesen BJ, van den Berg A. 2012. Generation of miRNA sponge constructs. *Methods* 58: 113-117*.*

Kluiver J, Gibcus JH, Hettinga C, Adema A, Richter MK, Halsema N, **Slezak-Prochazka I**, Ding Y, Kroesen BJ, van den Berg A. 2012. Rapid generation of microRNA sponges for microRNA inhibition. *PLoS One* 7(1):e29275.

Slezak-Prochazka I, Durmus S, Kroesen BJ, van den Berg A. 2010. MicroRNAs, macrocontrol: Regulation of miRNA processing. *RNA* 16: 1087-1095.

ACKNOWLEDGEMENTS

Every journey starts with a first step. My first step in Groningen was 5 years ago when I started my internship and I immediately knew that I wanted to do my PhD here. I would like to thank my promoter Prof. Anke van den Berg for giving me this opportunity. Anke, you showed me how to be a good scientist and how to make, sometimes difficult, decisions and cherish small successes. You made me believe in myself. You also knew when to push me and when to let go. I admire how you can do so much so quickly and always think logical.

I would like to acknowledge my co-promoters Dr. Bart-Jan Kroesen and Dr. Joost Kluiver. Bart-Jan, I admire your writing skills and ability to put thoughts into exactly the right words. Thank you also for your easy-going attitude. Joost, I learned a lot from you on how to design experiments and analyze data. I enjoyed our work-related and less work related conversations. Thank you for your help with solving my countless scientific and daily-life problems and for cheering me up when I needed it.

I would also like to express my gratitude to Prof. Gerald de Haan, Prof. Philip Kluin and Prof. Jan Jacob Schuringa. I appreciate that you accepted to be members of my reading committee and spent your valuable time on reading my thesis.

My utmost thanks go to all present and former members of the "miRNA group". It was a pleasure to work with you. Johan, you were an inspiring and motivating supervisor during my internship and as a colleague later on. I admired how you came up with new fascinating ideas and so passionately talked about them. Jan-Lukas, I am grateful that you shared your project that resulted in my chapter 4. I like your English sense of humor and stories about your daughter. Debora, you were a huge help in the lab, especially in the last months. You were understanding when I needed to have everything done before yesterday and enthusiastic when something worked out. I am very happy that you agreed to be my paranimf. Nancy, I appreciate especially your help with microarrays, how you calmed me down when I was jittery over pipetting samples on glass slides and when scanning didn't work. DNA-lab is not the same

without you… Gertrud, you made me smile every time I saw you. Thank you that you were eager to help and that you put so much heart into whatever you did. Bea, I appreciate your help with Western Blots and RNA isolations. Melanie, thank you for spending your holidays on handling the massive amount of work I had for you. Rikst-Nynke, you introduced me to the lab during my internship, patiently answered all my beginners questions and were so kind to me. Geert, your experience with qRT-PCR analysis and microarrays was very helpful and I am grateful for teaching me how to handle the plating robot. Chris, thank you for the 3 months when you handled the things I didn't have time for and for your Friday afternoon jokes. Pytrick, thanks for work discussions and sharing reagents.

I am also thankful to the co-authors and collaborators. Prof. Sibrand Poppema, thank you for your expert opinion on my research. I very much enjoyed the two Allersmaborg meetings, where we could discuss our projects from a global point of view in a very friendly atmosphere. Klaas, your help with designing and analyzing custom arrays is highly appreciated. I learnt a lot from you and Martijn about analysis of large datasets in a systematic way. Ye Ding, thank you for your expertise on designing miRNA sponges and for taking me for Chinese dinner in Vancouver.

I would also like to acknowledge Lydia and Arjan from the Malignant Lymphoma group. Lydia, thank you for your kind words just in the right time and for the delicious carrot cake on my farewell party. I also very much enjoyed the multicultural meeting with you and the PhD students at your place. Arjan, I appreciate your stimulating questions during my presentations.

I would also like to say that thank you to all the people from the DNA and O&O labs (Mirjam, Lorian, Weird, Klaas, Sippie, Inge, Jenny, Sicco, Eric, Sharon, Annelies, Hans, Rianne and others). I very much enjoyed working with you. You helped me whenever I had doubts and created a very nice working environment (and the labs were so well organized!).

A special thanks to fellow PhD students. Wouter, I liked talking to you about serious and not serious issues. I know that you keep a list of things I shouldn't have said… Sietse, thanks for your help with translating Dutch letters.

To my fellow foreign PhD students (Lu Ping, Chuanhui, Kushi, Ali, Mina, Yuxuan, Huang Xin, Richard, Zheng Liang, Rea, Achmed, Nato, Li Jun), I appreciate that we could talk about differences in our cultures, try traditional food (at Lydia's and Anke's place) and discuss difficulties that we encounter as foreigners. Lu Ping, you gave me some good pieces of advice when I was starting my PhD. Thank you for establishing Ago2-RIP-Chip technique in our lab. As you can see it works well! Kushi, I enjoyed listening to your stories about Indian weddings. Ali, you had a good conclusion, namely that Iranian and Polish people are very similar. Chuanhui, Huang Xin, Richard, I hope you are doing well in China. Kushi, Ali, Yuxuan, Zheng Liang, Rea, Achmed, Mina, Nato, Li Jun, good luck with your projects and I am looking forward to getting your dissertations!

I am also grateful to Geert, Henk and Roelof-Jan from FACS facility for patiently sorting my "difficult" cells and squeezing my sorts in the very busy sorting schedule. Big thanks to my two German students, Ann-Christin and Julian. You were great students and thanks to you I realized that I like teaching. Thank you Jan and Roel for help with computers and thanks to the secretaries from our department for being helpful and efficient.

I am also grateful to Prof. Hanna Rokita for mentoring me during my studies at the Jagiellonian University and encouraging me to participate in the Erasmus program.

Thank you to my Polish lunch team (Marta, Kasia, Paulina). Girls, thank you for always being there for me. You were like a family. Marta, I wish you all the best with your work as scientist/doctor/fitness instructor. I enjoyed our Friday evening outings. I will never forget that you drove all the way to Eindhoven and we made it 1 minute before the gate at the airport closed. Kasia, thank you for our long evening coffee chats. It was nice to have someone with similar problems and sometimes very different point of view. Good luck with your and Marcin's defense! Paulina, you were a great flatmate and I loved your sarcastic comments. Marta and Kasia, it is great that you are willing to be my paranimfen!

I would like to thank my family. Mamo i Tato, dziękuję Wam za to, że nauczyliście mnie by podążać za marzeniami i zmieniać je w plany i że wszystko,

co robię powinnam robić najlepiej jak potrafię (Mum and Dad, thank you for teaching me to follow my dreams and change dreams into plans and that whatever I do I should do my best). Kora, I could always call you when I felt lonely. Bartek, without your constant support, love, friendship and ability to make me laugh I couldn't finish it. I am so happy that we proved ourselves that long-distance relationship can work out!

I smile to my computer when writing these acknowledgements and recalling all the nice memories. It is time to move on, but the people I met in Groningen will always be in my mind and heart. Thank you all!